



ESCUELA TÉCNICA SUPERIOR DE INGENIERÍA (ICAI)  
INGENIERO SUPERIOR INDUSTRIAL MECÁNICO

**ANALYSIS AND IMPLEMENTATION OF A  
MATERIAL MODEL FOR SEMI-FINISHED  
FIBER PRODUCTS FOR AUTOMOTIVE  
CARBON COMPOSITES STRUCTURES**

Autor: Alba Rollano Corroto

Director: Sebastian Bender

Madrid  
Agosto 2015

## AUTORIZACIÓN PARA LA DIGITALIZACIÓN, DEPÓSITO Y DIVULGACIÓN EN ACCESO ABIERTO ( RESTRINGIDO) DE DOCUMENTACIÓN

### 1ª. Declaración de la autoría y acreditación de la misma.

El autor D. Alba Rollano, como estudiante de la UNIVERSIDAD PONTIFICIA COMILLAS (COMILLAS), **DECLARA**

que es el titular de los derechos de propiedad intelectual, objeto de la presente cesión, en relación con la obra Analysis & Implementation of a material model for semi-finished fiber products for...<sup>1</sup>, que ésta es una obra original, y que ostenta la condición de autor en el sentido que otorga la Ley de Propiedad Intelectual como titular único o cotitular de la obra.

En caso de ser cotitular, el autor (firmante) declara asimismo que cuenta con el consentimiento de los restantes titulares para hacer la presente cesión. En caso de previa cesión a terceros de derechos de explotación de la obra, el autor declara que tiene la oportuna autorización de dichos titulares de derechos a los fines de esta cesión o bien que retiene la facultad de ceder estos derechos en la forma prevista en la presente cesión y así lo acredita.

### 2ª. Objeto y fines de la cesión.

Con el fin de dar la máxima difusión a la obra citada a través del Repositorio institucional de la Universidad y hacer posible su utilización de *forma libre y gratuita* ( *con las limitaciones que más adelante se detallan*) por todos los usuarios del repositorio y del portal e-ciencia, el autor **CEDE** a la Universidad Pontificia Comillas de forma gratuita y no exclusiva, por el máximo plazo legal y con ámbito universal, los derechos de digitalización, de archivo, de reproducción, de distribución, de comunicación pública, incluido el derecho de puesta a disposición electrónica, tal y como se describen en la Ley de Propiedad Intelectual. El derecho de transformación se cede a los únicos efectos de lo dispuesto en la letra (a) del apartado siguiente.

### 3ª. Condiciones de la cesión.

Sin perjuicio de la titularidad de la obra, que sigue correspondiendo a su autor, la cesión de derechos contemplada en esta licencia, el repositorio institucional podrá:

<sup>1</sup> Especificar si es una tesis doctoral, proyecto fin de carrera, proyecto fin de Máster o cualquier otro trabajo que deba ser objeto de evaluación académica

(a) Transformarla para adaptarla a cualquier tecnología susceptible de incorporarla a internet; realizar adaptaciones para hacer posible la utilización de la obra en formatos electrónicos, así como incorporar metadatos para realizar el registro de la obra e incorporar “marcas de agua” o cualquier otro sistema de seguridad o de protección.

(b) Reproducir la en un soporte digital para su incorporación a una base de datos electrónica, incluyendo el derecho de reproducir y almacenar la obra en servidores, a los efectos de garantizar su seguridad, conservación y preservar el formato. .

(c) Comunicarla y ponerla a disposición del público a través de un archivo abierto institucional, accesible de modo libre y gratuito a través de internet.<sup>2</sup>

(d) Distribuir copias electrónicas de la obra a los usuarios en un soporte digital.<sup>3</sup>

#### **4º. Derechos del autor.**

El autor, en tanto que titular de una obra que cede con carácter no exclusivo a la Universidad por medio de su registro en el Repositorio Institucional tiene derecho a:

a) A que la Universidad identifique claramente su nombre como el autor o propietario de los derechos del documento.

b) Comunicar y dar publicidad a la obra en la versión que ceda y en otras posteriores a través de cualquier medio.

c) Solicitar la retirada de la obra del repositorio por causa justificada. A tal fin deberá ponerse en contacto con el vicerrector/a de investigación ([curiarte@rec.upcomillas.es](mailto:curiarte@rec.upcomillas.es)).

d) Autorizar expresamente a COMILLAS para, en su caso, realizar los trámites necesarios para la obtención del ISBN.

---

<sup>2</sup> En el supuesto de que el autor opte por el acceso restringido, este apartado quedaría redactado en los siguientes términos:

(c) Comunicarla y ponerla a disposición del público a través de un archivo institucional, accesible de modo restringido, en los términos previstos en el Reglamento del Repositorio Institucional

<sup>3</sup> En el supuesto de que el autor opte por el acceso restringido, este apartado quedaría eliminado.

d) Recibir notificación fehaciente de cualquier reclamación que puedan formular terceras personas en relación con la obra y, en particular, de reclamaciones relativas a los derechos de propiedad intelectual sobre ella.

**5º. Deberes del autor.**

El autor se compromete a:

- a) Garantizar que el compromiso que adquiere mediante el presente escrito no infringe ningún derecho de terceros, ya sean de propiedad industrial, intelectual o cualquier otro.
- b) Garantizar que el contenido de las obras no atenta contra los derechos al honor, a la intimidad y a la imagen de terceros.
- c) Asumir toda reclamación o responsabilidad, incluyendo las indemnizaciones por daños, que pudieran ejercitarse contra la Universidad por terceros que vieran infringidos sus derechos e intereses a causa de la cesión.
- d) Asumir la responsabilidad en el caso de que las instituciones fueran condenadas por infracción de derechos derivada de las obras objeto de la cesión.

**6º. Fines y funcionamiento del Repositorio Institucional.**

La obra se pondrá a disposición de los usuarios para que hagan de ella un uso justo y respetuoso con los derechos del autor, según lo permitido por la legislación aplicable, y con fines de estudio, investigación, o cualquier otro fin lícito. Con dicha finalidad, la Universidad asume los siguientes deberes y se reserva las siguientes facultades:

a) Deberes del repositorio Institucional:

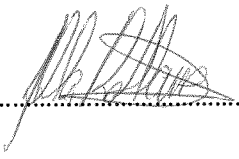
- La Universidad informará a los usuarios del archivo sobre los usos permitidos, y no garantiza ni asume responsabilidad alguna por otras formas en que los usuarios hagan un uso posterior de las obras no conforme con la legislación vigente. El uso posterior, más allá de la copia privada, requerirá que se cite la fuente y se reconozca la autoría, que no se obtenga beneficio comercial, y que no se realicen obras derivadas.
- La Universidad no revisará el contenido de las obras, que en todo caso permanecerá bajo la responsabilidad exclusiva del autor y no estará obligada a ejercitar acciones legales en nombre del autor en el supuesto de infracciones a derechos de propiedad intelectual derivados del depósito y archivo de las obras. El autor renuncia a cualquier reclamación frente a la Universidad por las formas no ajustadas a la legislación vigente en que los usuarios hagan uso de las obras.
- La Universidad adoptará las medidas necesarias para la preservación de la obra en un futuro.

b) Derechos que se reserva el Repositorio institucional respecto de las obras en él registradas:

- retirar la obra, previa notificación al autor, en supuestos suficientemente justificados, o en caso de reclamaciones de terceros.

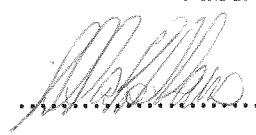
Madrid, a <sup>06</sup> de Agosto de 2015

**ACEPTA**

Fdo.....  


Proyecto realizado por el alumno/a:

Alba Rollano Corroto

Fdo.:  .....

Fecha: 26 / 08 / 2015

Autorizada la entrega del proyecto cuya información no es de carácter  
confidencial

EL DIRECTOR DEL PROYECTO

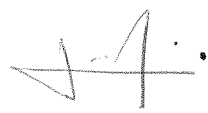
Sebastian Bender

Fdo.:  .....

Fecha: 24 / 08 / 2015

Vº Bº del Coordinador de Proyectos

José Ignacio Linares Hurtado

Fdo.:  .....

Fecha: 26 / 08 / 2015



## Table of Content

<b>Chapter 1. Introduction .....</b>	<b>9</b>
<b>1.1 Motivation .....</b>	<b>9</b>
<b>1.2 Aim and Scope of the thesis .....</b>	<b>12</b>
<b>1.3 Structure of the thesis .....</b>	<b>13</b>
<b>Chapter 2. Carbon Fiber Reinforced Plastics (CFRP) .....</b>	<b>15</b>
<b>2.1 Classification .....</b>	<b>15</b>
<b>2.2 Matrix .....</b>	<b>16</b>
<b>2.3 Reinforcements .....</b>	<b>17</b>
<b>2.4 Composites design .....</b>	<b>17</b>
2.4.1 Mechanical response .....	18
2.4.2 Laminate sequencing optimization.....	22
2.4.3 Failure modes .....	23
<b>2.5 Composite Manufacturing.....</b>	<b>25</b>
<b>Chapter 3. Semi- Finished Products (SFP) .....</b>	<b>28</b>
<b>3.1 Woven Fabric.....</b>	<b>30</b>
3.1.1 Woven mechanical properties .....	33
3.1.2 Woven fabric failure mode.....	48
<b>3.2 Non-Crimp Fabrics (NCF).....</b>	<b>54</b>
<b>3.3 Braiding.....</b>	<b>56</b>
<b>3.4 Prepregs.....</b>	<b>58</b>
<b>3.5 Simulation .....</b>	<b>59</b>
Fibersim (Siemens) .....	60
WiseTEX Suit .....	61
PAM-FORM (ESI-Group) .....	61
Digimat .....	62
<b>Chapter 4. Complexity .....</b>	<b>63</b>



---

<b>4.1</b>	<b>Drapability .....</b>	<b>66</b>
4.1.1	Deformation modes .....	70
<b>4.2</b>	<b>Permeability .....</b>	<b>72</b>
4.2.1	Definition .....	72
<b>Chapter 5.</b>	<b><i>Methodology .....</i></b>	<b>78</b>
<b>5.1</b>	<b>Problem description .....</b>	<b>78</b>
<b>5.2</b>	<b>Mechanical properties.....</b>	<b>79</b>
5.2.1	Layerwise optimization algorithm (LOA).....	84
5.2.2	Tsai-Wu Failure mode.....	86
<b>5.3</b>	<b>Material complexity .....</b>	<b>87</b>
5.3.1	Draping complexity.....	88
5.3.2	Draping validation.....	99
<b>Chapter 6.</b>	<b><i>Result and discussion .....</i></b>	<b>103</b>
<b>6.1</b>	<b>Mechanical properties. Case study .....</b>	<b>103</b>
<b>6.2</b>	<b>Drapability validation .....</b>	<b>104</b>
6.2.1	Knowledge-based rating.....	105
6.2.2	Time measurement .....	114
<b>6.3</b>	<b>Permeability validation.....</b>	<b>121</b>
<b>6.4</b>	<b>Ply stacking complexity.....</b>	<b>122</b>
<b>6.5</b>	<b>Draping simulation.....</b>	<b>124</b>
<b>Chapter 7.</b>	<b><i>Summary and Outlook .....</i></b>	<b>126</b>
<b>7.1</b>	<b>Future work .....</b>	<b>127</b>
<b>Appendix :</b>	<b><i>Survey.....</i></b>	<b>129</b>
<b>Used symbols</b>	<b>.....</b>	<b>132</b>
<b>List of tables</b>	<b>.....</b>	<b>134</b>
<b>List of figures</b>	<b>.....</b>	<b>136</b>
<b>Bibliography</b>	<b>.....</b>	<b>139</b>



## **ANALYSIS AND IMPLEMENTATION OF A MATERIAL MODEL FOR SEMI-FINISHED FIBER PRODUCTS FOR AUTOMOTIVE CARBON COMPOSITES STRUCTURES**

Autor: Alba Rollano

Director: Sebastian Bender

### **THESIS RESUME**

To find fast answers for future vehicle concepts with carbon reinforced plastics (CFRP) as structural material the institute of automotive technology in Munich develops a virtual vehicle model. With this model specific statements such as costs and production parameters of a CFRP-body in the early design phase should be answered quickly.

The target of the thesis is to investigate the influence of the fiber products of structural CFRP components to a complete body-in-white. Therefore, the initial is the familiarization with the current state-of-the-art of these composite materials. Important information is performance parameters, such as new analytical methods that estimate SFP properties, it was proved that the Mosaic Model based on fabric structure simplifications, show the best results when compared to experimental data. Additional failure criteria were applied in order to estimate composites degraded properties, and hence estimate if in case of failure it is required a change due to the lack of strength or stiffness left.

Despite the high quality of CFRP, the application of these materials in series-produced vehicles is limited by reason of material costs. Thereby, developing a manufacturing cost model has become a major factor of commercial success for composite products.

Without a doubt, it is much more efficient to reduce the cost in an early phase rather than in between the manufacturing process, as more than the 70% of the



overall cost are committed after the design phase.. Thus, cost modelling and estimation are indispensable to the development of price competitive composites.

From a material point of view, one of the ways to achieve an optimum cost model is through optimizing not only the used fabrics but also the lay-up sequence. Thus, Layerwise Optimization Algorithm was implemented to optimize the material lay-up, this means, thickness and orientation of each single ply of a laminate, as also the sequence on which the different layers are stack together to conform a laminate.

The developed methodology which is able to calculate the mentioned influence in the early design phase will be implemented as software model and integrated in the overall virtual vehicle model. Simulative and practical tests should provided information for further optimization and validation of the methodology.

Furthermore, in order to collaborate in the above named manufacturing cost model, the influence of the complexity of the fiber product on the manufacturing process was investigated. Two main parameters are responsible for material complexity, understanding complexity as additional efforts induced in the manufacturing process due to the use of different fabrics. It was initially assumed, based on literature, that the main mechanism responsible for inducing extra effort, here time, was draping process, affected by fabric shear angle.

In order to validate a proposed model, a knowledge-based rating was realized and a manufacturing-time measurement observe.

From both processes it was inferred that rather than shear, fabric areal weight played a larger role. But overall the time increment associated if compared to the overall manufacture procedure was insignificant. Other factors as orientation, used mold (female , male) or permeability were also analysed. In this case, tests show that rather than collaborating on a complexity, they are factors that should be optimized beforehand, in order to avoid this complexity.

One major conclusion of the thesis is due to the fact that realignment of fibers during preforming produces mechanical properties variations, along with variations in permeability. Hence, new values for sheared reinforcements must be estimated in order to estipulate if they are longer useful, or the mechanical



**UNIVERSIDAD PONTIFICIA COMILLAS**  
ESCUELA TÉCNICA SUPERIOR DE INGENIERÍA (ICAI)  
INGENIERO INDUSTRIAL

*ÍNDICE DE FIGURAS*

---

properties detriment is significantly big to require a new material. And hence, the increasing effort that should be done from an early design phase.

This thesis try to help through the implementation of the material optimization module into an overall BIW model



## **ANÁLISIS E IMPLEMENTACIÓN DE UN MODELO PARA LA OPTIMIZACIÓN DEL USO DE TEXTILES EN ESTRUCTURAS AUTOMOVILÍSTICAS DE FIBRA DE CARBONO**

Autor: Alba Rollano

Director: Sebastian Bender

Con el objetivo de encontrar respuestas rápidas a futuros conceptos de vehículos basados en el uso de fibra de carbono en matriz orgánica como material estructural, dentro de un proyecto del instituto de automoción de la Universidad Técnica de Múnich se desarrolla un modelo de vehículo virtual. Con este modelo, se buscan una respuesta rápida a la determinación de los costos y los parámetros de producción de un cuerpo de CFRP, desde una fase inicial de diseño.

El objetivo de la tesis es investigar la influencia de textiles a base de CFRP sobre el BIW del vehículo. Por lo tanto, la primera tarea aquí desarrollada es la familiarización con el estado de la técnica actual de estos materiales compuestos, prestando especialmente atención a los textiles, que serán el principal objeto the estudio, como nuevos métodos de análisis que estimen sus propiedades.

Tras un análisis teórico, tres de los principales modelos fueron implementados. De cuyo análisis se comprobó que el Mosaic Model basado en la homogenización de la estructura, mostraba los mejores resultados en comparación con los datos experimentales. Se aplicaron criterios adicionales de modos fallo con el fin de estimar las propiedades degradadas de estos materiales compuestos, y por lo tanto estimar si en caso de fallo es necesario un cambio de componente, porque los requerimientos no se cumplen por mas tiempo

A pesar de la alta calidad de CFRP, la aplicación de estos materiales en vehículos fabricados en serie está limitado por razón de costes de material. De este modo, el desarrollo de un modelo de coste de fabricación se ha convertido en un factor importante del éxito comercial para productos compuestos.

Sin duda, es mucho más eficiente para reducir el costo en una fase temprana en



lugar de en el medio del proceso de fabricación, ya que más del 70% del coste total se han comprometido después de la fase de diseño. Por lo tanto, modelos de costos y estimación son indispensables para el desarrollo de materiales compuestos a precios competitivos. Desde un punto de vista material, uno de los medios para lograr un coste óptimo es a través de la optimización no sólo los tejidos utilizados, sino también la secuencia de lay-up. Layerwise Optimization Algorithm se llevó a cabo para optimizar el lay-up del material, esto quiere decir, no solo la optimización del espesor y orientación de cada capa del laminado, sino también la secuencia en la que las diferentes capas se apilan juntos para conformar un laminado.

Además, con el fin de colaborar en el modelo de coste de fabricación mencionado anteriormente, se investigó la influencia de la complejidad de los textiles en el proceso de fabricación. Se entiende por complejidad del material, los esfuerzos adicionales inducidos en el proceso de fabricación debido al uso de diferentes tejidos. Se supuso inicialmente, en base a la literatura, que el principal mecanismo responsable de inducir un esfuerzo extra, en este caso esfuerzo fue medido en tiempo adicional, fue el proceso de conformación, condicionado en gran medida por el máximo ángulo que las fibras son capaces de girar en los puntos de interconexión.

Con el fin de validar el modelo propuesto, se llevó a cabo una encuesta a expertos en materiales compuestos a los que se les preguntó por la influencia que ejercían material, molde y dimensiones en la fabricación de componentes automovilísticos. Diferentes partes de un coche fueron evaluadas. Adicionalmente, se observó y midió un proceso de manufacturación.

De ambos procesos se infiere que el factor que predominantemente influye en la complejidad es el peso del textil. No obstante, en general el incremento de tiempo asociado si se compara con el procedimiento general de fabricación era insignificante. Se analizaron también otros factores como la orientación, molde utilizado (hembra, macho) o permeabilidad. En este caso, las pruebas muestran que en lugar de colaborar en una complejidad, son factores que deben ser



optimizados de antemano, a fin de evitar esta complejidad.

La realineación de las fibras durante el preformado produce variaciones en las propiedades mecánicas, junto con variaciones la permeabilidad. Por lo tanto, los nuevos valores para refuerzos cizallados deben ser estimados con el fin de estipular si son ya útiles, o las propiedades mecánicas en detrimento es significativamente grande como para requerir un nuevo material. Esta tesis trata de ayudar a través de la implementación del módulo de optimización de material en un modelo global de optimización del BIW.



## Chapter 1. INTRODUCTION

This chapter introduces the motivation (1.1), Aim & Scope of the Thesis (1.2) and an overall structure of the thesis (1.3).

### *1.1 MOTIVATION*

---

In 2009 the European Union adopted a legislation setting binding emission targets for the car manufactures vehicle fleets in order to reduce CO<sub>2</sub>-emissions and address by the restricted presence of non-renewable resources. Meeting these regulations will require unprecedented and fundamental changes in the automobile industry.

The top concern driving the development of new products in between the automobile sectors is regulation; different strategies are available in order to achieve fuel efficiency and emissions standards. However, the new requirements are so significant that implementing a single approach will not be enough. Automotive companies must have multiple strategies to meet the fulfillment of these regulations. The figure below shows the most followed strategies:

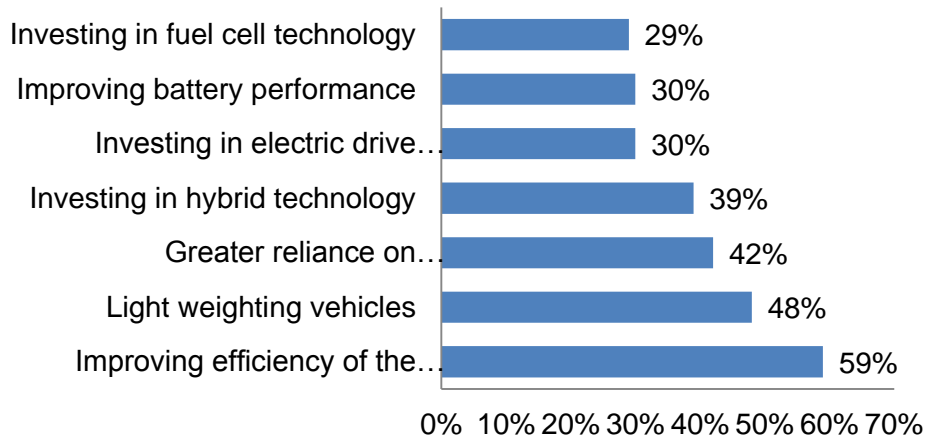


Figure 1.1 Emissions reduction strategies [39]

The largest followed strategy is the improvement of the drivetrain efficiency so that less fuel is burned. The next strategy is to reduce the weight so less fuel will be needed to propel it. This approach it is of great importance for electric vehicles where weight savings have a directly effect on power consumption

One of the most obvious ways to remove weight is to look at alternative materials that are lighter, yet strong enough to withstand the impact of a crash. Consequently, it is not too surprising that 88 % of automotive companies either have or plan to develop strategies for using new materials. [39]

Then, when looking at what these material strategies are, most plan to use aluminum, composites, or a combination of mixed materials. Carbon Fiber Reinforced Plastics (CFRP) offer significant strength while weighting very little. Applications for carbon fiber are expected to grow over the next decade and, by 2025, automotive companies expect 60% of their vehicles to be made at least with 20% carbon fiber. In this regard BMW developments in indeed pioneering. The German company has shown an increasing interest on CFRP, launching in the last years the hybrid BMW i8 and the electric i3. Further motivating this increase in carbon fiber is an expected drop up to 67% in price [39].

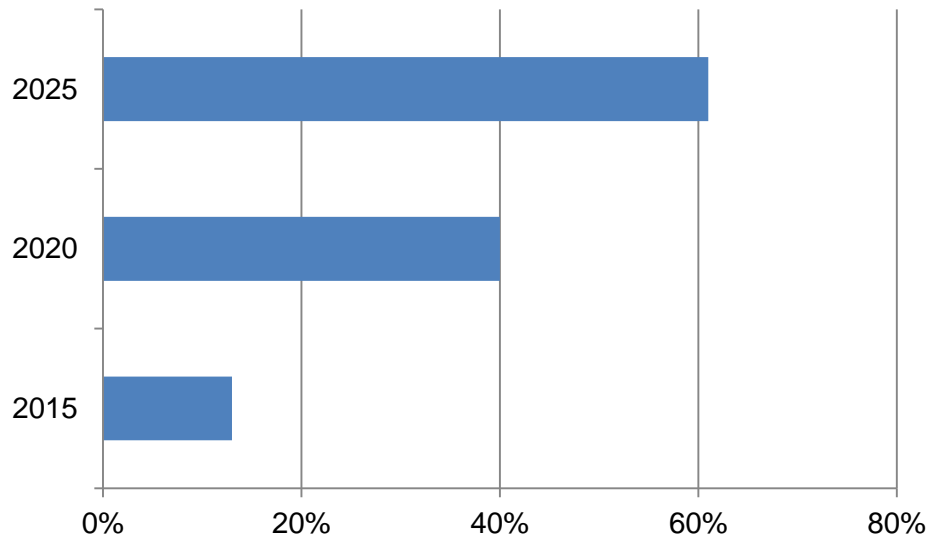


Figure 1.2 Expectations towards CFRP implementation

Carbon fiber, is not just a light weight material, in addition, less material is needed to achieve stiffness and impact resistance requirements. This make it a very appealing material, but at the same time, as illustrated above in Figure 1.2, there is some uncertainty when designing and manufacturing new components with it. Many companies turn to composite design software to help them design with this material. Those who use composite design software have been rewarded with 139 % greater weight reduction than non-users.

Most of the companies claim that the main reasons for not using carbon fiber were [39]:

- Cost of carbon fiber
- Lack of knowledge in designing parts in composites
- Lack of knowledge when manufacturing composite parts
- Manufacturing cycle time is too long for composite parts



The use of software makes it easier, improving the manufacturability of composite parts. Hence, it can be inferred that in order to facilitate the development of composite parts accurate software should be designed with the main aim of reducing costs and simplifying composites manufacturing process.

## ***1.2 AIM AND SCOPE OF THE THESIS***

---

The thesis at hand is realized on behalf of TUM CREATE Centre for Electromobility Limited, an international joint collaboration between the Technische Universität München (TUM) and the Nanyang Technological University (NTU). TUM CREATE is part of the Campus for Re-search Excellence And Technological Enterprise (CREATE) program in Singapore and is funded by the National Research Foundation. The main objective of the research work, done within TUM CREATE, is the development of concepts for a sustainable future in mobility. The key output is an electric vehicle prototype, explicitly designed as a taxi for tropical megacities, codenamed EVA [TUM2013].

The vehicle concept is focusing on the specific challenging demands of fast growing tropical mega cities. Within the development process of EVA, a team of scientists, engineers and de-signers from 20 countries is facing problems in different fields of research. One field is the development of a lightweight Carbon Fiber Reinforced Plastic (CFRP) body structure. It is one of the largest automotive body structures made of CFRP, facilitating a weight saving potential of 150 kg compared to steel structures with similar stiffness and strength performance. Subsequent to the completed body structure development process, research at TUM CREATE is partially focusing on its optimization [TUM2013].



Prior research focused on helping in the optimization of CFRP materials usage in the automotive body development process from an early design phase [AMJ2014], under the creation of a software (“CC-Fast”) that optimizes the overall design of the CFRP BIW. The objective of this thesis is to further investigate CFRP composite materials, especially when referring to semi-finish fabrics (SFP), also known as "textile composites".

Due to the fact that manufacturing cost estimation within the overall optimization needs to take into account the material complexity of parts [REH2014], a further analysis on material complexity based on SFP data will be developed.

### ***1.3 STRUCTURE OF THE THESIS***

---

The thesis at hand focuses on the investigation and analyses of SFP, and thereafter on a study on the influence exerted by these fabrics on manufacturing process. Hence two main objects of study can be here distinguished. In the first part, a complete understanding of SFP characteristics and behavior is described. The second part of this work concentrates in the evaluation and determination of a material complexity.

Chapter 2 focuses on a brief introduction to CFRP to understand the further development of this work. It is of great importance the description of their mechanical behavior, since part of the here presented methodologies can be further implemented with SFP. In Chapter 3 an overview of the main SFP fabrics is given with a deeper analysis on woven fabric and non-crimp-fabrics (NCF), most used fabrics amongst the automotive industry. Different models for predicting woven fabrics properties are here also described. At the end of the chapter, available software for composites design are explained in order to infer which areas are necessary to be investigated on future work or in which



market is worth it to introduce a new competitive software . A definition for complexity is given in Chapter 4, along with an exhaustive investigation on possible influencing parameters. Later on Chapter 5, a methodology on estimating a material complexity model is hereby introduced. The results are described and discuss on Chapter 6. While on Chapter 7, a summary of the information inferred during the thesis at hand is given. Recommendations for future works are also included in this last chapter.



## Chapter 2. CARBON FIBER REINFORCED PLASTICS (CFRP)

Composite materials are the combination of two or more materials in such a way that certain improved or desired properties are achieved. In practice, most composites consist of a bulk material, the matrix, and reinforcement, added to increase the strength and stiffness of the matrix.

### *2.1 CLASSIFICATION*

---

Today, the most common man-made composites can be divided into three main groups according to the matrix material:

- Metal matrix Composites (MMC). Increasingly found in the automotive industry, these composites use metal such as aluminum as matrix, and reinforce it with fibers or particles.
- Ceramic Matrix Composites (CMC). Used in high temperature environments, these composite materials reinforce a ceramic matrix with short fibers or whiskers.
- Polymer Matrix Composites (PMC). Also known as Fiber Reinforced Fabrics, these materials use a polymer-based resin as matrix, and a variety of fibers such as aramid, glass or carbon as reinforcement. Hereafter, the thesis will consider exclusively PMC, by reason of automotive application.



## 2.2 *MATRIX*

---

Matrix used for fiber reinforced composites are commonly referred as resins. They can be classified under, thermoplastic and thermoset, according to the effect of heat on their properties. Among this, thermoset matrix composites are predominantly used. Matrix selection is performed under chemical, thermal, electrical, cost, performance, and manufacturing requirements constraints, it is determinant on infusion and curing procedures.

- Thermoplastic. In general, ductile and tougher than thermoset materials. Thermoplastics can be melted by heating and solidified by cooling, which render them capable of repeated reshaping and reforming. Their lower stiffness and strength, as well as their poor creep resistance and their complicated repairing process , have led to a lack of implementation in the automotive industry. For further detail, refer to [42].
- Thermoset: Once cured cannot be remelted or reformed. They offer easy processability, better fiber impregnation, greater thermal and dimensional stability, better rigidity and higher electrical, chemical and solvent resistance. The most common resin materials used in thermoset composites are:
  - Polyester
  - Epoxy
  - Vinylester



## **2.3** *REINFORCEMENTS*

---

Reinforcements for composites can be in form of fibers, particles or, flakes. Each has its unique application, although fibers are the most widely employed, due to the extra strength and stiffness they provide to the composite. Fibers generally follow a specific pattern or structure for increasing handability and manufacturability. Depending on the structure that the fibers defined, different properties are obtained. The main forms fibers can be find in a composite are:

- Yarns : set of fiber yield together
- Mats
- Fabrics: defined as layers of long and continuous fibers with a variety of orientations These layers are held together either by mechanical interlocking of the fibers themselves such as woven fabrics or with a secondary material to bind them together and hold them in place, giving the fabric the enough integrity to be handled. Fabric types, also named semi-finished products, are categorized by the orientation of the fibers used and their distribution along the fabric. A further analysis is undertaken in the following sections.

## **2.4** *COMPOSITES DESIGN*

---

The concept of designing a material for a structural part, required of a preliminary material selection that may be based on mechanical properties for which experimental values are not always available. Hence, analytical methods resulted from mainly micromechanics studies need to be implemented from an early design phase as a path in estimating composites properties and behavior, and thus, the most optimum option for a certain part. When designing composites one must



additionally consider several alternatives such as best stacking sequence, optimum fiber angles in each layer as well as the number of layers itself, based on different criteria such as meeting load and moments constraints.

## 2.4.1 MECHANICAL RESPONSE

---

The determination of the mechanical properties of composites structures is complex due to the fact that existing vehicle structure design philosophies applied for metal structures cannot be directly ported over as the fact that manufacturing processes are time-intensive.

Composite properties result from the individual properties of each of the components, the ratio of fiber to resin (Fiber Volume fraction,  $V_f$ ), their interaction and the fibers geometry and orientations. The fiber volume fraction derives largely from the manufacturing process, and it will be defined by the user as a minimum required constraint. Nevertheless, it is highly governed by the type of resin and the fibers arrangement within the yarn (bundle of twisted fibers filaments).

### 2.4.1.1 Rule of Mixtures (ROM)

Rough estimation of composite effective elastic constants can be estimated based on the distribution of each of the material compounding a composite. This approach is referred to as the ROM. For a fiber & resin composite:

$$V_f + V_m = 1 \quad (2.1)$$

Where  $V_f$  is the fiber volume fraction, and  $V_m$  the matrix fiber volume.

Taking account that the fiber volume will be defined as a user input, composite properties are defined as follows:



- The Young's modulus ( $E_1$ ) parallel to the fiber direction:

$$E_1 = E_{1f} \cdot V_f + E_{1m} \cdot (1 - V_f) \quad (2.2)$$

- The Young's modulus ( $E_2$ ) perpendicular to the fiber direction:

$$E_2 = \frac{E_{2f} \cdot E_{2m}}{(E_{2f} \cdot (1 - V_f) + E_{2m} \cdot V_f)} \quad (2.3)$$

- The Density ( $\rho$ ) of the composite material:

$$\rho = \rho_f \cdot V_f + \rho_m \cdot (1 - V_f) \quad (2.4)$$

- The Shear modulus ( $G_{12}$ ):

$$G_{12} = \frac{G_{12f} \cdot G_{12m}}{(G_{12f} \cdot (1 - V_f) + G_{12m} \cdot V_f)} \quad (2.5)$$

- Finally, the Poisson's ratio ( $\nu_{12}$ ):

$$\nu_{12} = \nu_{12f} \cdot V_f + \nu_{12m} \cdot (1 - V_f) \quad (2.6)$$

Where  $E_{1f}, E_{2f}, G_{12f}, \nu_{12f}$  and  $\rho_f$  are the Young moduli, shear moduli, Poisson's ratio and mass density respectively, of the fiber, while  $E_m, G_m, \nu_m$  and  $\rho_m$  are the corresponding properties for the matrix.

#### ***2.4.1.2 Classical Laminate Theory (CLT)***

ROM models are valid for determining single-ply properties but more complex methodologies are required to enable characterization of multiplied laminates.



CLT is a compound but a well-established and accepted approach. Two major assumptions required are:

- Fiber and resins properties can be smeared into an equivalent homogenous material with orthotropic behavior. This assumption allows stress-strain relations development.
- In-plane stress components, considered in the (X,Y) plane of the principal coordinate system, are considered much larger than out-of-plane stresses, thereby, they are set to zero.

In order to obtain the laminate mechanical properties, a number of sequential steps should be followed. A scheme with the procedure is shown in Figure 2.1.

Where  $A$ , extensional stiffness matrix,  $B$ , bending extensional coupling stiffness matrix and  $D$ , bending stiffness matrix, are calculated as follows:

$$\begin{aligned} A_{ij} &= \sum_{k=1}^N \overline{Q}_{ijk} \cdot (z_k - z_{k-1}) \\ B_{ij} &= \frac{1}{2} \cdot \sum_{k=1}^N \overline{Q}_{ijk} \cdot (z_k^2 - z_{k-1}^2) \\ D_{ij} &= \frac{1}{3} \cdot \sum_{k=1}^N \overline{Q}_{ijk} \cdot (z_k^3 - z_{k-1}^3) \end{aligned} \quad (2.7)$$



Carbon Fiber Reinforced Plastics (CFRP)

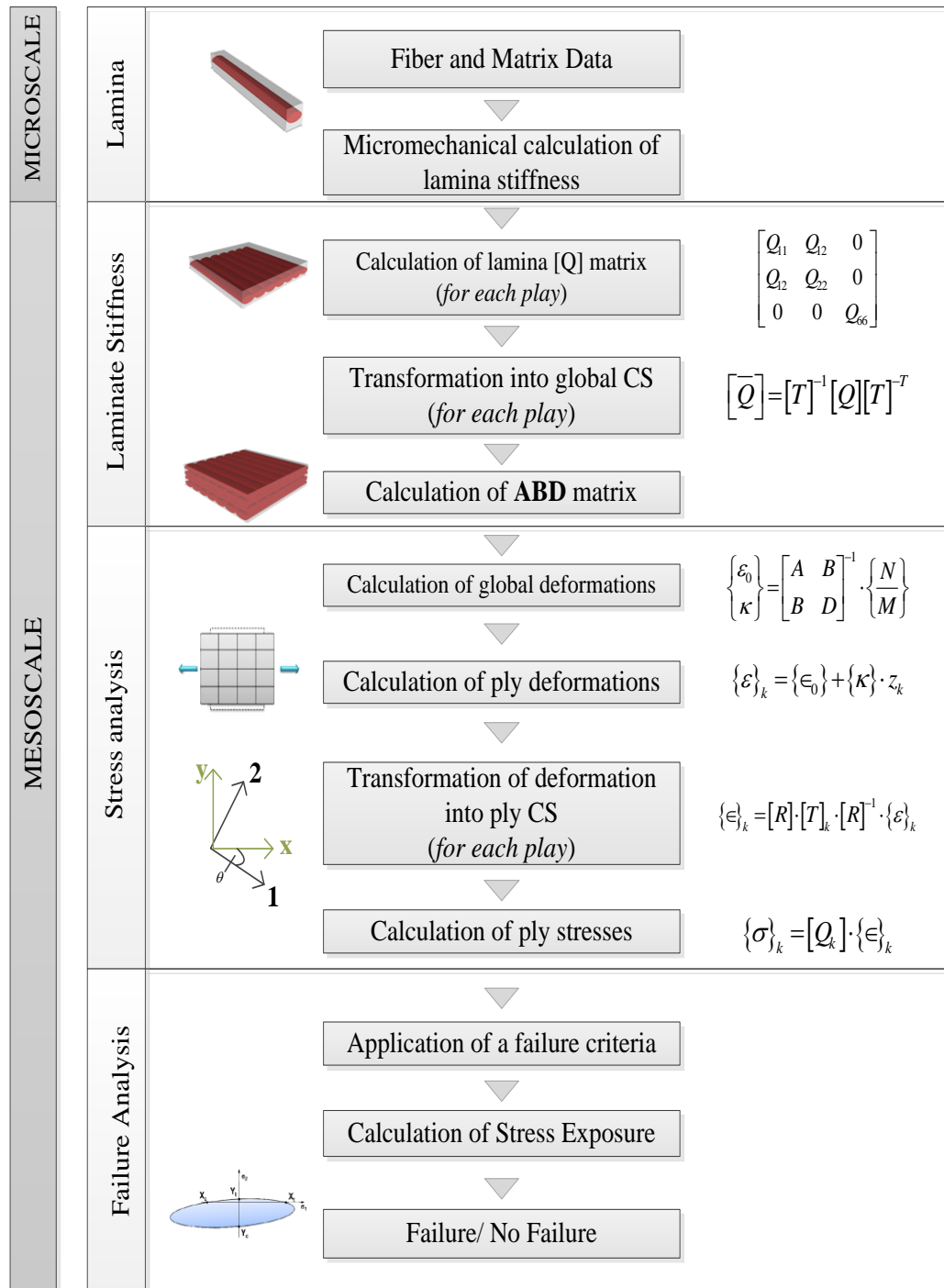


Figure 2.1 CLT Flowchart



## 2.4.2 LAMINATE SEQUENCING OPTIMIZATION

---

The sequence, in which the layers stack on top of each other, influences the resultant stiffness matrix of the laminate. Thus, in order to meet loading and stiffness requirements it is as vital to optimize the stacking order as the orientation per ply. [2]

Numerous studies have been developed with the aim of streamlining composites lay-up. Special attention is paid to are the models Gradient Based Optimization, Search Optimization, Genetic Algorithm and Layerwise Optimization, among others. The Gradient Based Optimization approach was developed to optimize the orientation of a single layer composite [37], further modifications [45] allowed to optimize the thickness of a predetermine specific sequence. In 1970, Search Optimization was used to determine the lightest composite design [50] assuming a constant thickness per- ply. The optimization technique par excellence, Genetic Algorithm [4], was also applied to laminate composites. Despite their advantages, the obtained results were proved to be influenced by the population size as well as the impossibility of the results to achieve a global optimum. Lastly, the Layerwise Optimization proposed by [35] performs a sequential algorithm, optimizing layer by layer, maximizing the constraints in each step.

Given the stated objective of implementing an overall model that optimizes, from a material point of view, carbon fiber reinforced plastics structures, it is crucial that the performed method enables variation on part thickness. Furthermore, the simulation starting point will have no impact regarding the component thickness, but it should converge faster as the number of plies (thickness) increases when the constraints are not met. For the previously mentioned reasons, and after comparing the different approaches [1], it is concluded that the Layerwise Optimization approach is the most suitable method to implement when multi-objective optimizations are involved (sequence and angles).



### 2.4.3 FAILURE MODES

---

Fatigue and fracture behavior of composite materials are crucial in design phase in order to determine the component behavior under static and fatigue loadings. It is well established that the mechanisms that reduce strength and stiffness are related to a variety of complex modes of failure. [40]

Structures can be limited by the structure deformation, stiffness predominance, or by the material strength. Therefore, it is crucial to estimate which type of failure may occurred.

Failure criteria proposed to predict lamina failure could be divided in:

(a) Failure criteria not associated with failure modes

This group includes all tensorial and polynomial criteria using material strength to describe the failure. In general, these relations are obtained by applying regression models to curves based on experimental tests. The most known general polynomial was proposed by [49]. This criterion will be introduced in Section 3.1 as a measurement on woven failure. Other popular and well-known quadratic failure modes include those propose by Hoffman, Chamis or Tsai-Hill, distinguished in the way in which the tensor stress components are determined.

(b) Failure criteria associated with failure modes

The criteria considered that the non-homogeneous behavior of composites leads to failure amongst their constituents. The main advantage of this criteria is their ability on predicting failure modes, being thereby optimal to be used in a progressive damage analysis.

Most of the named criteria identify the following failure modes



## Carbon Fiber Reinforced Plastics (CFRP)

- Inter Fiber Failure (IFF): describes cracks that run parallel to the fibers through the entire thickness of a layer. Cracks that may occur owing to the presence of residual tensile stress in the matrix. Different art of stresses lead to different forms of IFF. It is of great importance to distinguished among IFF, since cracked layers can be no longer stressed in tension and limited under shear and compression stresses.

As it can be shown on Figure 2.2, both transverse tension and longitudinal shear lead to longitudinal cracks while transverse compression and shear result in inclined fracture planes that suppose a great risk for the lamina performance.

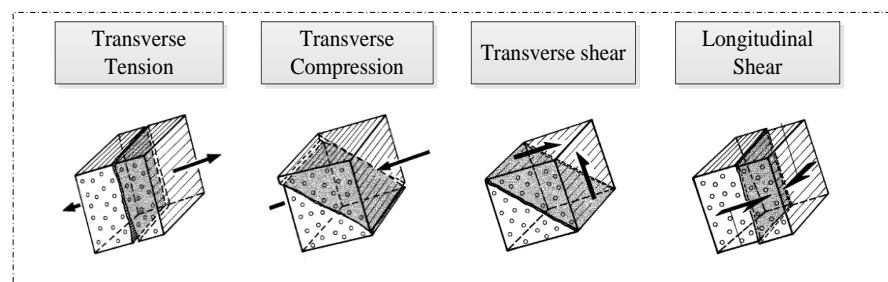


Figure 2.2 IFF Failure modes

- Fiber Failure (FF): denotes the simultaneous rupture of several bundles of fibers. In this type of failure it is important to distinguish if the predominant stress is either tensile or compressive. In the first case, the fibers will split along the axis. Compression stresses are generally due to shear, micro-buckling and kinking.

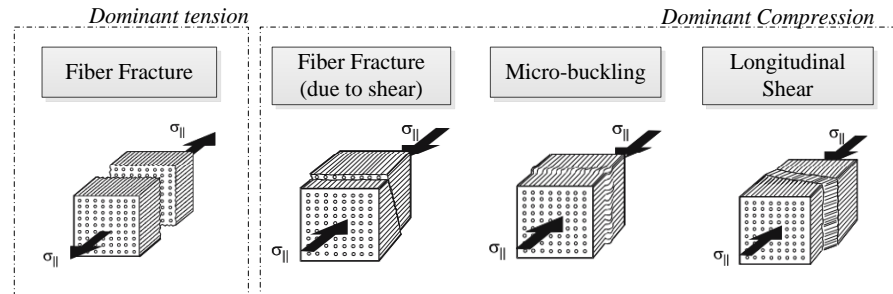


Figure 2.3 FF Failure modes

A further division can be done depending the type of failure:

- Non-interactive: Do not take account of stresses/strains relations occurring on a lamina. Commonly known non-interactive criteria are maximum strain criterion or maximum stress criterion, which was used by [1] for optimizing composites structures.
- Interactive: Hashin-Rotem [20], Hashin [19] and Puck [36] are known interactive criteria that takes into consideration stress/strain relation.

## 2.5 COMPOSITE MANUFACTURING

Composites manufacturing is defined as the process, along which raw material is transformed into a specific form or shape. According to the type of reinforcement, production rate, performance and cost requirements, there are various processing techniques available. A classification gathering these parameters is shown in Figure 2.4



## Carbon Fiber Reinforced Plastics (CFRP)

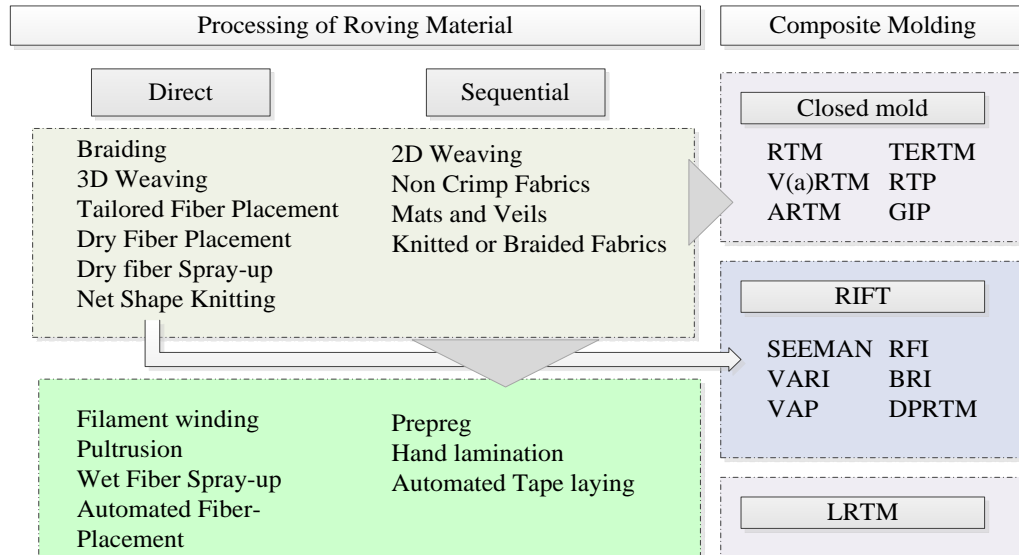


Figure 2.4 Manufacturing processes

Furthermore, as can be seen above, preforming raw material could be done on a sequential process or either by direct preforming. Their inclusion in the overall manufacture chain is designed in Figure 2.5. However, for detailed information on composites manufacturing refer to [46].



## Carbon Fiber Reinforced Plastics (CFRP)

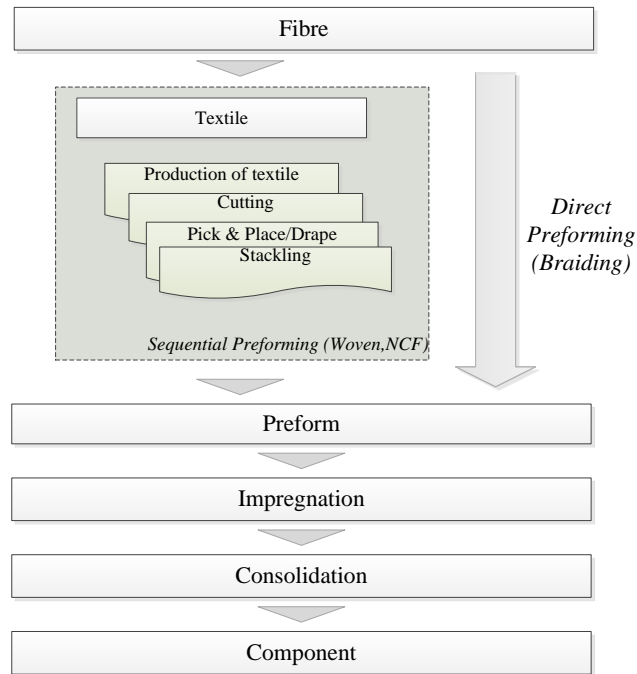


Figure 2.5 Sequential vs. direct

Despite the high quality of CFRP, the application of these materials in series-produced vehicles is limited by reason of material costs. Thereby, developing a manufacturing cost model has become a major factor of commercial success for composite products. [10]

Without a doubt, it is much more efficient to reduce the cost in an early phase rather than in between the manufacturing process, as more than the 70% of the overall cost are committed after the design phase [41]. Thus, cost modelling and estimation are indispensable to the development of price competitive composites.

From a material point of view, one of the ways to achieve an optimum cost model is through optimizing not only the used fabrics but also the lay-up sequence.



## Chapter 3. SEMI- FINISHED PRODUCTS (SFP)

Upcoming stringent regulations on emissions and fuel efficiency are driving the automotive industry towards lightweight vehicle design. Thus, many traditional materials which have served in engineering applications for a long time are being replaced by the so called 'new materials' [23]. These new materials are characterized by a high ratio between the stiffness parameters and the density. Thereby, a higher share of carbon fiber composite materials in vehicle structures is expected. Today not only cover parts or interior parts are made of CFRP but also structural parts like crash elements or doors. Therefore more processes and material combinations are under investigation to identify the best composites from the early stages of prototype up to series production. [16]

In recent years, there has been an increasing interest in textile preform reinforced composites due to their attractive capabilities for a variety of structural applications. The unique mechanics properties of these advanced materials include increased transverse moduli and strength, and improved shear resistance and damage tolerance. Textile preforms also provide dimensional stability and near-net-shape manufacturing capability. [3]

The terms textile structural composites or SFP are used to discern a sort of advanced composites utilizing fiber preforms, for structural application. [8]. Textiles increasing analysis and applicability are due to their unique capacity to be tailored according to the composite performance needs.

The major criteria for deciding on textile preform are:

- In-plane multiaxial reinforcement capability
- Through-thickness reinforcement
- Ability to form different shapes



The selection of the fulfillment of either some or all of the above mentioned features, remains on the processing and end use requirements.

Consequently, performing textile composites require background knowledge of the fabric structure as well as of the involved procedures resulting into the prespecified final product.

The major textile shaping techniques are waving, knitting, stitching and braiding. All of which are able to manufacture either two-dimensional (2D) or three-dimensional (3D) fabrics. Due to the lack of agreement on a common benchmark to differentiate them, [7] a definition is considered. The bound between two-dimensional and three-dimensional textiles is defined as the threshold at which the integrations of yarns in the thickness direction influence considerably the resultant strengthening. Consider, as an example, angle-interlock woven or solid braids, they form packed integrated structures that without a doubt strengthen the fabric on the thickness direction.

Figure 3.1 shows the most commonly 2D textiles and their classification according to the yarn interlacing pattern.

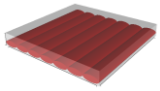
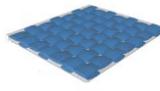
2D TEXTILES					
Veils/Mats	Non-loop-stitched systems			Loop stitched systems	
	NCF	Woven	2D braid	Weft Knit	Warp knit
					

Figure 3.1 2D SFP classification

Today, mainly woven and non-crimp fabrics (NCF) are used in the automotive industry. Hence, the thesis at hand will focus on the material modelling of these



types of reinforcements. In addition, and from a theoretical point of view, prepreg & braiding technology will be introduced.

### 3.1 *WOVEN FABRIC*

---

High cost and the impossibility of having optimum out of-plane mechanical properties, which greatly reduces impact resistance, made unidirectional fabrics not the most favorable option.

The need for a new reinforcement capable of bear high stresses in three directions, crash, impact, energy absorption and multiaxial fatigue, resulted in the emergence of new materials, weaves, following the technique that clothing textile industry has been implementing for decades.

These sort of reinforcement, also known as woven fabric, is produced by interlacing longitudinal yarns, also known as warp ( $0^\circ$ ) fibers, and widthwise yarns, known as weft ( $90^\circ$ ) fibers, over and under each other alternating according to a specified pattern called weave [8]. Weaving pattern (Figure 3.3) has a significant impact on the reinforcement of the mechanical properties, and simultaneously on hand ability since the friction in the interlacing points influences the shearing.

Woven fabrics are characterized by a set of parameters that define or influence, at the same point, their properties:

- Fabric count ( $n_{warp} \times n_{weft}$ ):  $n_{warp}$  denotes that a weft yarn is interlaced with every  $n_{warp}th$  warp yarn, and  $n_{weft}$  vice versa. The present thesis is confined to  $n_{warp} = n_{weft} = n_{ng} = 2$  (Plain woven fabrics)
- Warp & weft linear density



- Areal weight [ $g/m^2$ ]
- Crimp: Undulation angle in between tows. Stellbrink estimated the angle  $\Omega_{weft}$  as:

$$\Omega_{weft} = \arcsin[l_{0,warp}/(l_{0,warp}^2/h_{warp} + h_{matrix}) + (h_{warp} + h_{matrix})] \quad (3.1)$$

Where,

$h_{warp}$ : warp yarn height

$h_{matrix}$ : matrix height

$l_{0,warp}$ : yarn density in warp direction

- Spacing
- Weave pattern

Relative to the weave pattern, identifiable by the amount of warp fibers that each weft interlace with, three common styles can be distinguished, either plain, twill or satin Figure 3.2.

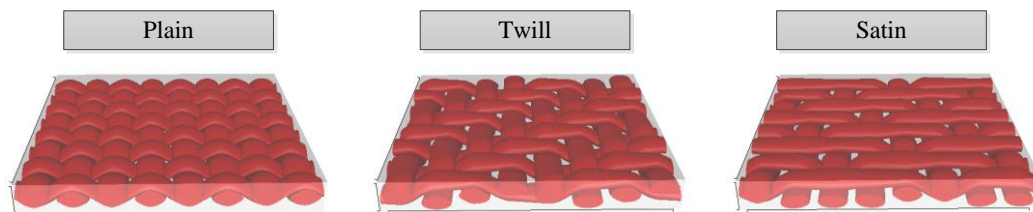


Figure 3.2 Weave pattern styles

Due to the crimp, plain weave shows the lowest mechanical properties, as the fibers are not directly aligned to the load. On the other hand, given the density of crossing points, damage tolerance and impact resistance values have been shown to be greater than those on the other styles [32]. Plain weave is general restricted for heavy fabrics given the over crimp that arise when using large fibers (high tex).

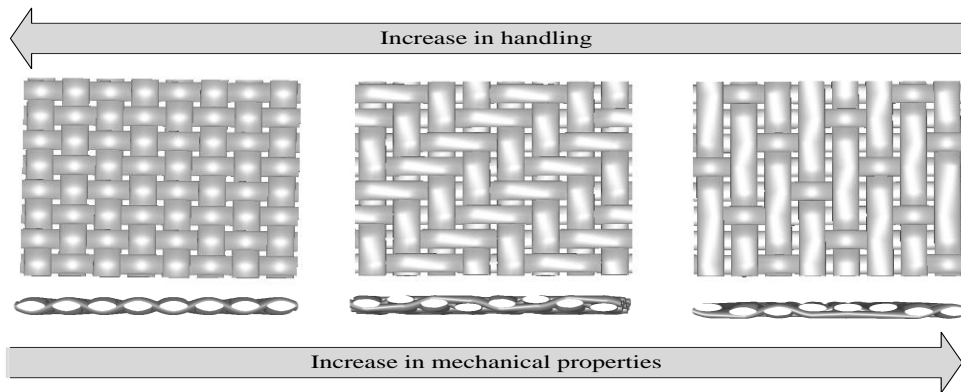


Figure 3.3 Woven comparison

As seen above, a decrease in the number of warp and weft intersections causes a decrease in the fabric stability and crimp along with an increase on the textile drapability.

A summary of the main differences between each one of the aforementioned styles can be founded on the following table:

Table 3.1 Properties Comparison [28]

	Plain	Twill	Satin
Good stability	+	0	-
Good drapability	-	+	++
Low porosity	0	+	++
Smoothness	-	0	++
Balance	+	+	-
Symmetrical	++	0	--
Low crimp	-	0	++



In order to reduce crimp influence and enhance mechanical properties, spread tow fabrics have been lately developed and introduced in the CFRP markets [47] [21]. These special tows enable thinner laminates and reductions in tandem undulations Figure 3.4. Lower crimp leads to an easing of excess matrix in the laminate which in turn also reduces the weight up to 20% percent. In Table 3.2, example values from the literature [28] illustrate the role played by crimp.

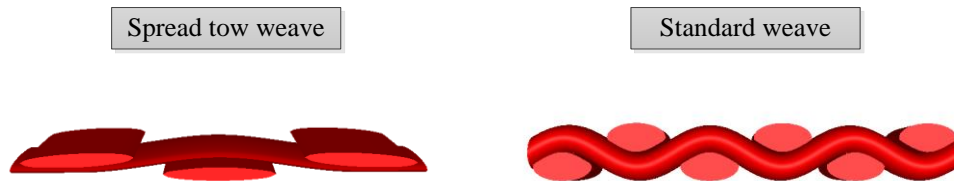


Figure 3.4 Spread vs. standard

Table 3.2 Mechanical properties comparison

	Tensile Strength (MPa)	E-Modulus (GPa)	Ultimate Strain
Spread Tow	928	73	1.3
3 K	820	71	1.2
12 K	807	61	1.3

### 3.1.1 WOVEN MECHANICAL PROPERTIES

---

The use of woven materials is increasing due to their symmetric and balanced properties, the ease of manufacturing and handling, and the greater impact their



properties. Hence, an accurate estimation of mechanical properties is of importance for structural composites designs where there are tough requirements to meet.

Methods for predicting the mechanical properties of 2D fabrics are more complex than those for laminated composites due to the presence of non-straight fibers presence. Therefore, both micro- and mesoscale analysis must evolve.

Several models for prediction of the above named elastic properties have been proposed in the last decades. They are based mainly in homogenization schemes that simplify the microstructure consisting of a repeating cell, representative volume element (RVE), that stand for the smallest representative unit of the fabric. RVE for different patterns are shown in Figure 3.5.

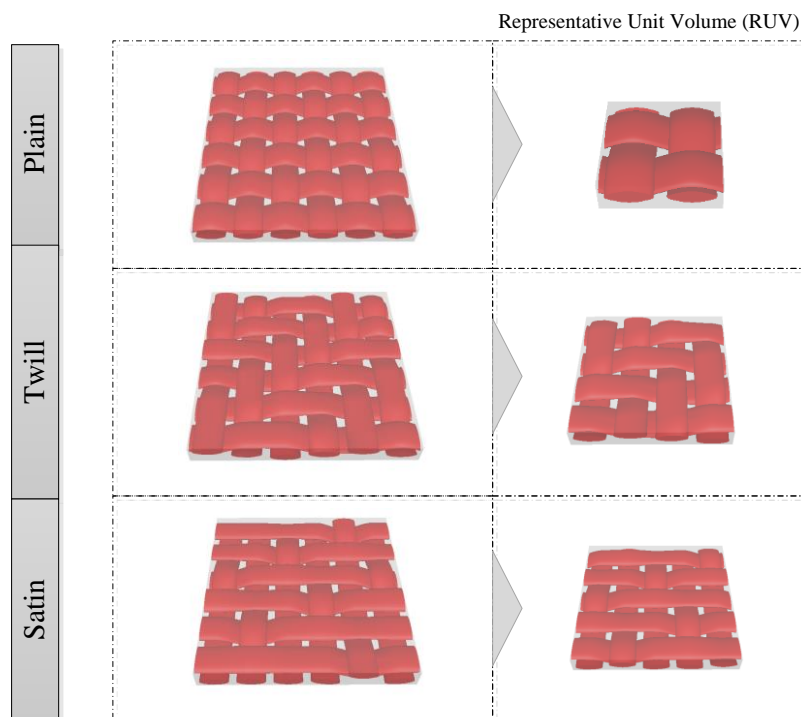


Figure 3.5 RVE Examples



An overview of some of the analytical models that can be used to predict the laminated composites mechanical properties are presented. Chou and Ishikawa [7] provided three one-dimensional models, namely Mosaic Model, Crimp Model and Bridging Model. All these methods make use of the CLT to derive the effective elastic properties. They will be explained in the following sections. Other 2D models were developed by Naik et al. to predict the properties of plain woven fabrics using CLT and incorporating undulation and fiber continuity in both warp and weft directions. Naik et al. also developed two 2D orthogonal models, namely, the Element Array Model (EAM) and the Slice Array Model (SAM), to predict the on axis elastic properties based on a unit cell. Additional models were developed for specific fiber architectures. Karayaka et al. introduced a micromechanics model for satin weaves, incorporating the variation on the weave parameters and loading directions.

### ***3.1.1.1 ROM & Halpin-Tsai***

In view of material mechanical behavior, two approaches are widely used: Rule of Mixtures (ROM) and Halpin-Tsai. The basic assumptions considered in both stated methods are: both matrix and fiber are linearly elastic, homogeneous and isotropic, fibers are perfectly aligned and distributed through the free void matrix, and, lastly, fiber and matrix bend together in perfect concordance.

Based on the fiber and resin volume fractions, and ignoring fiber crimp and weave, the rule of mixtures method, determines the plain woven elastic properties as in the case of unidirectional (UD) laminas by homogenization approaches.

A simple estimation for the longitudinal, transverse modulus ( $E_1, E_2$ ) and the Poisson's ratios are computed as follows:

$$E_1 = E_2 = 0.5 \cdot V_f \cdot (E_{1f} + E_{2f}) + E_m \cdot (1 - V_f) \quad (3.2)$$



$$\nu_{12} = \nu_{21} = 0.5 \cdot V_f \cdot (\nu_{12f} + \nu_{21f}) + \nu_m \cdot (1 - V_f)$$

Where  $E_{1f}$  is the fiber longitudinal modulus,  $E_{2f}$  is the fiber transverse modulus,  $E_m$  is the matrix modulus,  $V_f$  fiber volume,  $\nu_{12f}$  and  $\nu_{21f}$  are the fiber major and minor Poisson's ratio and  $\nu_m$  is the matrix Poisson's ratio. The factor 0.5 is due to the equal amount of fibers in warp and weft directions. Nevertheless, in order to apply a generalized rule of mixtures for further types of reinforcement, a corrective coefficient was introduced by [25]:

$$E = \eta_L \cdot \eta_o \cdot (E_{1f} + E_{2f}) \cdot V_f + E_m(1 - V_f) \quad (3.3)$$

With  $\eta_L$  as a length correction factor that typically takes the value of  $\eta_L \approx 1$  for fibers longer than 10 mm. On the other hand,  $\eta_o$ , non-unidirectional reinforcement correction factor, considers values from zero to one, with one representing unidirectional fabrics, in the same orientation as the load, while zero expresses lesser share of fibers line up in direction of the load . Some usual values are:

Table 3.3  $\eta_o$  typical values

	$\eta_o$
Unidirectional	1.0
Biaxial	0.5
Biaxial at $\mp 45^\circ$	0.25
Random (in plane)	0.375
Random (3D)	0.20



Finer solutions are obtained in case of taking into consideration yarn longitudinal properties:

$$E_1^y = V_f \cdot E_{1f} + E_m \cdot (1 - V_f) \quad (3.4)$$

The rule of mixtures estimates accurately the longitudinal modulus. However, applying Halpin-Tsai equation one can obtain finer solutions for the transverse modulus:

$$E_{2y} = \frac{(1 + \xi \cdot \eta \cdot V_f) \cdot E_m}{1 - \eta \cdot V_f} \quad (3.5)$$

Where  $\eta = \frac{E_{2f}/E_m - 1}{E_{2f}/E_m + \xi}$ .  $\xi$  acquire different values depending on the fibers geometry, packing and loading. Halpin and Tsai [24] obtained veracious agreement with results for circular fibers in a square assemblage when  $\xi = 2$  was used for the estimation of  $E_{2y}$  and  $\xi = 1$  in the following calculation of  $G_{12}^y$ :

$$G_{12}^y = G_m \cdot \frac{(G_{12f} + G_m) + V_f \cdot (G_{12f} - G_m)}{(G_{12f} + G_m) - V_f \cdot (G_{12f} - G_m)} \quad (3.6)$$

In which  $G_{12f}$  and  $G_m$  are fibers and matrix shear modulus, respectively. Similarly, the mayor and minors Poisson's ratios can also be calculated via Halpin-Tsai equations:

$$v_{12}^y = V_f \cdot v_{12f} + v_m(1 - V_f) \quad (3.7)$$

$$v_{21}^y = v_{12}^y \cdot \frac{E_2^y}{E_1^y} \quad (3.8)$$



Lastly, the elastic properties for a single ply are determine according to rule of mixtures homogenization method.

$$E_1 = E_2 = 0.5 \cdot (E_1^y + E_2^y) \quad (3.9)$$

$$v_{12} = v_{21} = 0.5 \cdot (v_{12}^y + v_{21}^y) \quad (3.10)$$

The results obtained have led to a first rough estimation of the different singly-ply elastic properties. However, in order to achieve preferable values, more involved models need to be applied.

### 3.1.1.2 Mosaic model

Developed by Chou in the earlies 1980s, this method idealizes the crossover regions as cross-ply laminates, excluding fiber continuity and undulation in the interlacing points and using the CLT as a theoretical basis Figure 3.6.

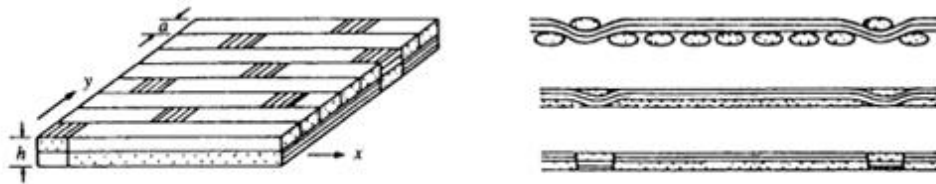


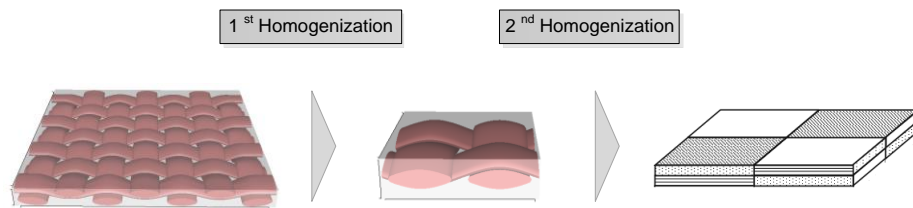
Figure 3.6 Idealization of the mosaic model

In general, a textile idealize by the mosaic model can be accounted as an assemblage of asymmetric cross-ply laminates.

In order to obtain the elastic stiffness constants of a woven fabric, the consequent procedure is followed: [9]



1. Lamina homogenization. Procedural simplifications have to be made. In first place, the representative unit volume is exclusively considered, since a woven fabric is assumed symmetrical. On a second level of homogenization, sub cells are view as cross-ply laminates.



2. Sub cell properties estimation. Cross-ply laminates are assumed to be comprise of two orthogonal unidirectional plies [44] half the thickness of the woven lamina,  $h/2$ .

As a reminder, Q-Matrix of a UD lamina which has orthotropic symmetry is:

$$Q_{ij} = \begin{bmatrix} E_{11}/D_v & \nu_{12} \cdot E_{22}/D_v & 0 \\ \nu_{12} \cdot E_{11}/D_v & E_{22}/D_v & 0 \\ 0 & 0 & G_{12} \end{bmatrix} \quad (3.11)$$

Where  $D_v = 1 - \nu_{12} \cdot \nu_{21}$ .  $E_{11}$  and  $E_{22}$  are the Young's moduli,  $G_{12}$  is the in-plane shear modulus, and  $\nu_{12}$  denotes the Poisson's ratio.

From Equation 3.12 and Equation 2.7 the stiffness constants from a cross-ply laminate can be derived:

$$\begin{aligned} A_{11} &= (E_1 + E_2) \cdot h/2 \cdot D_v & D_{66} &= G_{12} \cdot h^3 / 12 \\ A_{12} &= \nu_{12} \cdot E_2 \cdot h/D_v & D_{12} &= \nu_{12} \cdot E_2 \cdot h^3 / 12 \cdot D_v \end{aligned}$$



$$\begin{aligned}
 A_{66} &= G_{12} \cdot h & D_{11} &= D_{22} = (E_1 + E_2) \cdot h^3/24 \cdot D_v & (3.12) \\
 A_{11} &= A_{22} & B_{11} &= -B_{22} = (E_1 - E_2) \cdot h^2/8 \cdot D_v
 \end{aligned}$$

In terms of stress and strains, extension  $A_{ij}$ , bending-extension coupling  $B_{ij}$ , and bending  $D_{ij}$  stiffnesses are calculated relative to the midplane by applying:

$$\begin{Bmatrix} \varepsilon_0 \\ \kappa \end{Bmatrix} = \begin{bmatrix} A & B \\ B & D \end{bmatrix}^{-1} \begin{Bmatrix} N \\ M \end{Bmatrix} \quad (3.13)$$

$$\begin{bmatrix} N_1 \\ N_2 \\ N_6 \end{bmatrix} = \begin{bmatrix} A_{11} & A_{12} & 0 \\ A_{21} & A_{11} & 0 \\ 0 & 0 & A_{66} \end{bmatrix} \cdot \begin{bmatrix} \varepsilon_1^0 \\ \varepsilon_2^0 \\ \varepsilon_3^0 \end{bmatrix} + \begin{bmatrix} B_{11} & 0 & 0 \\ 0 & -B_{11} & 0 \\ 0 & 0 & 0 \end{bmatrix} \cdot \begin{bmatrix} \kappa_1 \\ \kappa_2 \\ \kappa_3 \end{bmatrix} \quad (3.14)$$

$$\begin{bmatrix} M_1 \\ M_2 \\ M_6 \end{bmatrix} = \begin{bmatrix} B_{11} & 0 & 0 \\ 0 & -B_{11} & 0 \\ 0 & 0 & 0 \end{bmatrix} \cdot \begin{bmatrix} \varepsilon_1^0 \\ \varepsilon_2^0 \\ \varepsilon_3^0 \end{bmatrix} + \begin{bmatrix} D_{11} & D_{12} & 0 \\ D_{12} & D_{11} & 0 \\ 0 & 0 & D_{66} \end{bmatrix} \cdot \begin{bmatrix} \kappa_1 \\ \kappa_2 \\ \kappa_3 \end{bmatrix} \quad (3.15)$$

3. Average strain and stress values of the unit cell, together with the effective stiffness constant matrices that correlate them, are obtained by assembling asymmetric cross-ply laminates. Two methodologies based upon either iso-stress or iso-strain assumption are able to estimate these constants:

- a. Series model: Cross-ply laminates are displaced in series along the loading direction (
- b. Figure 3.7). Strain is assumed to remain constant (Iso-strain assumption), neglecting the disturbance of stress and strain close to the interface. Iso-strain assumption leads to the definition of average midplane strain and curvature, which results in upper bounds of the compliance constants. Lower bounds are then determined by the inverse of the compliance constant matrix.

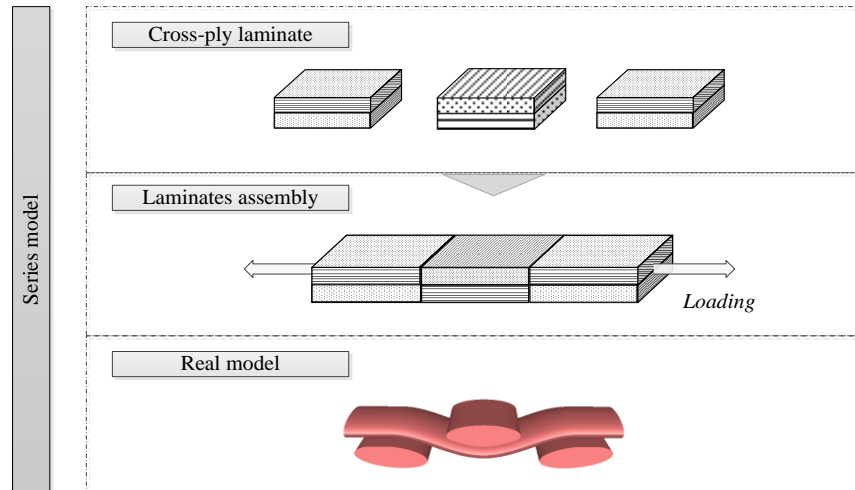


Figure 3.7 Series-model flowchart

- c. Parallel model: On the other hand, this approach assembles the cells parallel to the loading direction. (Iso-stress assumption- See figure below)).

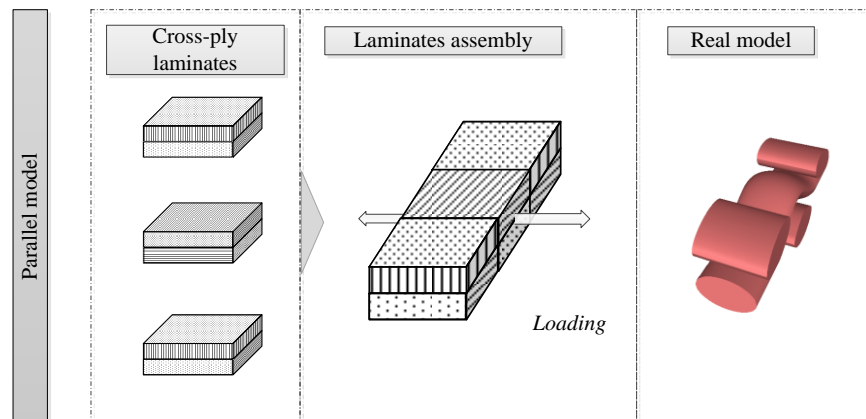


Figure 3.8 Parallel-model flowchart

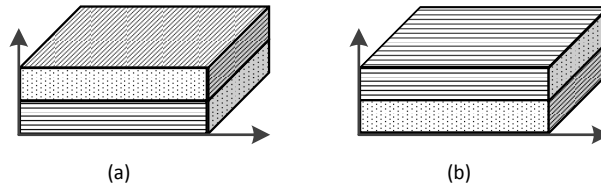
Uniform state of strain,  $\epsilon^0$ , and curvature,  $\kappa$ , is assumed in the laminate midplane. Assumption that gives rise to stress and overall moment's definition, and consecutively to the upper bound of the stiffness constants. As proceed with the series model, lower bounds are obtained by considering the inverse of stiffness constant matrix.



Average stress resultant,  $\bar{N}$ , and moment,  $\bar{M}$ , are related with strain,  $\varepsilon^0$ , and curvature,  $\kappa$ , within the RUV, through the matrix  $\bar{A}_{ij}$ ,  $\bar{B}_{ij}$  and  $\bar{D}_{ij}$ .

$$\begin{aligned}\bar{A}_{ij} &= A_{ij} \\ \bar{B}_{ij} &= \left(1 - \frac{2}{n_g}\right) B_{ij}^L \\ \bar{D}_{ij} &= D_{ij}\end{aligned}\tag{3.16}$$

The factor  $\left(1 - \frac{2}{n_g}\right)$  appears because the element  $B_{11}$  for the interlaced regions ( $B_{11}^T$ ) and non-interlaced ( $B_{11}^L$ ) have opposite signs,  $B_{11}^T = -B_{11}^L$ . Note that  $B_{11}^L$  is the term for a cross-ply laminate where the upper surface is orientated in the load direction (Figure (a)). On the other hand,  $B_{11}^T$  (Figure (b)), is the term for a cross-ply laminate with inverted order of plies.



In the case of plain woven fabrics, these matrices are derived directly [48] from the cross-ply laminate ones,  $A_{ij}$ ,  $B_{ij}$ ,  $D_{ij}$  [48]:

$$\begin{aligned}\bar{A}_{ij} &= A_{ij} \\ \bar{B}_{ij} &= 0 \\ \bar{D}_{ij} &= D_{ij}\end{aligned}\tag{3.17}$$

On the thesis at hand, the parallel model will be the method selected and implemented.



4. Elastic constants. On the basis of the ABD- Matrix, the effective properties of the woven composite are defined by [48]:

$$\begin{aligned} [\bar{a}^*] &= h \cdot [\bar{A}]^{-1} \\ E_1 &= \frac{1}{a_{11}^*} \\ E_2 &= \frac{1}{a_{22}^*} \\ v_{12} = v_{21} &= \frac{-a_{12}^*}{a_{11}^*} \\ G_{12} &= \frac{1}{a_{66}^*} \end{aligned} \quad (3.18)$$

Notice that as  $\bar{A} = A$ , where  $A$  change linearly with respect to the thickness,  $h$ , (see equation 2.13)  $[\bar{a}^*] = h \cdot [\bar{A}]^{-1}$  is independent of  $h$ . Hence, the effective estimated elastic properties of a plain woven fabric are independent of the RVE thickness.

Mosaic results are always overestimated due to the lack of yarn crimp influence in the properties. Furthermore, this outcome may not be so accurate in case of satin weaves, where interlaced regions are not connected. [6]

Owing to the low complexity of the model and the suitable agreement reported with tests, especially regarding woven fabrics, the mosaic model pose a proper first approximation of the fabric mechanical properties. However, modern models provide more accuracy on the results as a consequence of considering crimp.



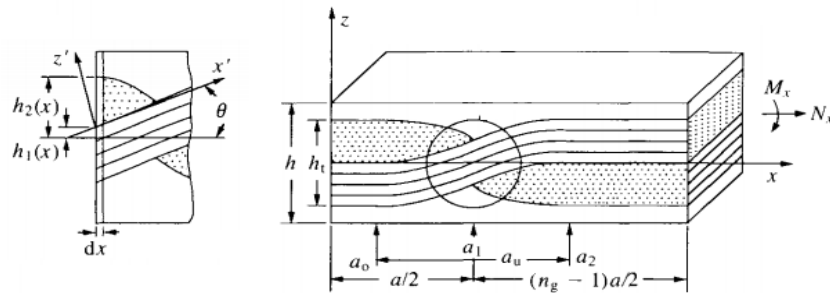
### 3.1.1.3 Crimp model

In contrast to the mosaic model, the crimp model was developed awaiting fiber undulation and continuity. Optimal results are obtained when applied to low  $n_g$  values.

As explained in [6], the weft crimp is represented by the expression:

$$h_1(x) = \begin{cases} 0, & (0 \leq x \leq a_0) \\ \left[1 + \sin \left\{ \left(x - \frac{a}{2}\right) \cdot \frac{\pi}{a_u} \right\}\right] \cdot \frac{h_t}{4}, & (a_0 \leq x \leq a_2) \\ \frac{h_t}{2}, & (a_2 \leq x \leq n_g \cdot \frac{a}{2}) \end{cases} \quad (3.19)$$

Where  $a_0 = (a - a_u)/2$ ,  $a_2 = (a + a_u)/2$  and  $a, a_u, h_t$  are geometrical factor that characterize the crimp, as it is shown in the figure above:



Besides, the warp sectional shape is assumed:

$$h_2(x) = \begin{cases} \frac{h_t}{2}, & (0 \leq x \leq a_0) \\ \left[1 + \sin \left\{ \left(x - \frac{a}{2}\right) \cdot \frac{\pi}{a_u} \right\}\right] \cdot \frac{h_t}{4}, & (a_0 \leq x \leq \frac{a}{2}) \\ - \left[1 + \sin \left\{ \left(x - \frac{a}{2}\right) \cdot \frac{\pi}{a_u} \right\}\right] \cdot \frac{h_t}{4}, & (\frac{a}{2} \leq x \leq a_2) \\ - \frac{h_t}{2}, & (a_2 \leq x \leq n_g \cdot \frac{a}{2}) \end{cases} \quad (3.20)$$



Under the conjecture that CLT is applicable to each of the infinitesimal parts along the  $x$  direction,  $A_{ij}, B_{ij}, D_{ij}$  are calculated as functions of  $x$  ( $0 \leq x \leq a/2$ ) by:

$$\begin{aligned}
 A_{ij}(x) &= Q_{ij}^M \cdot \left[ h_1(x) - h_2(x) + h - \frac{h_t}{2} \right] + Q_{ij}^F(\theta) \cdot \frac{h_t}{2} + Q_{ij}^W \\
 &\quad \cdot [h_2(x) - h_1(x)] \\
 B_{ij}(x) &= \frac{1}{2} \cdot Q_{ij}^F(\theta) \cdot \left[ h_1(x) - \frac{h_t}{4} \right] \cdot h_t + \frac{1}{4} \cdot Q_{ij}^W \cdot [h_2(x) - h_1(x)] \cdot h_t \\
 D_{ij}(x) &= \frac{1}{3} \cdot Q_{ij}^M \cdot \left\{ \left[ h_1(x) - \frac{h_t}{2} \right]^3 - h_2^3(x) + \frac{h^3}{4} \right\} + \frac{1}{3} \cdot Q_{ij}^F(\theta) \\
 &\quad \cdot \left[ \frac{h_t^3}{8} - 3 \cdot h_t^2 \cdot \frac{h_1(x)}{4} + 3 \cdot h_t \cdot \frac{h_1^2(x)}{2} \right] + \frac{1}{3} \cdot Q_{ij}^W \\
 &\quad \cdot [h_2^3(x) - h_1^3(x)]
 \end{aligned} \tag{3.21}$$

Where the superscripts  $M, F, W$  signify matrix, weft and warp, respectively, and

$$\theta = \arctan \left( \frac{dh_1(x)}{dx} \right) \tag{3.22}$$

Similar expression can be repeated for  $a/2 \leq x \leq n_g \cdot a/2$ .

On the other hand,  $Q_{ij}^F(\theta)$ , mention above, is estimated as a function of  $\theta(x)$  as follows:

$$Q_{ij}^F(\theta) = \begin{bmatrix} E_{xx}^F(\theta)/D_v & E_{xx}^F(\theta) \cdot v_{yx}^F(\theta)/D_v & 0 \\ E_{xx}^F(\theta) \cdot v_{yx}^F(\theta)/D_v & E_{yy}^F(\theta)/D_v & 0 \\ 0 & 0 & G_{xy}^F(\theta) \end{bmatrix} \tag{3.23}$$

Where  $i, j = 1, 2, 6$  and  $D_v = 1 - \left( v_{yx}^F(\theta) \right)^2 \cdot E_{xx}^F(\theta) / E_{yy}^F(\theta)$ .



By replacing Equation 2.24 in Equation 2.22, local plate stiffness constants can be determined. In last term, the compliance constants, are evaluated inverting the stiffness constants as follows:

$$\begin{aligned} \bar{A}'_{ij} &= \left(1 - \frac{2 \cdot a_u}{n_g \cdot a}\right) A'_{ij} + \frac{2}{n_g \cdot a} \cdot \int_0^{n_g \cdot a/2} A'_{ij}(x) dx \\ \bar{B}'_{ij} &= \left(1 - \frac{2}{n_g}\right) B'_{ij} + \frac{2}{n_g \cdot a} \cdot \int_{a_0}^{a_2} B'_{ij}(x) dx \\ \bar{D}'_{ij} &= \left(1 - \frac{2 \cdot a_u}{n_g \cdot a}\right) D'_{ij} + \frac{2}{n_g \cdot a} \cdot \int_{a_0}^{a_2} D'_{ij}(x) dx \end{aligned} \quad (3.24)$$

Based on Table 2.4, where an overview with Tsai- Chou approaches is illustrated, it is concluded that due to the aim of implementing a model that emerges computationally fast when optimizing various material and wherein a lot of input effort is not required, mosaic model should be chosen.

Table 3.4 Tsai-Chou approaches comparison

	Mosaic model	Crimp Model	Bridging Model
Consider undulation	✘	✔	✔
Used for	Plain	Low $n_g$	Satin
Input	Warp & Weft mechanical properties	Warp & Weft mechanical properties, crimp & RUV dimensions	Warp & Weft mechanical properties, crimp & RUV dimensions



Disadvantages	Overestimated mechanical properties	Reduced use	High load of input data.
---------------	-------------------------------------	-------------	--------------------------

### 3.1.1.4 Cross-ply approach

Lastly, it is to remarked, due to their lack of complexity, one last simple method. The cross-ply method reproduces woven fabrics as two plies orthotropic laminates. [27]. They are assumed to behave as the composition of two UD, which have been pile together with their fibers, equal number in each orientation, in perpendicular direction Figure 3.9)

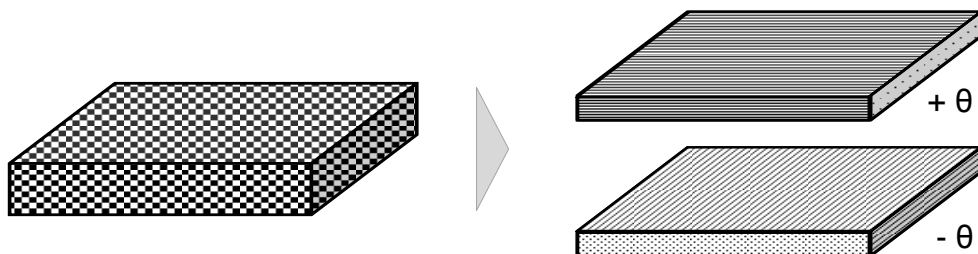


Figure 3.9 Cross-ply model

Hence, the stiffness matrix is calculated as follows:

$$Q_{ij}^{woven} = \frac{1}{2} \cdot \left[ (\overline{Q}_{ij})_{\theta} + (\overline{Q}_{ij})_{-\theta} \right] \quad (3.25)$$

$(\overline{Q}_{ij})_{\theta}$  and  $(\overline{Q}_{ij})_{-\theta}$  are defined as the stiffness matrices of plies oriented in  $\theta$  and  $-\theta$  directions, respectively. Applying Equation 3.26 we obtain:



$$Q_{ij}^{woven} = \begin{bmatrix} Q_{11}^{woven} & Q_{12}^{woven} & Q_{16}^{woven} \\ Q_{12}^{woven} & Q_{22}^{woven} & Q_{26}^{woven} \\ Q_{16}^{woven} & Q_{26}^{woven} & Q_{66}^{woven} \end{bmatrix} \quad (3.26)$$

With:

$$\begin{aligned} Q_{11}^{woven} &= c^4 \cdot Q_{11} + s^4 \cdot Q_{22} + 2 \cdot c^2 \cdot s^2 \cdot (Q_{12} + 2 \cdot Q_{66}) \\ Q_{22}^{woven} &= s^4 \cdot Q_{11} + c^4 \cdot Q_{22} + 2 \cdot c^2 \cdot s^2 \cdot (Q_{12} + 2 \cdot Q_{66}) \\ Q_{12}^{woven} &= c^2 \cdot s^2 \cdot (Q_{11} + Q_{22} - 4 \cdot Q_{66}) + (c^4 + s^4) \cdot Q_{12} \\ Q_{66}^{woven} &= c^2 \cdot s^2 \cdot (Q_{11} + Q_{22} - 2 \cdot Q_{12}) + (c^2 - s^2) \cdot Q_{66} \\ Q_{16}^{woven} &= Q_{26}^{woven} = 0 \end{aligned} \quad (3.27)$$

Where  $c = \cos \theta$  and  $s = \sin \theta$ .

Results obtained using cross-ply method were overestimated, mainly due to the fact that no crimp was considered. This means that different patterns of woven fabrics will lead to the same values of the mechanical properties.

### 3.1.2 WOVEN FABRIC FAILURE MODE

---

Due to the complex architecture of weave fabrics that lead to elastic properties estimation, especial attention need to be paid in order to understand the fabric limits, what the maximum load that a certain fabric can resist until it starts losing their capacities or until it finally breaks. All these circumstances are reflected when analyzing failure modes.

Although numerous techniques have been used to predict woven stiffness properties, there are only a few of them have been develop to predict the strength of textiles composites. Dow und Ramnath [12] assumed a linear undulation path



for warp and fills yarns when modelling woven fabrics. They computed constituent fiber and matrix stresses from local stresses, which were estimated under iso-strain assumption and predicted failure based on the fiber and resins average stresses along with a maximum stress criterion.

R.A.Naik [34] developed a general approach for the prediction of failure initiation, damage progression and strength of 2D woven composites, including the effects of non-linear shear and material response. Naik predicted failure within the RUV discretizing the yarns into slices and averaging the stresses over the RUV volume, in order to estimate the main stiffness matrix. Failure was predicted at each sequential step of the analysis, using the accumulative stresses in each yarn slice together with applicable failure modes.

Notice that HASHIN and PUCK failure modes were designed for Uni-directional fibers and, hence, they cannot be applied to woven fabrics.

The fact that we consider homogenization methods to estimate woven fabrics properties, allow the application of laminated composite failures approaches to the local strains within the yarn, avoiding the consideration of interface delamination within the RUV.

The present thesis will attempt to introduce a progressive structural failure mode that account for failure within the yarns with reasonable noncomplex assumptions. A quadratic failure criterion is applied to the local strains along with a strength and stiffness reduction to judge damage within the yarns.

As consider in the mosaic model, in between RUC, each yarn is treated locally as unidirectional laminates with transversely isotropic mechanical properties. Tsai-Wu failure mode [48] was selected to determine the progressive degradation of yarns strength and stiffness. Thereby, mainly five basic material strengths are account (see following Table):



Table 3.5 Yarn Strengths for Tsai-Wu failure mode

$X_t$	Tensile Strength in the fiber direction
$X_c$	Comprehensive Strength in the fiber direction
$Y_t$	Tensile Strength in the transverse direction
$Y_c$	Comprehensive Strength in the transverse direction
$S$	In-plane longitudinal shear strength

Tsai-Wu quadratic criterion in strain space can be expressed as a function from material strengths and  $\varepsilon_0$ . Where  $\varepsilon_0 = [\varepsilon_1 \ \varepsilon_2 \ \varepsilon_3 \ \gamma_{23} \ \gamma_{31} \ \gamma_{12}]$ .

Under the assumptions:

- CLT is applicable locally for the yarns
- Yarn are locally in a state of plane stress
- Kirchhoff hypothesis apply to the local displacement field

The scalar equation in strains can be obtained as follows:

$$G_{ij} \cdot \varepsilon_i \cdot \varepsilon_j + G_i \cdot \varepsilon_i = 1 \quad i = 1,2,6 \quad (3.28)$$

When enlarged:

$$G_{11} \cdot \varepsilon_1^2 + 2 \cdot G_{12} \cdot \varepsilon_1 \cdot \varepsilon_2 + G_{22} \cdot \varepsilon_2^2 + G_{66} \cdot \varepsilon_6^2 + G_1 \cdot \varepsilon_1 + G_2 \cdot \varepsilon_2 = 1 \quad (3.29)$$

Where



$$\begin{aligned}G_{11} &= F_{11} \cdot Q_{11}^2 + 2 \cdot F_{12} \cdot Q_{12} \cdot Q_{22} + F_{22} \cdot Q_{22}^2 \\G_{22} &= F_{11} \cdot Q_{12}^2 + 2 \cdot F_{12} \cdot Q_{12} \cdot Q_{22} + F_{22} \cdot Q_{22}^2 \\G_{12} &= F_{11} \cdot Q_{12} \cdot Q_{11} + F_{12} \cdot (Q_{11} \cdot Q_{22} + Q_{12}^2) \\G_{66} &= F_{66} \cdot Q_{66}^2 \\G_1 &= F_1 \cdot Q_{11} + F_2 \cdot Q_{12} \\G_2 &= F_1 \cdot Q_{12} + F_2 \cdot Q_{22}\end{aligned} \tag{3.30}$$

On the other hand, strength parameters [F] are given by:

$$\begin{aligned}F_{11} &= \frac{1}{X_t \cdot X_c} & F_1 &= \frac{1}{X_t} - \frac{1}{X_c} \\F_{22} &= \frac{1}{Y_t \cdot Y_c} & F_2 &= \frac{1}{Y_t} - \frac{1}{Y_c} \\F_{66} &= \frac{1}{S^2}\end{aligned} \tag{3.31}$$

In the Tsai-Wu criterion, due to the complexity on performing combined stress-tests,  $F_{12}$  is normalized by:

$$F_{12} = \frac{F_{12}^*}{\sqrt{X_t \cdot X_c \cdot Y_t \cdot Y_c}} \tag{3.32}$$

On this study, a default von Mises value  $F_{12}^* = -1/2$  is implemented. The reduced stiffness for each of the yarns in local coordinate system can be obtained from Equation 2.12.



### 3.1.2.1 Material degradation model

Once Tsai-Wu criterion is formulated according to material local strains and reduced stiffnesses in each yarn, failure is detected if Equation 3.29 is not verified or exceeds the value.

Two failure modes associated with the local yarn degradation are defined:

- If  $\varepsilon_2 > 0$ , and there are no prior yarn failure  $\rightarrow$  MATRIX FAILURE  
+ material transverse strength and stiffness degradation
- If  $\varepsilon_2 < 0$ , or there a prior yarn failure has occurred  $\rightarrow$  FIBER FAILURE + material axial stiffness degradation

A matrix failure can precede a fiber failure but fiber failure is just allowed once per yarn. The second fiber failure within a yarn, is interpreted as ultimate failure. There by, just four different situations are possible. Either matrix failure, single fiber failure, matrix failure followed by a fiber failure (ultimate failure) or non-failure states are distinguished.

Owing to the plain woven RUV symmetry, the two warp yarns, and respectively, the weft yarns, are in the same failure state, allowing the simplicity of the RUV to one warp/weft.

As suggested by Tsai [48], to degrade the stiffness and strengths, the empirical constants used in his model are appraise. Their values are found in table

Table 3.6 Empirical degradation constants

	Empirical Constant	Value
Matrix degradation factor	$E_m^*$	0.15
Fiber degradation factor	$E_f^*$	0.01
Stress partitioning parameter I	$\eta_2$	0.5161



Stress partitioning parameter II	$\eta_{12}$	0.3162
Axial compressive strength reduction	$n$	0.1

A modified rule of mixtures is used to determine both matrix and fiber degraded properties:

$$\begin{aligned} \frac{1}{E_2^{degraded-m}} &= \frac{1}{(1 + v_2^*)} \cdot \left[ \frac{1}{E_{f2}} + \frac{v_2^*}{E_m \cdot E_m^*} \right] \\ \frac{1}{G_{12}^{degraded-m}} &= \frac{1}{(1 + v_{12}^*)} \cdot \left[ \frac{1}{G_{f12}} + \frac{v_{12}^*}{E_m \cdot E_m^*} \right] \end{aligned} \quad (3.33)$$

$$\begin{aligned} \frac{1}{E_2^{degraded-f}} &= \frac{1}{(1 + v_2^*)} \cdot \left[ \frac{1}{E_{f2}} + \frac{v_2^*}{E_m \cdot E_f^*} \right] \\ \frac{1}{G_{12}^{degraded-f}} &= \frac{1}{(1 + v_{12}^*)} \cdot \left[ \frac{1}{G_{f12}} + \frac{v_{12}^*}{E_m \cdot E_m^*} \right] \end{aligned}$$

Where  $E_m, G_m, E_{f2}, G_{f12}$  are matrix moduli and transverse fiber moduli, respectively. In addition,  $v_{12}^*$  and  $v_2^*$ , are obtained from the stress partitioning parameters and the overall fiber volume fraction,  $V_f$ :

$$v_2^* = \eta_2 \cdot \frac{1 - V_f}{V_f} \quad v_{12}^* = \eta_{12} \cdot \frac{1 - V_f}{V_f} \quad (3.34)$$

Axial compressive strength degradation is given by:

$$X_c^{degraded-m} = X_c \cdot \left( \frac{G_{12}^{degraded-m}}{G_{12}} \right)^n \quad (3.35)$$



$$X_c^{degraded-f} = X_C \cdot \left( \frac{G_{12}^{degraded-f}}{G_{12}} \right)^n$$

It must also be considered, the reduction in the Tsai-Wu interaction term after failure:

$$F_{12}^{*degraded-m} = E_m^* \cdot F_{12}^* \quad F_{12}^{*degraded-f} = E_f^* \cdot F_{12}^* \quad (3.36)$$

In conclusion, in case the matrix or the fiber fails, degraded stiffness and strengths must be determined.

### 3.2 *NON-CRIMP FABRICS (NCF)*

---

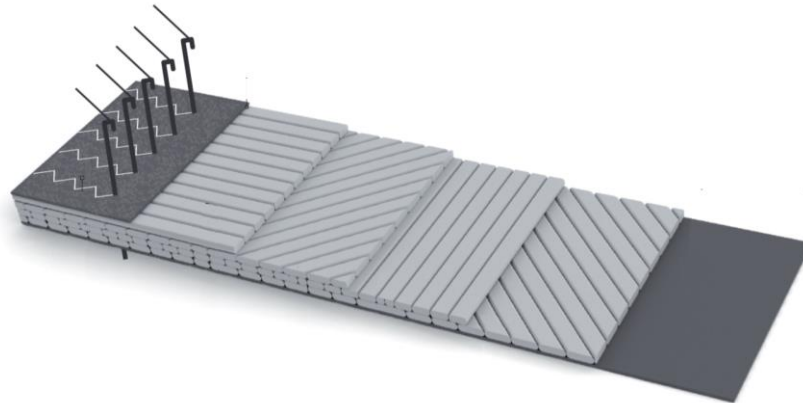
NCF are defined as a laminate composed of unidirectional fibers orientated under different angles, fix by woven threads or chemical binders. The two advantages over woven fabrics are the improved mechanical properties, primarily from the fact that the fibers are always straight and non-crimped, and in second place, the improved component build speed based on the possibility of manufacturing thicker fabrics with multiple fiber orientations, avoiding multiple layers lay-up. NCFs can reach 5-20 % higher strengths and stiffness than woven fabrics [SCHU05, pg.61]

Due to the different fiber orientations and the lack of interlacing points, NCF eases draping although it can be restrained by the amount of stitch. Furthermore, NCF layers with a +/- 45° orientation don't cause that much cutting scrap as cutting these layers out of a normal 0/90° fabric.

On the other hand, NCF manufacturing processes can be slow and with a high machinery and fibers cost as low tex fibers are required to get good surface



coverage for the low weight fabrics. Furthermore, extremely heavy fabrics, which enable incorporating high number of fibers instantly to a component, hinder infusion processes where not automated processes are considered



.Non-crimp fabrics behave as a laminate composed by various plies of unidirectional fabrics, stacked following a specific sequence and orientation. Therefore, NCF mechanical properties can be obtain applying directly CLT. It is assumed that the amount of stitching material compared to the lamina weight is negligible, and for that reason it does not influence on the stack properties.

As an overview, differences between NCF and woven fabrics are shown in Table 3.7.

Table 3.7 Woven vs. NCF

	Advantages	Disadvantages
2D Woven Fabric	<ul style="list-style-type: none"><li>- Good hand ability &amp; impact resistance</li><li>- Highly automated preform</li></ul>	<ul style="list-style-type: none"><li>- Lower mechanical properties (crimp influence)</li></ul>



	manufacturing process	
Non-Crimp Fabric	<ul style="list-style-type: none"> <li>- Good drapability</li> <li>- Good in-plane mechanical properties</li> </ul>	<ul style="list-style-type: none"> <li>- Low out-of-plane properties</li> </ul>

### 3.3 *BRAIDING*

Braiding technology offers the possibility to produce preforms with a near net shape and load-adapted fiber direction. Unlike woven and non-crimp fabrics, where a sequential preforming is required, over braiding is a direct preforming process (Figure 2.4), where owing to the lack of scrap material and the high level of process automation, cost effectiveness is greatly achieved.

As exposed on Figure 3.10, the studied braiding process is based on over braiding mandrels or cores. Due to the high fiber stresses the braid tightly encloses the core, by contrary movements of bovin carriers, giving the preform the form and geometrical stability. For multi-layer preforms, the process can be repeated along the over braid core.

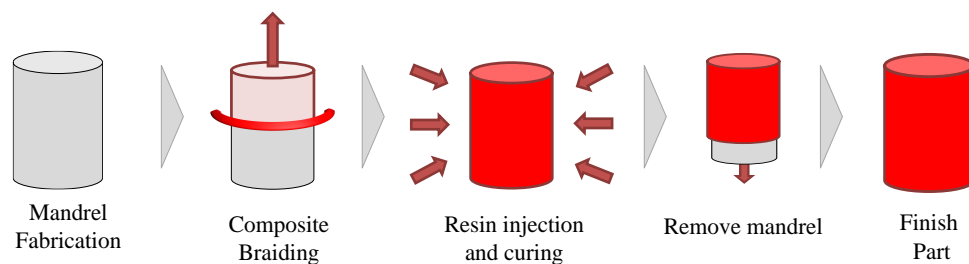


Figure 3.10 Braiding process



As with woven fabrics, braids can be classified depending on the number of fiber directions they cover. Therefore, biaxial (two bias fiber directions), triaxial (three) and unidirectional (UD-one fiber direction) braids can be distinguished in **¡Error!**  
**No se encuentra el origen de la referencia. .**

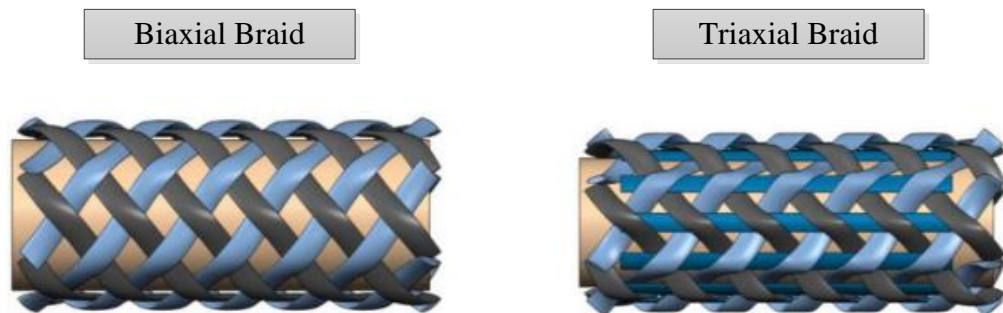


Figure 3.11 Braid styles

Similar to the weave fabrics, braids are conformed following diamond, regular or Hercules patterns, where the braiding angle, angle between the longitudinal axis of the braid and the thread path, is decisive determining their mechanical properties. Other parameter to consider when analyzing braids behavior is the above named, amount of fiber directions. The larger it is, major the number of interlacing points, and hence, lower the mechanical properties, and higher the hand ability.

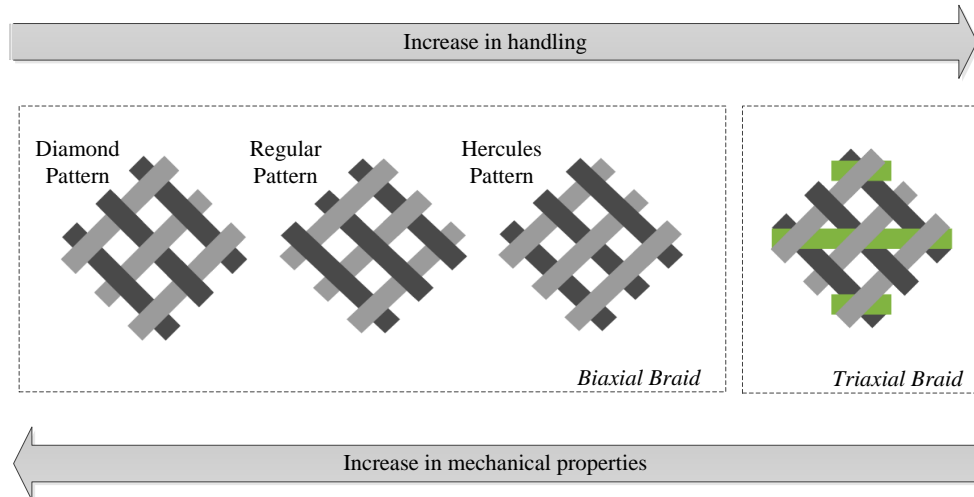


Figure 3.12 Braids mechanical properties

### 3.4 *PREPREGS*

Prepreg are PRE-impREGnated UD tapes or woven fabrics. Woven prepregs are normally used to manufacture curved parts in which material flexibility is , or when designing sandwich structures using honeycomb as a core material. The main disadvantage regards to the high costs of the fabrics, the maximum shelf time of approx. six months under -20 C and the necessity of storing the material in cooled conditions (e.g. -20 C), what means extra costs. Thereby, their use is limited to low productions volume, especially when Class-A surfaces are demanded (Figure 3.13).

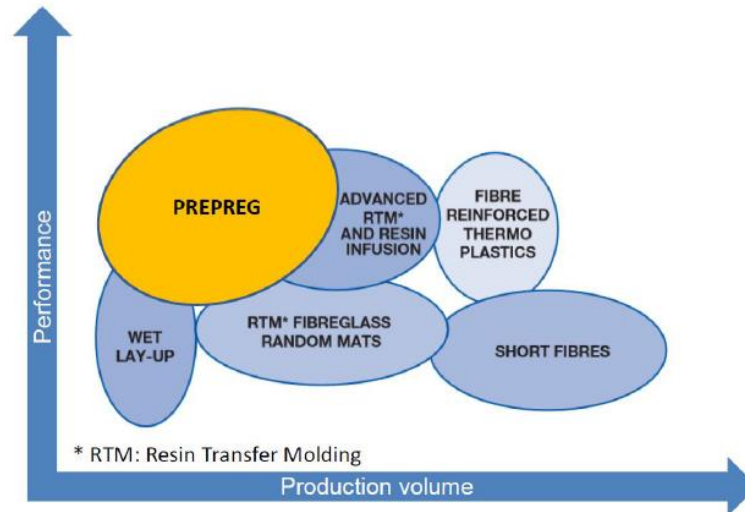


Figure 3.13 Prepreg production volume

On the other hand, they provide more controlled properties, high fiber volumes and higher stiffness and strength properties than other composite materials.

For all the reason mentioned, their use is limited mainly to prototype automobiles, sports car and racing industry; and will not be considered in this study.

The aim of the study is to estimate the elastic properties of SFP parts, in order to optimize, from a material point of view, the overall Body-in-White (BIW) structure of CFRP automobiles when stringent requirements must be fulfilled. Thus, simple analytical models without imploring high-accuracy but lesser time-consuming calculation schemes must be implemented.

### 3.5 *SIMULATION*

Engineering processes and the supporting automotive design software applications must evolve to enable engineers to efficiently make the optimal design choices required to deliver cost-effective, lighter, more fuel-efficient products to market in



a timely manner. In the end, the optimal choice will depend on how much a company is willing to pay for efficiency and performance at a lighter weight. These considerations will help automotive companies achieve the success they need to meet upcoming regulations, creating a competitive advantage.

Although these days a large variety of software specialized in carbon fabrics is available, all failed in offering the user a general program that optimizes the automobile BIW structure from a simultaneously topology, material, manufacturing or assembly point of view. Hence, the aim of the overall program. Nonetheless a brief summary with the most known and used carbon software is hereafter exposed.

### **FIBERSIM (SIEMENS)**

Fibersim provides a digital model that serves as the backbone for the entire automotive composites product development process. Used by Formula one race teams to develop a variety of key composites components, such as chassis, gear box, side pod and double diffuser (floor). Fibersim main advantages are: cost and weight feedback early in the design process, structural and crash performance analysis, multi-layer material simulation, insight into the drapability of non-crimp fabrics (NCF) and other new materials as well as the manufacturing process [43]. Siemens portfolio includes the following modules:

- Composite Engineering Environment
- Advanced Composite Engineering Environment
- Automated Deposition Design
- Analysis Interface
- Composite Viewer
- Fiber Placement Interface
- Flat Pattern Export
- Laser Projection



- Tape Laying Interface
- Ply development
- Material requirement \& optimization

## **WISETEX SUIT**

Depending on the desired study, they have developed different submodules. Below each subgroup is identified with the aim of study:

- Internal geometry and deformability of textiles
  - ✓ WiseTex : Modelling of the structure of the internal structure and deformability of textiles
  - ✓ LamTex : models of textile laminates
  - ✓ WeftKnit : models of weft-knitted structures
  - ✓ FETex : transfer of textile models to FE packages
- Micro-mechanics of textile composites
  - ✓ TexComp : Calculation of stiffness of textile composite using method of inclusions. The reinforcement model should be done with WiseTex
- Permeability of textile composites
  - ✓ FlowTex: calculation pf permeability of textile using finite difference or Lattice Boltzmann solutions of Stokes or Navier-Stokes equations. The reinforcement model should be built with WiseTex

## **PAM-FORM (ESI-GROUP)**

PAM-FORM enables realistic and predictive pre-forming and forming (simulation) of laminated composites. Simulates the entire forming process, allowing engineers to select the most appropriate material, the right tooling design, and the best process parameters. Taking into account the physics of the



forming process, PAM-FORM enables the user to predict manufacturing defects such as wrinkling and to correct these by optimizing the process parameters. It is also available for a wide range of materials such as UD, fabrics, dry textiles, preregs or NCF reinforcement, thermoset and thermoplastic matrix.

### **DIGIMAT**

Digmat is a software platform for material analysis, and it comprises of two base technologies: Digimat MF (Mean-Field homogenization that predicts the nonlinear constitutive behavior of multi-phase composite materials) and Digimat FE (homogenization software based on the nonlinear Finite Element modeling of realistic Representative Volume Elements of complex material microstructures). They are dedicated to composite materials, and can be used for individual materials for the appropriate application.



## Chapter 4. COMPLEXITY

One of the major problems avoiding the inclusion of composites in the automotive industry over conventional materials in mainstream applications is cost, both raw materials and processing. Whence, cost models are decisive when designing CFRP parts in the early design phase.

Cost models for composite materials derive their formulation by identifying the drivers that may play a role on the overall cost of the component. [11, 14, 31]. Therefore, the greater number of cost drivers that may be identified, the higher the accuracy of the cost model.

The major focus of the thesis at hand is to examine material cost drivers under the assumption that cost is directly proportional to manufacturing time, and hence, estimating the influence on time will be sufficient. As an example, cost-driving parameters are for instance those that influence the cycle time. As higher cycle time means higher cost per finished product.

A study on adverse increment of manufacturing time related with the employment of one material or other is here conducted.

Henceforth, when referring to the material influence on the manufacturing chain, the term Material Complexity will be used. Furthermore, it will be defined as the amount of additional effort required to produce a composite part [29] due to the different material structural parameters and manufacturability. Additional effort that is ordinarily not included in manufacturing time estimation equations. Therefore, a new model is developed and implemented in order to estimate the time increment owing to the necessary extra effort.

In order to understand where and when material complexity has a role, the different manufacturing process involved in CFRP production must be analyzed.



However, instead of going through each procedure, it is possible to dissect the considered manufacturing methods into three parts, as show:

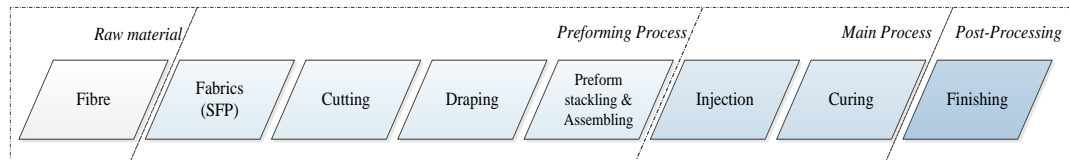


Figure 4.1 Composites manufacturing process

Preforming is one of the most important procedures involved in the manufacturing chain when considering material influence, if not the most. The process can vary from simple, with the cut of the fabrics to advance with the forming of a complex 3D-solid. The impact of the preforming process on the overall cost depends on the complexity of the process.

As appears from the above, the preforming process can be subdivided in three sequential steps:

- Cutting.
- Draping
- Stackling and assembling

Within the above named procedures, material plays a decisive role in draping, as cutting and stackling, commonly are automatized process, where the influence is solved changing the machine set up. As an example, when cutting, the use of stiffer fibers lead to a change on the cutter speed but have no relevant influence neither on time nor cost.

The change of draping time under different materials was reported by [29] where different time estimation equations were proposed according to the reinforcement. (See Figure below)

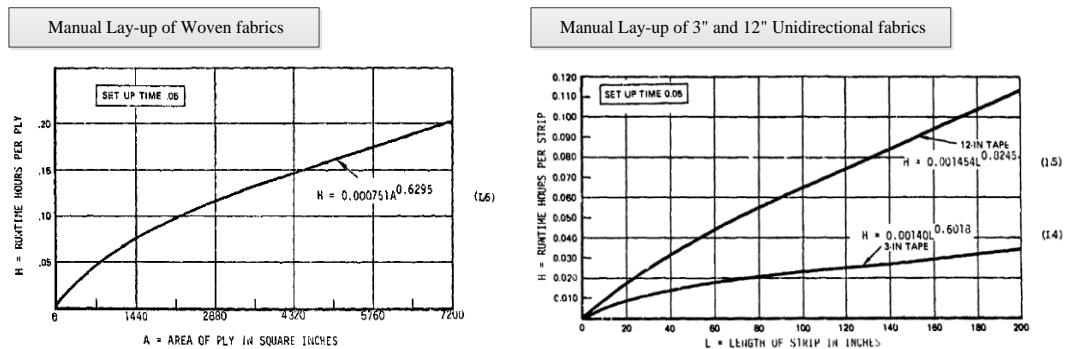


Figure 4.2 Woven and UD lay-up equations

Similarly to the preforming, post-processing is highly dependent on the capability of the process as well as the complexity of the manufactured component. It can be from actual machining of material such as drilling holes to surface painting. However, as we are considering early design phase, post-processing procedures are not in between our object of study.

The main process involves the procedures that regards to the consolidation of the composite final properties, commonly infusion and curing. As curing times are set, a change in material will just lead to a different curing time, but no adverse effect is hereby linked.

On the other hand, infusion has been widely studied, by reason of lack of understanding on flow phenomena. The most discussed of these flow phenomena are permeability variation, fabric compressibility and dynamic viscosity, among others. [18]

A depth analysis on the influencing parameters is shown in Appendix 3.

Hence, the two main procedures to examine in detail, drapability and permeability, are studied below.



## 4.1 DRAPABILITY

In the field of textile reinforcements structures drapability describes the behavior of the textile fabric during the forming process from its flat initial state in a three-dimensional form. The drapability of textiles fabrics is a decisive factor when designing and manufacturing reinforced plastics and therefore vital in manufacturing process of composite parts.

In order to understand the draping process, influencing parameters must be identified (Figure 4.3). Other factors not included are order of draping and temperature.

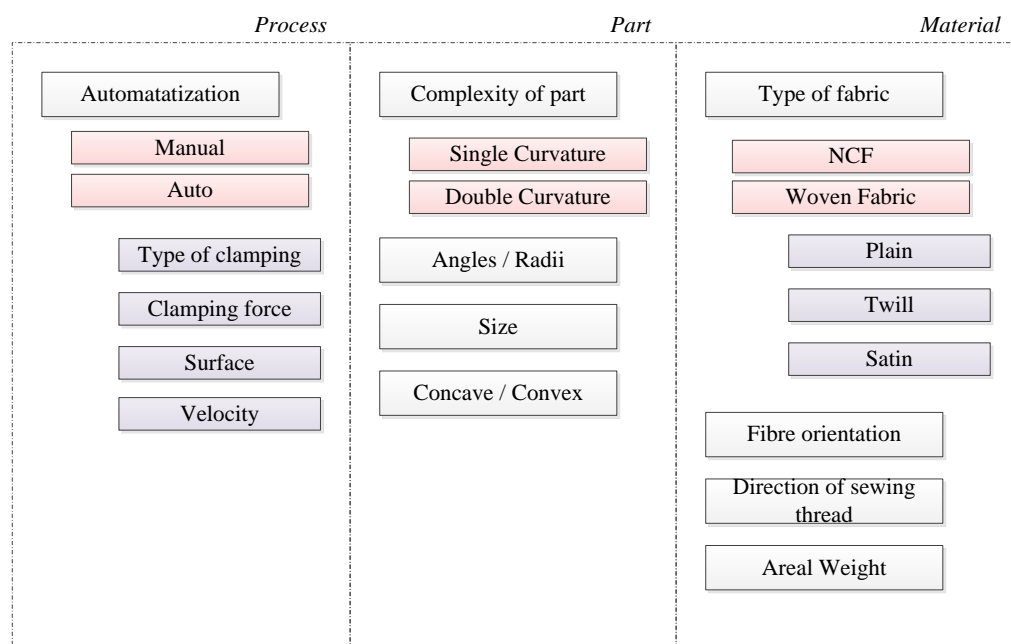


Figure 4.3 Draping influencing parameters

Henceforth, exclusively material influence is investigated in depth.

Although this process can be quite complex, understanding fabrics behavior when shaping is crucial for assessing their application and use.



One of the major reasons on analyzing draping process is to avoid the emergence of defects on the final product, which will lead to a decrease of the mechanical properties of the composite. [51].

Major defects associated with unsatisfactory forming procedures are:

- Wrinkling (Out-of-plane and In-plane): Initiated either by compression forces in fiber direction that lead to buckling and consequently wrinkling of the fibers, or once the locking angle (maximum shear deformation) is exceeded.
- Gaps/Voids: Induce resin rich areas which weaken the part locally.
- Fiber Pull-out: Due to mismatched tensile forces along the composite layers. Mainly driven by the part geometry and the fiber alignment.

However, any kind of defect should be avoided in the production phase. In fact, the aim of optimizing a composite manufacturing process is to achieve final products with the highest quality at the lowest prices. Indeed, especially importance. This is particularly relevant when considering automotive structural components as they must meet a number of requirements, especially with regards to load resistance.

As follows from the above, some of the mentioned influencing parameters cannot be longer considered, and rather optimize during designed phase such as fiber alignment or fabrics stitching.

The present study focuses on the influence of semi-finished products. A first rough idea on how different textiles drape in comparison to other reinforcements is illustrated below:

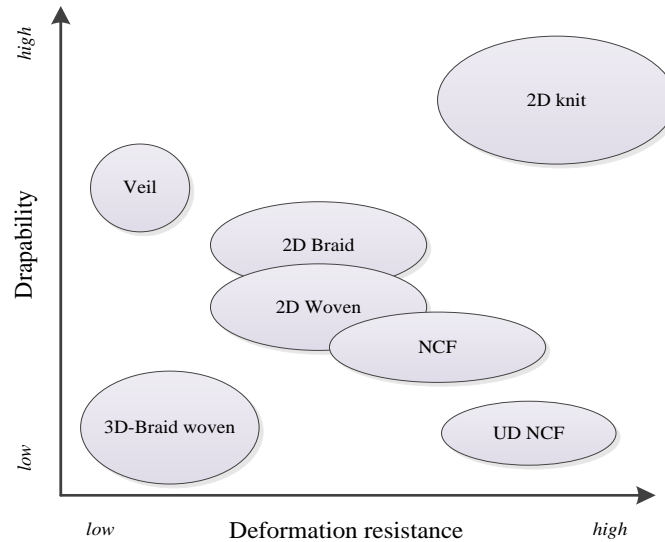


Figure 4.4 SFP Drapability

Several methods based on geometrical changes have been defined to obtain a physical measure of the draping mechanism, named kinematic models. These methods evaluate the interlacing point position before and after the forming process obtaining the concern strain.

The kinematic mapping model is based on the assumption that deformation is restricted to in-plane shear. It is also called 'pin-jointed net' (PJN), because the yarns are considered inextensible and pin-jointed at crossover points with no relative slippage. The fabric behaves as a 'fishnet' and is mapped accordingly onto the surface of the forming tool. Hereby only geometric information about the draping process is provided. Stresses or applied forces are not considered. The main problem that this model has regards to the lack of material properties consideration, resulting in the same draped patter whether the fabric is prereg, twill or satin woven.

Since the forming procedure is governed by the fabric structure, difficult to investigate physically by reason of scale and detail, the development of



sophisticated numerical simulations is required when looking forward meticulous results, mechanical approaches are used in this case.

The mechanical approach offers the benefit to represent the resistance against deformation using a non-linear material model and to include realistic boundary conditions at the price of being computationally more expensive. Traditional mechanical forming simulations are preformed using the finite element (FE) method .

The nonlinear finite element method supports the process optimization by predicting the fiber orientations and other deformations on the product. This requires the development of suitable material models that incorporate the anisotropic drape behavior of these textiles and that track the fiber orientations.

ABAQUS FE package and PAM-FORM (ESI Group) are normally used for modelling of forming processes.

Based on the foregoing, research on forming of fabrics can be classified into two general categories:

Table 4.1 Forming research overview

	Fabric properties	Weave Structure	Material Structure ("Mesh")	Low Computational Effort	Processing Conditions	Simple Model
Kinematic model	✗	✗	✓	✓	✓	✓
FEM model	✓	✓	✓	✗	✓	✗

The fabric ability to conform different forms is mainly due to the deformations that yarns experiment in order to adapt the flat textile structure into a three-dimensional shape. These movements of the yarns respect to their original



positions are known as deformation modes. It is of vital importance to comprehend how they perform, so that the shaping process can be optimized to manufactured part of the best quality. In the next section, involved deformation modes will be object of study.

#### 4.1.1 DEFORMATION MODES

In the thesis at hand, a classification according the scale of influence of the deformation is adopted. Thereby, three mayor levels can be distinguished:

- Macro-level: Allude to distortions that take place within layers.

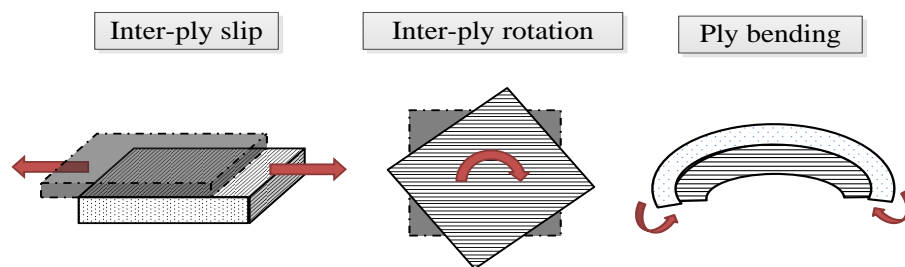


Figure 4.5 Macro-level deformations

- Meso-level: Refers to deformations that occur when looking at a ply like a whole. The four common deformation modes at macro-scale are transverse compression, in-plane tension, in plane shear and off-plane bending as shown in Figure 4.6 In plane shear is considered the primary deformation mechanism that occur during drapability. It can be experimentally calculated via picture frame test and the bias extension test.

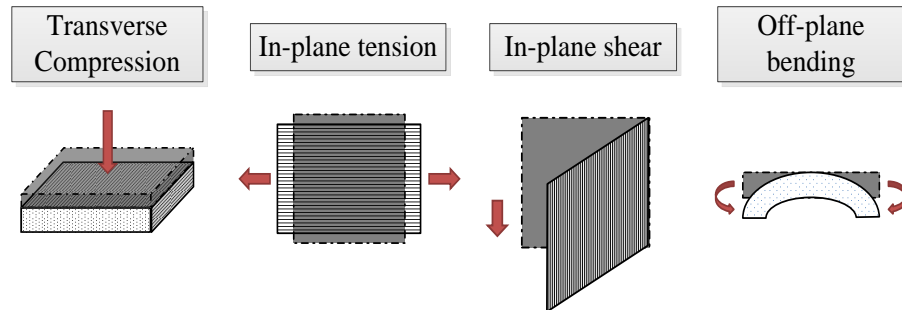


Figure 4.6 Meso-level deformations

- Micro-level: Deformations within yarns

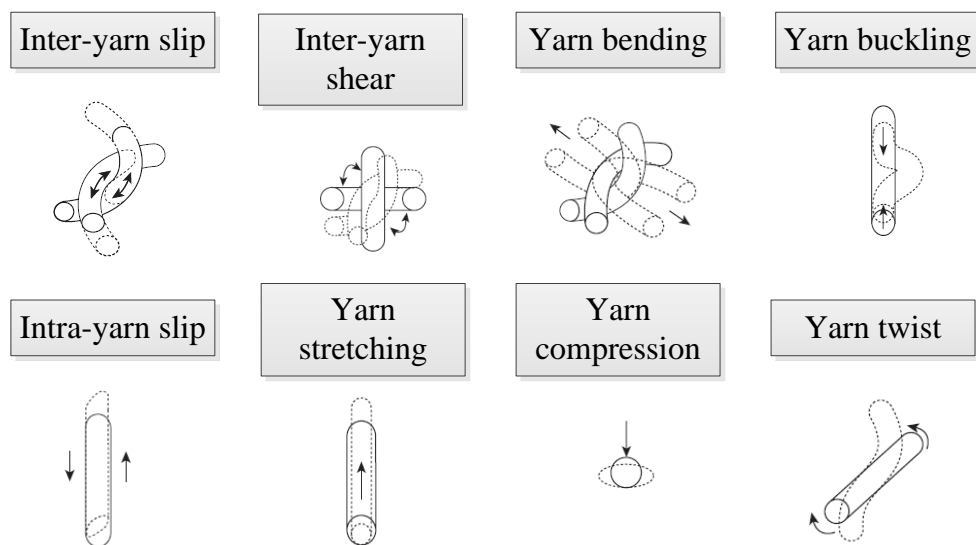


Figure 4.7 Micro-level deformations

For woven fabrics, it has been shown that draping process eventuates as a result of a change on the initial angle between weft and warp. Hence, the in-plane shear deformation, which governs the locking angle dimension, is the main responsible when draping. The lower the locking angle is, the better the fabric drapes since it can be sheared to a smaller grade. Wrinkles or buckling may occur as soon as the



locking angle is exceed. The amount of in-plane shear induced in a laminate to generate the part form is a good indicator of the difficulty of manufacturing a part. Therefore, shear is examined as a possible complexity metric in the cost modeling of composites.

While for NCF, drapability is influenced by: stitching, construction and areal weight, showing optimal behavior when using either low areal weight, low compaction or bidiagonal fabrics. [28]

When comparing both fabrics, it was observed that lamina performance produce with the same fibers differ when changing the number of interlacing point. [15]. Decreasing the drapability in the same proportion as the number of crossing point rise.

## **4.2** *PERMEABILITY*

---

Permeability is a measure of the ability of a porous material to transmit fluids. Thus, it is a crucial input to evaluate in impregnation stages of a composite material fabrication process, as it influences the required time to complete the phase.

The microstructural distribution of fibers, not only influences lamina mechanical properties but also within a preform, dictate the pore geometry, distribution and fiber path along the composite, giving rise to a harder or easier matrix infiltration and consolidation process.

### **4.2.1 DEFINITION**

---

Flow in porous media was first studied experimentally by Darcy's in 1856. Observing the flow of water through a bed of sand, Darcy's deduced that the volume of fluid running through a media is proportional to the pressure drop:



$$Q = \frac{K \cdot A}{\mu} \cdot \frac{\Delta P}{L} \quad (4.1)$$

The stated equation is known as Darcy's law, where the total volumetric discharge in unit time is  $Q$ ,  $A$  is the cross sectional area of the porous medium,  $\Delta P/L$  is the pressure gradient,  $\mu$  is the fluid viscosity and  $K$  is the static permeability of the porous medium.

Permeability value,  $K$ , relies on the geometry and the structure of the flow channels in the porous medium. Thus, it is a characteristic of the material.

In the general case, permeability is defined as a three-dimensional tensor:

$$[K] = \begin{bmatrix} K_{xx} & K_{xy} & K_{xz} \\ K_{yx} & K_{yy} & K_{yz} \\ K_{zx} & K_{zy} & K_{zz} \end{bmatrix} \quad (4.2)$$

Hence to the orthotropic behavior of woven fabrics,  $K_{xy} = K_{yx}$ ,  $K_{xz} = K_{zx}$ ,  $K_{yz} = K_{zy}$ ; additionally, exists a principle coordinate system with a principle permeability tensor:

$$[K] = \begin{bmatrix} K_1 & 0 & 0 \\ 0 & K_2 & 0 \\ 0 & 0 & K_3 \end{bmatrix} \quad (4.3)$$

Where  $K_3$  is the through thickness permeability while  $K_1$  and  $K_2$  are the medium in-plane permeability: along the fiber ( $K_{||}$ ) and perpendicular to the fiber ( $K_{\perp}$ ). Due to the real anisotropy of textile fabrics these permeability values differ from each other. In the case of woven fabrics, permeability should involve yarn crimp angle.

The presence and the size of gaps between yarns influences fabric permeability, as it does fiber arrangement inside the yarn. Real fabrics do not show fibers with a uniform array, however it can be said that one type of disposition accounts mainly



within the main yarn portion. Gap size allows the distinction between loose and tight fabric. For loose fabrics, the clear gaps between yarns gives rise to fluid channels, which due to the repeatability of fabrics, are assumed to be identical and dependent upon weave density, yarn type and weave pattern. In contrast, in tight fabrics the fluid has to transfer through the yarns. In this case, fiber volume, radius and arrangement are the major parameters affecting permeability.

The study of this thesis is within the manufacturing process of automotive structural components made out of CFRP. Thus, merely tight fibers are here considered.

Gebart [17] developed an analytical method for predicting the permeability of fiber bundles depending on the fiber arrangement, either quadratic or hexagonal:

$$K_{\parallel} = \frac{8 \cdot R_f^2 \cdot (1 - V_f)^3}{c \cdot V_f^2} \quad (4.4)$$
$$K_{\perp} = C_1 \cdot \left( \sqrt{\frac{V_{fmax}}{V_f}} - 1 \right)^{5/2} \cdot R_f^2$$

Where  $R_f$  is the fiber radius,  $V_{fmax}$  is the maximum possible volume fiber fraction and  $c$  and  $C_1$  are constants which depend on the fiber arrangement. Values for  $c$ ,  $V_{fmax}$  and  $C_1$  are  $57, \pi/4$  and  $16/(9\pi\sqrt{2})$  respectively when the fibers follow a quadratic arrangement and  $53, \pi/2\sqrt{3}$  and  $16/(9\pi\sqrt{6})$  respectively when it is hexagonal. This approach has excellent agreement with experimental results.

On the other hand, an analytical method to determine through-thickness permeability was developed by Kulichenko [26] by simplifying gaps in a fabric as a system of straight channels as shown in Figure 4.8

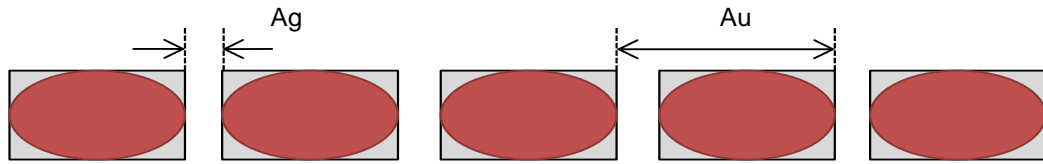


Figure 4.8 Gaps simplification

The permeability was predicted as:

$$K = \frac{\theta \cdot d_h^2}{80} \quad (4.5)$$

Where  $d_h$  is the hydraulic perimeter of the pore,  $Ag$  is the gap area, while  $Au$  is the area of a unit cell.  $\theta$ , denoted as fabric porosity can be estimated as the quotient between  $Ag$  between  $Au$ . In comparison with experiments, no method can give an accurate value neither for porosity nor for the hydraulic perimeter.

Infusion models generally employ values obtained from literature or experiments to avoid possible mismatches. Nevertheless, these values normally referred to one-ply fabric. Therefore, further authors have developed methods to obtain multi-layer fabrics permeability.

Mogavero [33] compared experimental data with effective permeability prediction, to conclude defining the effective permeability,  $\bar{K}$  as:

$$\bar{K} = \frac{1}{L} \cdot \sum_{i=1}^N l_i \cdot K_i \quad (4.6)$$

Where  $K_i$  is the in-plane permeability of the  $i$ -th layer,  $l_i$  is the thickness of the named  $i$ -th layer and  $L$  is the preform total thickness. It was found to be an accurate approach with errors between 14,2% and 23,8%. Furthermore, an equation for through-thickness permeability of multilayer preforms was proposed



by Chen [5], considering inter-layer continuity and coupling between in-layer and trans-layer flow :

$$\bar{K} = \frac{1}{\sum_{i=1}^N \frac{l_i}{L} \cdot K_i} \quad (4.7)$$

In conclusion, multilayer preforms permeability depends on the permeability of each layer, which at the same time, is influenced by the fabric geometric features, such as gap size or preform thickness.

One extra important factor to consider is small interfiber spacing,  $\delta$ , direct consequence of higher volume fractions, as it could lead to less ease for the resin to penetrate into the bed of fibers. It was shown that plane permeability ( $K_x$ ) is roughly  $\delta^2$ . Small interfiber spacing can be then determined as:

$$\delta = d \cdot \left[ \frac{V_{fmax}}{V_f} - 1 \right] \quad (4.8)$$

Where  $d$  is the fibers diameter,  $V_f$  volume fiber and  $V_{fmax}$  maximum volume fiber attainable by reason of fibers displacement. For example, if the actual microstructure is approximated as a square array,  $V_{fmax} = \pi/4$ .

In the specific case of NCF, Lundström [30] and Drapier [13] suggested that neither the stacking sequence nor stitching pattern influence the transverse permeability, but it is the yarns density that has the largest influence.

Permeability is a determining factor on composites manufacturing, more concrete on infusion procedures. However, obtaining accurate geometrical parameters is crucial for obtaining good agreements. Tests have exhibit statistical variation even when reproducing the same conditions, parameters configuration and material. This is explained by the unlike paths that the fluid follows during the infusion



process of each of the test repetitions. Leading to the conclusion that experimental determination is the only accurate method to determine permeability. [18]



## Chapter 5. **METHODOLOGY**

This chapter is introduced with the problem description in order to approach afterwards the development of a material complexity

### **5.1** *PROBLEM DESCRIPTION*

---

The object of this research is contributing to the development of a new tool for fast modelling up from the early design phase of CFRP BIW, optimizing in a parallel effort time and cost.

By reason of optimizing automotive carbon composites structures, the main constraints that define the overall BIW optimization are cost, weight, strength, stiffness and user score. Material optimization is one of the module on the overall tool that emprises, at the same time, manufacturing processes, topology and assembly optimization. In Figure 5.1 a scheme of the tool overview is illustrated:

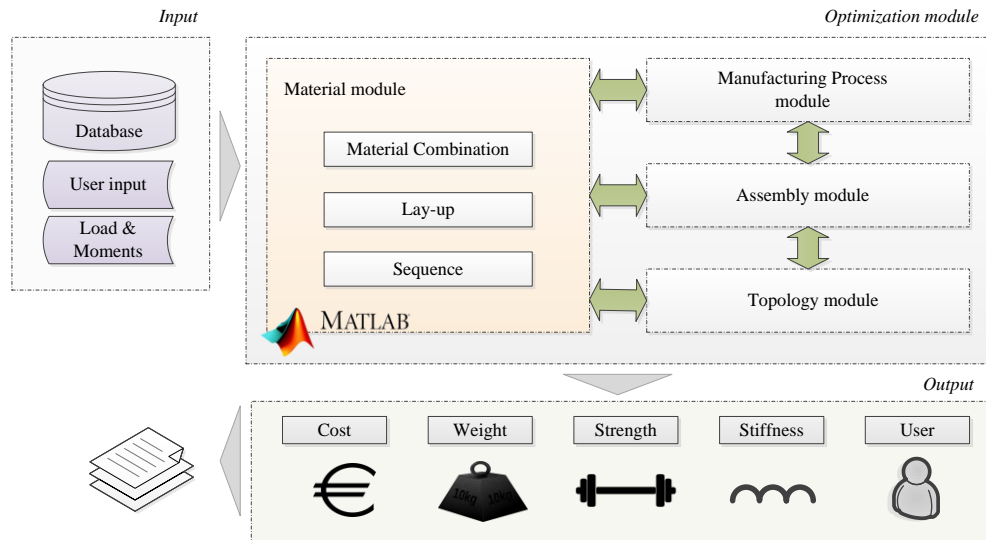


Figure 5.1 Tool overview

The present thesis will concentrate on the material module, concretely on semi-finished products, which will be presented and explained in the next sections. For the further implementation, MATLAB will be used.

## 5.2 MECHANICAL PROPERTIES

Material optimization process provides the user with the best material combination, lay-up orientation and sequence under the premises that all the manufacturing, topology, and user constraints are fulfilled.

The approach that this thesis is focused on is, further than optimizing from a material side (already implemented- [1]), is in the optimization of the use of textile composites in structural components. Hence, as introduced before, new models must be investigated and implemented.

As presented in Section 3.1.1, different models are available when it comes to estimate composites mechanical properties. However, due to the lack of



information regarding textiles geometry parameters, bridging model is excluded. On the case study, the optimum model, based on accurate result and simplicity, will be determined since our main goal is computation effortlessness. Nevertheless, for user interests, the program flowchart will show all the mechanical properties models available. This could be also made, on future work, with failure modes, as it is done in actual composites software.

As mentioned before it is crucial, that the algorithm converges faster. Thereby, a parallel model was implemented, paying special attention to preselection factors since they reduce the number of iterations.

In order to reduce the number of iterations or paths available, the user is given the option of selecting different types of reinforcements (Woven Fabrics or Non-Crimp Fabrics), as also the possibility of selecting the database to use. This is due to the fact that reinforcement properties are normally referred to as one single or double plies laminates. Thus, the approach can optimize the material either optimizing layers or also starting from a microscale point, with fibers and resins.

Figure 5.2; **Error! No se encuentra el origen de la referencia.** illustrate a scheme of what the user could choose between, as earlier indicated, although just one mechanical model is implemented, in the flowcharts all the options are shown.

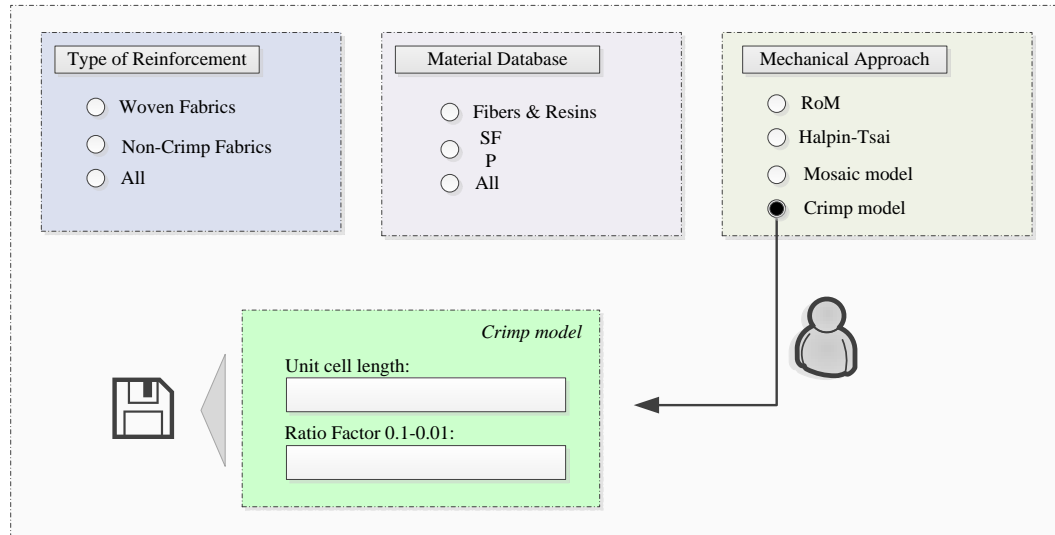


Figure 5.2 SFP GUI flowchart

Following the user election, the material optimization algorithm begins with the aim of achieving the best solution in compliance with the requirements. Best solution is hereby referred as the combination of material, lay-up and sequence that best satisfy or fit a determine number of parameters.

As previously stated, integrating SFP within material optimization module is the object of optimization.

The main difference optimizing SFP lies on estimating their mechanical properties. While with NCF and UD fabrics, CLT is applicable (see Section 2.2.1), for woven fabrics, due to their undulation pattern, other models must be implemented. As it will be analyzed in the case study, mosaic model has proven to be the most suitable approach. In conformity with this method, the guidelines to follow are shown in the next flowchart:

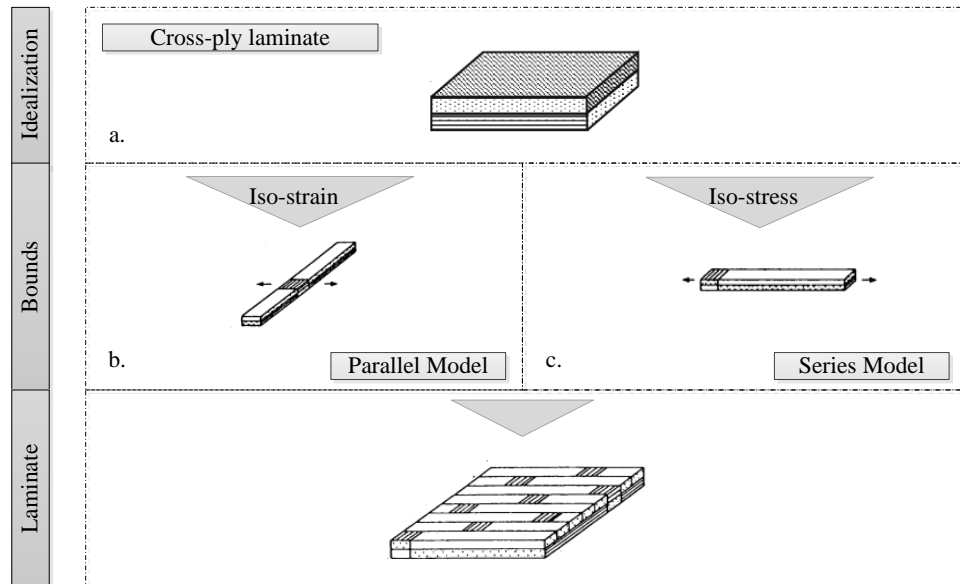


Figure 5.3 Mosaic model flowchart

For each step, the equations explained in Section 3.1.1.2 will be applied. Taking into account that either the parallel-model or the series-models are usable, the first one is chosen in the present procedure.

An overview of the complete algorithm follows (Figure 5.4):

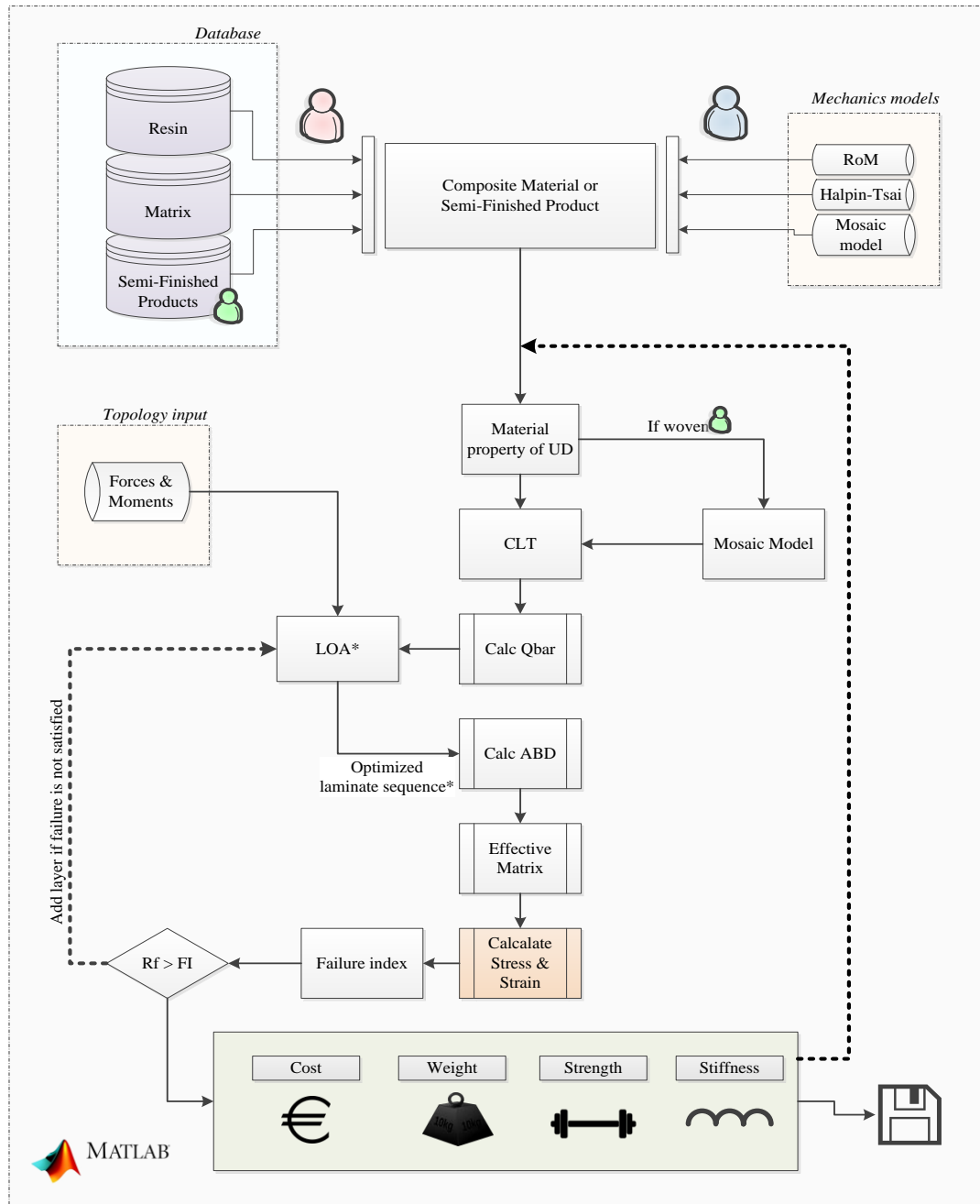


Figure 5.4 Material Optimization flowchart

(\*) When woven fabrics are involved LOA is adapted



---

## 5.2.1 LAYERWISE OPTIMIZATION ALGORITHM (LOA)

---

As mentioned above (section 2.2.2), due to the multi-objective purposes of our model, the LOA must be considered. It must be applicable to all fabrics, this means that a new factor should be introduced in order to make it suitable to woven fabrics. For this reason, the term SFP is introduced, which acquires the value 1 if it is a woven fabric or 0 if not.

The LOA determines the lay-up that maximizes the stiffness of the lamina based on the minimum strain energy principle.

The strain energy of a symmetrically composite plate of length 'a' and width 'b' subject to uniformly distributed loads and moments can be expressed as:

$$U = \frac{1}{2} \cdot \iint (\varepsilon_x \cdot N_x + \varepsilon_y \cdot N_y + \gamma_{xy} \cdot N_{xy} + \kappa_x \cdot M_x + \kappa_y \cdot M_y + \kappa_{xy} \cdot M_{xy}) dx \cdot dy \quad (5.1)$$

Where  $N_x$ ,  $N_y$  and  $N_{xy}$  are the normal and shear loads per unit length, respectively. On the other hand,  $M_x$ ,  $M_y$  and  $M_{xy}$  are out of plane moments. A representative scheme follows:

Due to the assumption of performing symmetric laminates, only top half has to be optimized. Thus, a laminate plate consists of 2N unidirectional layers which value is a function of the part and material thickness.

It is hence considered the fiber alignment algorithm as first optimization.

$$[\theta_1, \theta_2, \dots, \theta_k]_{Sopt} \quad (5.2)$$

Where  $\theta$  denotes the fiber orientation and  $\theta_k$  and  $\theta_1$  the outermost and innermost layer, respectively.

To achieve the desired optimization, the algorithm proceeds in two iterations:

### 1<sup>st</sup> Iteration:



Step 1: Assume a hypothetical N layers composite plate.

Step 2: Optimize the outermost layer angle  $[\theta_{1opt}]$  applying the minimum strain energy to different angles configurations  $[0^{\circ}, 90^{\circ}, 45^{\circ}, -45^{\circ}]$ .

Step 3: Similar procedure and  $[\theta_{2opt}]$  is determined

Step N:  $[\theta_{Nopt}]$  is estimated.

When considering woven fabrics (SFP=1), although they can be homogenized as a cross-ply laminate in order to apply LOA, a further constraint must be implemented. This regards to the fact that one woven fabrics layer is equal to a two UD layers laminate. Thereby, the orientation optimization must be developed every two layers. A resume chart is show below:

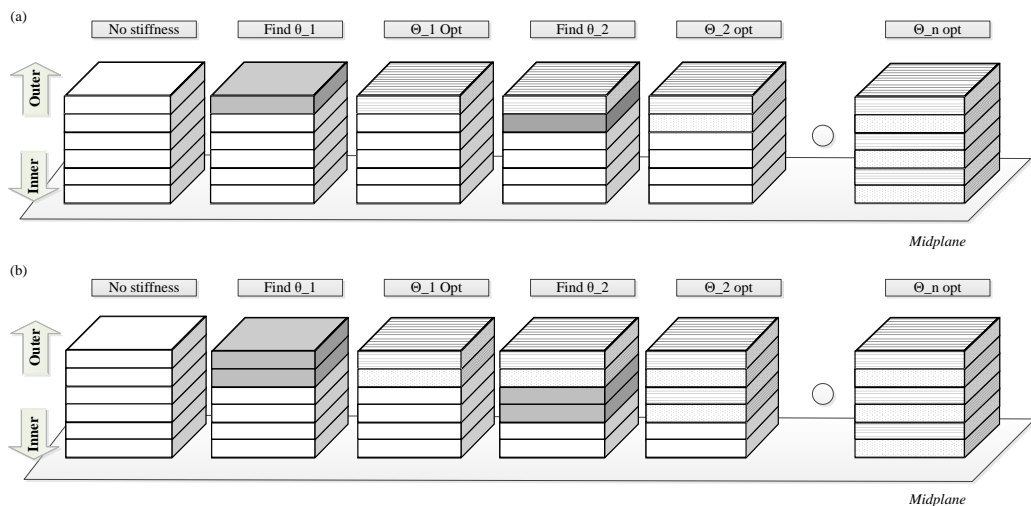


Figure 5.5 LOA for (a) laminate (b) woven fabrics

**2<sup>nd</sup> iteration:**



Once the fiber orientations are fixed, the algorithm is repeated under no assumption of hypothetical number of layers. This second iteration ends as soon as two consecutive layup sequences are equal.

## 5.2.2 TSAI-WU FAILURE MODE

---

As mentioned in Section 2.2.3, it is crucial to estimate composites properties under fracture and fatigue loading conditions, since it is required that after failure parts must still offered enough strength and stiffness. It is to be recalled that structural automotive components are hereby considered. This fact it is of great importance, as structural parts support the vehicle weight while absorbing collision energy and road shock.

Based on the above statement, one structural part failure can lead to a problem on the overall body-in white. Prediction of failure modes and mechanical properties reduction is crucial when optimizing the complete structure, as in case of failure, the rest of parts must be able to assumed the extra load.

Composite components generally require replacement or sectioning if any deformities, cracks, tears or misalignment are present. However, this is done in case the load constraints are no longer verified. Reason by, failure analysis is also useful.

The selection of failure criteria that comprises the beforehand mentioned statements was conditioned by the capability of determining the component degraded properties. Thus, Tsai-Wu, explained in Section 3.1.2.1, is implemented as follows:

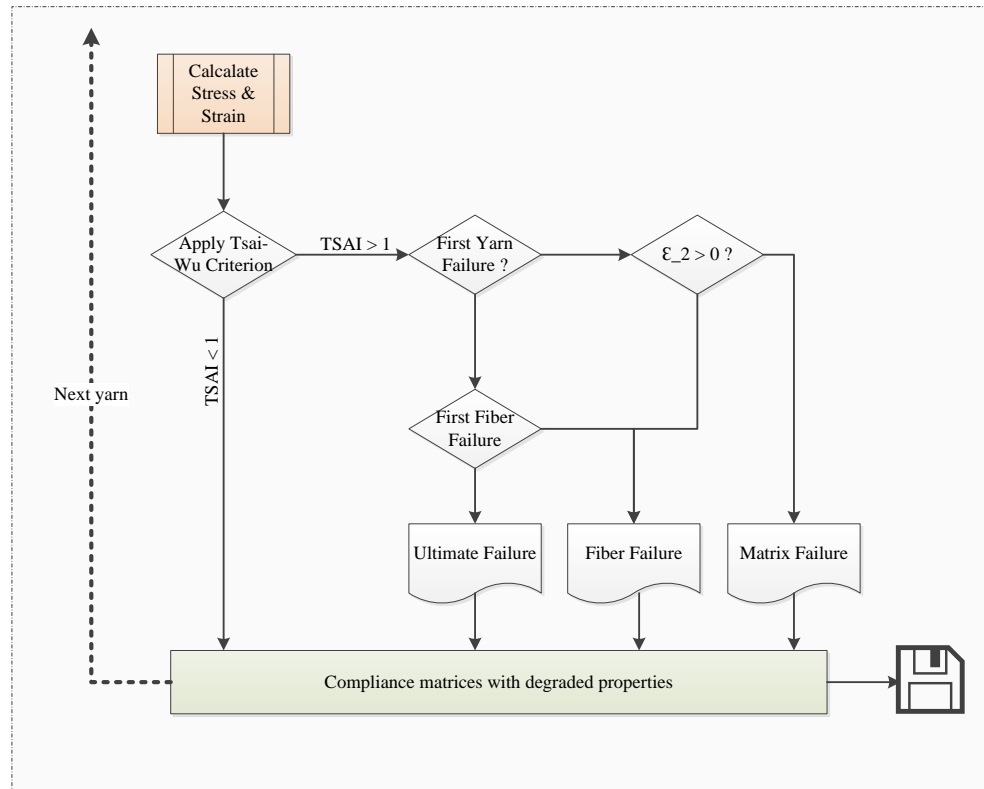


Figure 5.6 Tsai-Wu failure mode implementation

### 5.3 MATERIAL COMPLEXITY

In order to address manufacturing requirements at the early design phase, it is necessary to establish relationships between manufacturing levels and materials influence or parameters. As exposed in Section 2.5, material complexity is defined as the additional effort required producing a component due to material adverse influence. Impact not considered in the process and considered as a cost driver

The manufacturing time index associated with a complexity factor can be expressed in a generic form as:



$$MTI = \sum_{i=1}^n C_i \quad (5.3)$$

Where  $i$  refers to the different manufacturing steps involved in the composites structural parts production and  $C_i$  to the complexity associated to each of the steps.

As explained in Section 2.5, material influence can be reduced to two sub-processes: draping and infusion

$$MTI = C_{draping} + C_{infusion} \quad (5.4)$$

Costs can be reduced by integrating many components into one mold in order to reduce the quantity of material used or shortening the cycle time of the molding process. The main process time is being addressed through advanced resin chemistry and optimization of the resin injection and curing through improved tool design, heating methods and simulation software. Major cost drivers are nowadays required in preform procedures to bring the preforming cycle times shorter whilst allowing large and complex components to be produced reliably and accurately. Hence, the analysis will be focused on draping complexity, leaving permeability (infusion) excluded, as the new estimations are expected to be included in a further manufacturing time estimation model.

### 5.3.1 DRAPING COMPLEXITY

---

The drape behavior of woven fabric is complex mainly due to the underlying structure of the weave, but it has been observed that the fabric undergoes nearly pure shear during draping, with the constituent tows rotating freely at the crossing



points, as shear resistance is normally lower than other deformation modes. The angle between two yarns is called the inter-yarn angle ( $\varphi$ ), with the change in the inter-yarn angle defined as shear angle ( $\theta_s$ ), complementary of the inter-yarn angle:

$$\theta_s = 90 - \varphi \quad (5.5)$$

In view of the foregoing equation, higher shear angles are synonym of minor locking angles and thus, larger rotation of the yarns in the interlacing points allowing a finer drapability.

Based on experimental results [22] it was proved that under the same mechanical properties circumstances shear angle change with different weave pattern:

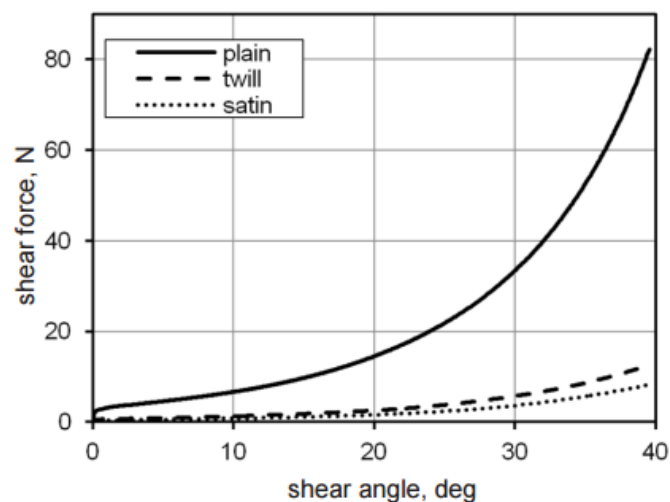


Figure 5.7 Shear angle [22]

The minimum angle between yarns ( $\varphi_{min}$ ) that a fabric can deform to before wrinkling appears is known as ultimate shear angle or locking angle. A method for predicting locking angle of woven fabrics was proposed by Prodromou and



Chen, based on the fabric packing limit of a unit cell and depending on yarn spacing  $L_{yarn}$  and width  $W_{yarn}$ :

$$\theta = \sin^{-1} \left( \frac{W_{yarn}}{L_{yarn}} \right) \quad (5.6)$$

In order to estimate shear angles different methods have been proposed based on woven garment textiles measurements among them the so called bias extension method that measures the load/displacement characteristics of fabrics under  $45^\circ$  bias tensile loads conditions. Attention should also be drawn to the parallelogram method, where a force is applied to opposite diagonals of the frame, altering the geometry and shearing the fabric.

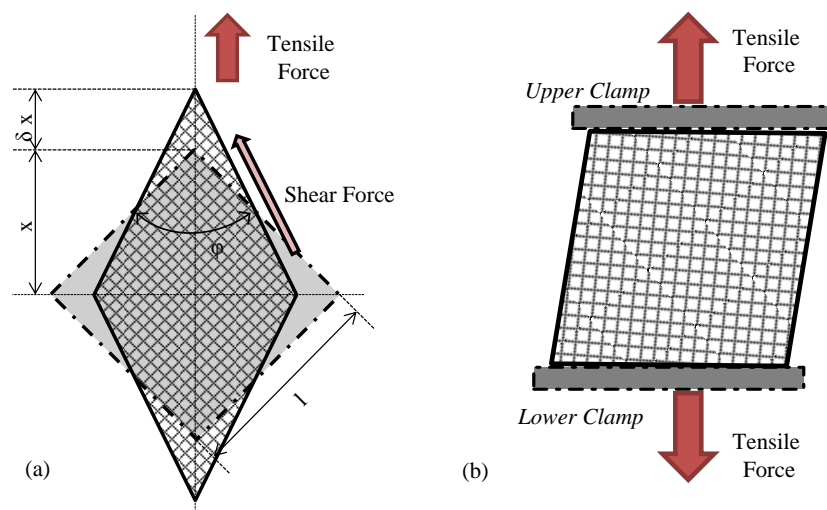


Figure 5.8 Shear angle measurement methods (a) parallelogram (b) bias-extensional

Using these methods some locking angles values found in literature are:



Table 5.1 Summary of published locking angles

Author	Fabric	Material	Locking Angle	Method
Wang	Carbon PW	189 $g/m^2$	37°	Bias extension
Wang	Carbon 5HS	289 $g/m^2$	28°	Bias extension
Wang	Glass 4HS	107 $g/m^2$	35°	Bias extension
Wang	Glass 8HS	289 $g/m^2$	36°	Bias extension
Breuer	Carbon PW	350 $g/m^2$	50°	Parallelogram
Breuer	Carbon TW	204 $g/m^2$	30°	Parallelogram
Breuer	Carbon SW	285 $g/m^2$	37°	Parallelogram
Breuer	Glass PW	345 $g/m^2$	50°	Parallelogram
Breuer	Glass TW	295 $g/m^2$	35°	Parallelogram
Breuer	Glass TW	167 $g/m^2$	38°	Parallelogram
Breuer	Glass SW	294 $g/m^2$	52°	Parallelogram
Prodromou	Glass PW	250 $g/m^2$	32°	Parallelogram
Prodromou	Glass PW	333 $g/m^2$	33°	Parallelogram
Prodromou	Glass PW	200 $g/m^2$	24°	Parallelogram
Prodromou	Glass PW	800 $g/m^2$	40°	Parallelogram

The lack of information about unit cell geometry factors that help estimating the locking angle, and the aim of obtaining a simple parameter that doesn't depend on simulation approaches or experimental tests, lead to the definition of a



dimensionless factor. In order to deduce it, a detailed analysis on the parameters that may influenced forming ability is followed. Areal weight, shear modulus, young's modulus, pattern, stitch type, number of plies, orientation and yarn linear density are the most significant properties among the ones defined by the manufacturer.

In the light of the foregoing, a first rough estimation can be drawn by contemplating exclusively those parameters that influence shear deformation behavior. On this aspect, with the goal of evaluating how areal weight exerts influence, a fabrics comparison according to pattern, material and areal weight and based on Table 5.1 , is here submitted:

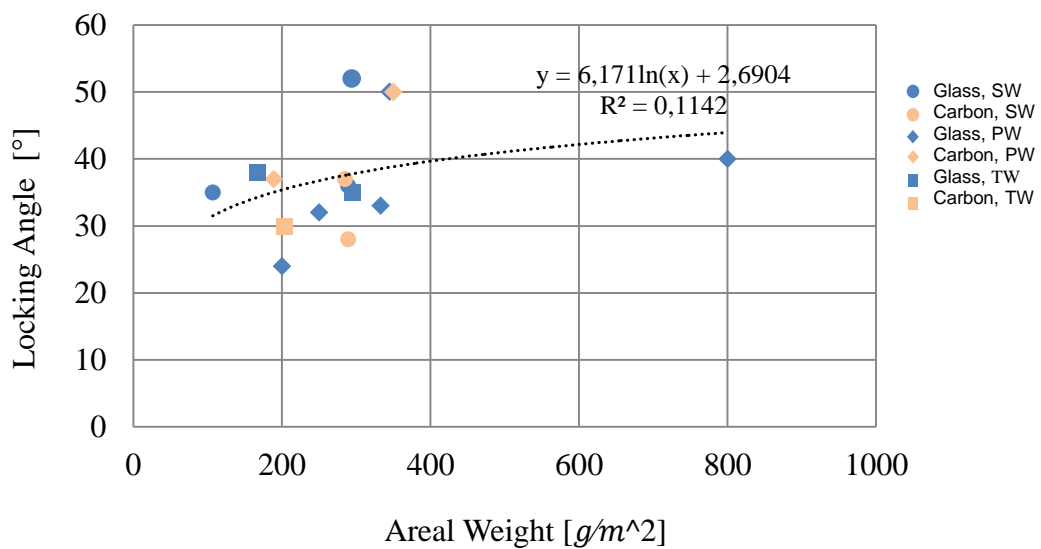


Figure 5.9 Locking angles for different fabrics

Including uniquely carbon fabrics, which are object of study:

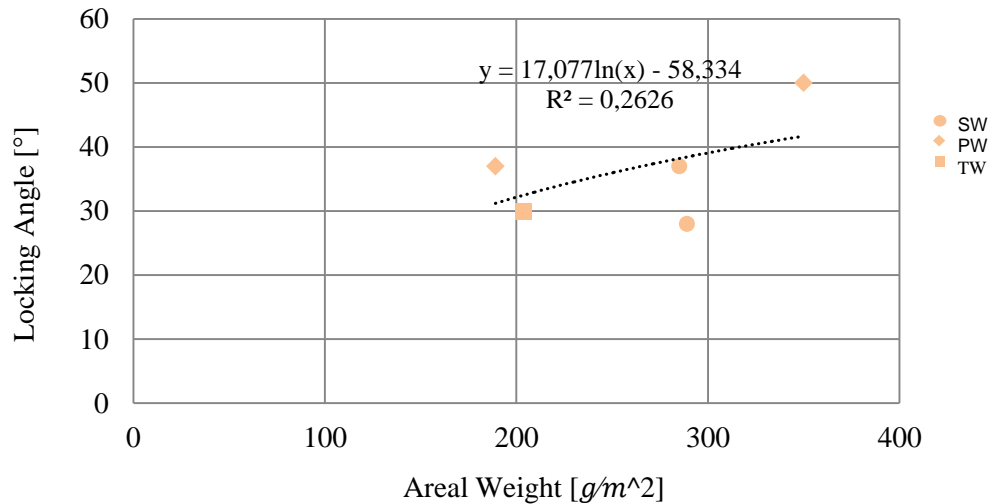


Figure 5.10 Carbon fabrics locking angles

From Figure 5.10 it can be inferred:

- Plain woven fabrics with reduced areal weight show a smaller locking angle. In fact, what it comes down to is that the yarns can rotate a higher degree in the interlacing points and hence drape easily into 3D forms.
- As exposed on Section 3.1, results revealed that satin woven fabrics, although they are heavier, achieve minor locking angles amongst twill fabrics, which at the same time can lock lesser than plain woven fabrics. Hence, fabrics with lessen weave influence and comparable weights, will have similar draping properties. Smaller differences are ow to different yarn interactions in the different weaves. Therefore, in a 3/3 satin fabric yarn interactions (crossing points) are higher than those on a 5/5 satin fabric, leading to unlike shear rigidities and hence to less draping behavior. An example of this behavior can be deduced from Figure 5.11 were satin woven



of similar areal weight shown highly different ultimate shear angles.

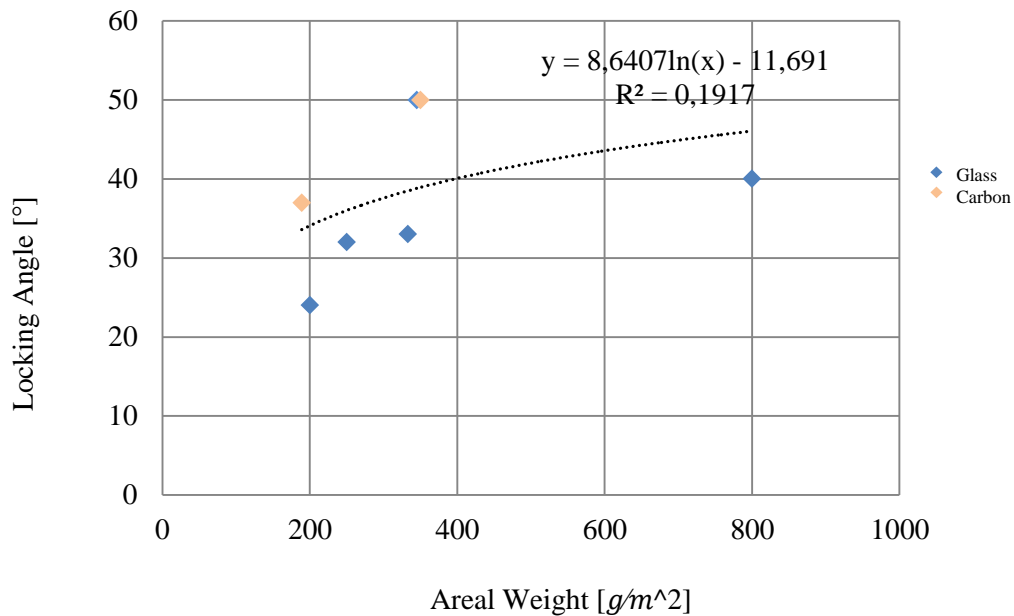


Figure 5.11 Locking angles

In this condition as also deduced from experts' opinions areal weight plays an important role, especially when fabrics need to be fitted into narrow corners or high complex shapes. Manifesting a decrease on the locking angle when larger areal weights are involved. This was mainly attributable to the reduction on bending stiffness that it brings about a rise on areal weight. More specifically, [52] reported that rather than fabric weave it is areal weight the dominant factor determining bending rigidity.

Ascribed to the assumption that only plain woven and NCF fabrics are taken into consideration including the number of interlacing points is meaningless as plain woven pattern remains always equal.



In the thesis on hand, the preforming process is assumed to be done ply by ply, this means that only parameters that influenced one fabric layer are further considered. Thereby, number of layers input is excluded. Such as fabric orientation, as it is understood to be optimized prior in the lay-up design phase. Areal density is proportional to yarn linear density and yarn crimp, therefore they could be excluded as well from the analysis.

Furthermore, NCF's shear resistance is affected by the type, amount and pattern of stitch used. If the fabric is sheared parallel to the stitching, as the shear angle increases, the stitching which holds the fibers bundles together becomes tighter, increasing the friction between intersecting yarns. In this case, the shear limit of the fabric, known as beforehand mentioned locking angle, is dependent upon the stitch (known as *stitch limited locking*) if the stitch is in tension and upon the fiber packing limit (*packing limited locking*) when the stitch is not in tension. Thus, shearing parallel to the stitch require double the effort of shearing the fabric perpendicular to the fibers. As an example, fabrics using chain stitch locked at approximately  $12^\circ$  shear ( $78^\circ$  inter-yarn angle) when loaded parallel, but can achieve more than  $58^\circ$  ( $32^\circ$  inter/yarn angle) when loaded perpendicular to the stitch. As happens with fibers orientation, stitch is assumed to be optimized beforehand.

At low shear angles ( $0^\circ - 30^\circ$ ) plain woven and stitched fabrics show similar in-plane shear resistance, but at higher shear angles the interlocking of the yarns within the plain weave provide a higher shear resistance than in non-crimp fabrics. Main differences between using woven and NCF will be observed during the validation stage.

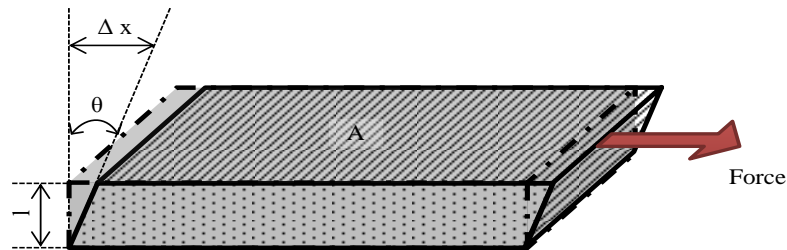
On last term, stiffness is hereby analyzed. As nearly pure shear is assumed to be the main deformation that fabric undergoes when draping, among the stiffness mechanical properties, shear modulus will focus the study.

Shear modulus or modulus of rigidity ( $G$ ) is defined as:



$$G = \frac{\tau_{xy}}{\gamma_{xy}} = \frac{F/A}{\Delta x/l} \cong \frac{F}{A \cdot \theta} \quad \left[ \frac{N}{m^2} \right] \quad (5.7)$$

Where the parameters can be derived from:



From Figure 5.8 and Figure 5.12 the hereunder equivalence can be gathered:

$$\theta = 90 - \varphi \quad (5.8)$$

Where  $\varphi$ , as mentioned in Equation 5.5 is the inter-yarn angle, which minimum value is denoted as locking angle. Therefore, G can be expressed as function of the name angle as:

$$G \cong \frac{F}{A \cdot (90 - \varphi_{min})} \quad (5.9)$$

As is evidenced in the foregoing, achieving lower locking angles (better drapability) is possible with minor values of G. Thus, evaluating shear modulus gives a subjective measure of forming 3D shapes for fabrics with equal area (A) and applied force (F).

With the objective of validating the above explained influencing parameters a composite manufacturing process was examined in detail.



In order to determine the combined effect of fabric mechanical properties on draping a regression equation is derived with respect to all influencing parameters discussed above. It is assumed that the fabric mechanical properties are linearly associated with the drape procedure and all input parameters follow normal distributions. A linear regression model as given in Equation is used:

$$Y = a + b_1 \cdot X_1 + \dots + b_n \cdot X_n \quad (5.10)$$

Where  $X_1 \dots X_n$  are the fabric mechanical properties,  $a, b_1 \dots b_n$  are the constants and  $Y$  is a parameter measuring drapability.

Defined then as:

$$Y = a + b \cdot \bar{G} + c \cdot W \quad (5.11)$$

Where  $G$  is shear stiffness,  $w$  is fabric weight per unit area defining the size of the material and  $a, b$  and  $c$  are constants that reflect the influence of each of the parameters.

A high shear stiffness in any direction will inhibit a good drapability in that direction, and would thus have a major influence on the overall effect. Thereby, it is appropriate to use the simple average  $\bar{G}$  :

$$\bar{G} = \frac{1}{3} \cdot (G_{12} + G_{23} + G_{31}) \quad (5.12)$$

Where the out-of-plane shear modulus  $G_{23}$  and  $G_{13}$  can be derived assuming that the ply is transversely isotropic with the plane of isotropy 23 . This yield:



$$G_{31} = G_{12}$$
$$G_{23} = \frac{E_2}{2 \cdot (1 + \nu_{23})} \quad (5.13)$$

Where:

$$\nu_{23} = \frac{(1 - V_f) \cdot E_{2f} \cdot \nu_m + V_f \cdot E_m \cdot \nu_{23f}}{(1 - V_f) \cdot E_{2f} + V_f \cdot E_m} \quad (5.14)$$

As stated at the outset, semi-finished fabrics reinforcements are produced using a process adapted from the textile industry. Thereby the analysis of fabric may be based on deformation mechanisms observed during earlier performed work by the textile industry . In their case, a drape coefficient (DC) is employed to describe the drape ability. After analyzing different research results, it was shown that there was a lineal relation between this coefficient and the areal weight of the fabric:

$$DC = 44.9 + 0.127 \cdot m_{m^2} \quad (5.15)$$

Or Behera, who estimated the drape coefficient to be:

$$DC = 0.24 \cdot G + 0.25 \quad (5.16)$$

Combining Equation 5.9, Equation 5.10 and Equation 5.11, a value for draping complexity can be obtained using:

$$Y = DC = 22.575 + 0.12 \cdot G + 0.0635 \cdot W \quad (5.17)$$



As mentioned in Section 4.1 such as seen on the subsequently real manufacturing process analysis. Fabric structure influences the manufacturing process on a greater or lesser degree depending on part geometrical form (GCF) as on the degree of automation. Hence, an overall draping complexity can be defined as:

$$C_{draping} = f(DC, GCF, \alpha) \quad (5.18)$$

Where  $\alpha$  is defined as grade of process automation. One process requires more or less effort depending on who performs the process.  $\alpha = 1$  when considering hand drapability, while  $\alpha = 0$  if the process is completely automatized, and hence, the fabric influence is almost none. On the other hand, fabrics do not have the same impact on a flat panel or simple part as in a complex case (high GCF), especially when double curvature is involved, where fabric must be carefully fit in all the edges.

Geometrical complexity factor, rated from 1 to 5, should be normalized, in order to define a final complexity factor:

$$C_{draping} = \alpha \cdot \frac{GCF}{5} \cdot DC \quad (5.19)$$

Draping complexity applicability will be analyzed on Section 6.2.

### 5.3.2 DRAPING VALIDATION

---

Based on the procedure followed when determining geometrical complexity factor [38], a knowledge-based rating and a process time measurement will be develop, with the aim of validating our material complexity approach.



### ***5.3.2.1 Knowledge-based rating***

Material complexity was deducted and assumed to be influenced mainly by shear rigidity and areal weight. By reason of validation, a knowledge-based rating survey was performed.

In order to design the named rating, account must be taken of a number of aspects. In first place, it is vital that the set of geometries cover a wide range of complexities. Complexity rating varies from 1 (simple geometry, therefore easy to manufacture) to 5 (complex geometry, therefore difficult to manufacture).

The number of rated parts is limited to eleven to allow for an acceptable time investment for experts participating. The parts are listed and briefly described in Appendix B, additionally; the survey layout for one part is included.

Every part on the survey is marked with red arrows which represent the demolding directions. Depending on the demolding direction the composites lay-up has either to be done on a female or on a male mold. In the Figure 5.12 demolding directions are illustrated.

Based on each part geometry, the experts were asked to conduct the following steps:

1. Rate the general geometrical shape complexity of each particular part, under no material or manufacturing influences. However the following constraints apply:
  - Sequential preforming
  - Liquid molding process
2. Evaluate the specific complexity of the parts based on a set of reference attributes. Attributes that will remain equal for all parts within the 2<sup>nd</sup> question:
  - Molding direction: male



- Material: biaxial NCF (i.e. each fabric comprises two orthogonal UD layers)
- Areal Weight: 200 gsm per ply

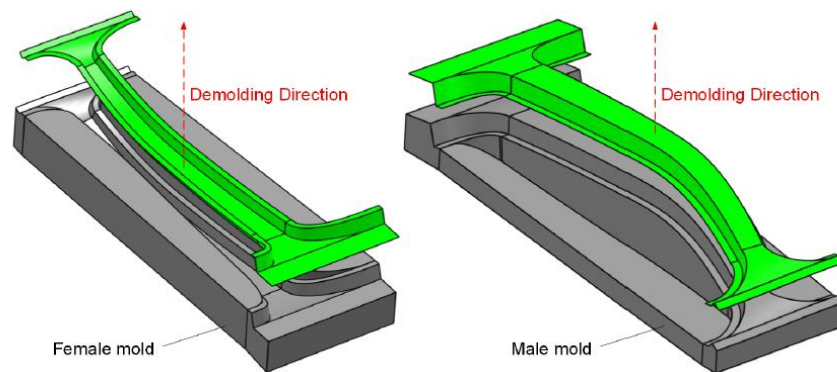


Figure 5.12 Molding directions

3. Determine the complexity change in case of each altered attribute (female mold, woven fabric or 600gsm ply). Specifying the direction of the change (+: more complex, 0: neutral, -: less complex) and, if possible, the respective numerical value.
4. For some parts, a 4<sup>th</sup> specific question to design variation is asked.

This 4<sup>th</sup> question refers to a deeper analyze on size variation as on sandwich structures use. The obtained results will be evaluated on chapter 6.

### 5.3.2.2 Time-Measurement

On a second level of analysis, to optimize and revalidate the material complexity model, the production of composite parts at a local Singaporean company was observed. A set of tests (Figure 5.13) were evaluated and measured.

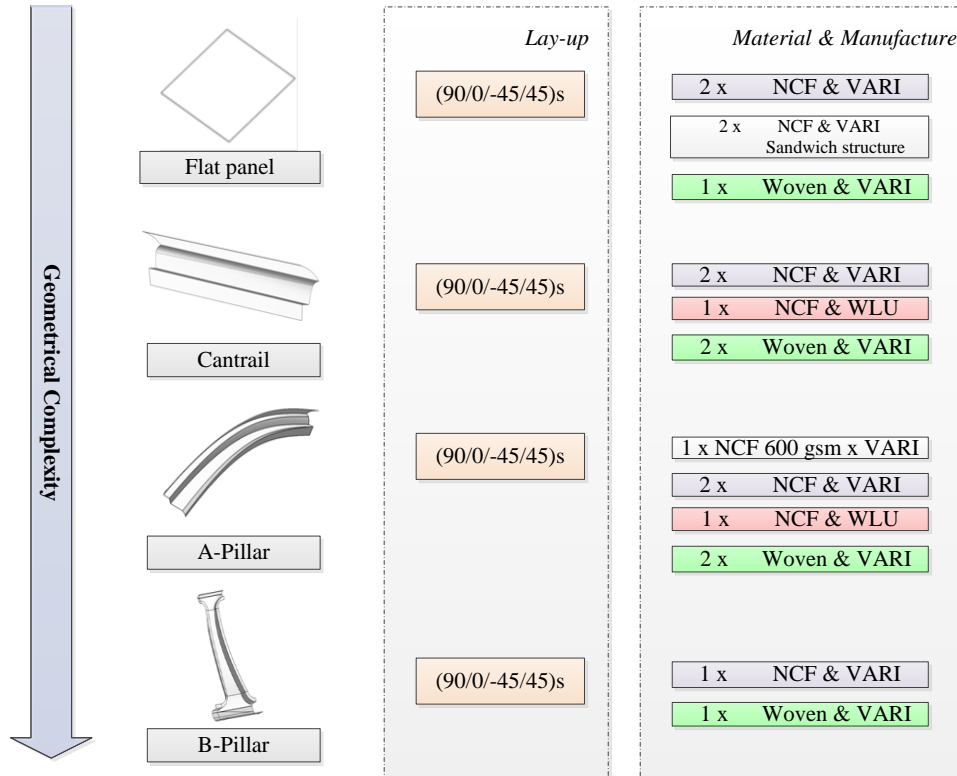


Figure 5.13 Time-measurement scheme



## Chapter 6. RESULT AND DISCUSSION

### 6.1 MECHANICAL PROPERTIES. CASE STUDY

In order to determine which of the proposed approaches is more suitable to experimental results, a case study is here introduced.

The mechanical properties of a woven laminate were estimated using three different models:

- Mosaic model
- Rule of Mixtures
- Halpin-Tsai

The exclusive consideration of these three methods is due mainly to the lack of geometry factor when using the crimp model and the fact that the cross-ply approach results, as mentioned, show to be overrated.

For the case study the following material properties will be considered:

Table 6.1 Material Data

Material	$E_l$	$E_T$	$G_{Lt}$	$G_{TT}$	$\nu_{LT}$
T-300 Carbon	230	40	24	14.3	0.26
Epoxy Resin	3.5	3.5	1.3	1.3	0.35

$$V_f = 0.47 \quad a = 1.0 \text{ mm} \quad H = 2 \cdot t = 0.1 \text{ mm}$$



The results obtained implementing both three methods on MATLAB interface are resume on the table below. Additionally, experimental results found in literature are included:

Table 6.2 Results comparisson

	$E_x, E_y$	$G_{xy}$	$\nu_{xy}$
Mosaic model	59.4	3.19	0.0415
Rule of Mixtures	65.305	2,34	0,3077
Halpin-Tsai	59,64	3.1959	0,1672
R.A.Naik [34]	60.0	3.16	0.0450

As it can be inferred, mosaic model show the most accurate results, and hence, will be the model implemented on the material optimization module.

## 6.2 DRAPABILITY VALIDATION

---

For material complexity validation a knowledge based rating survey was developed. The change of geometrical complexity because of changes on material properties or structure will be analyzed, with the aim of clarifying the range of influence.

As indicated in Section, an additional validation was done by analyzing the results observed during a manufacturing process.



Both cases are explained in the following sections.

### 6.2.1 KNOWLEDGE-BASED RATING

---

The aim of this survey was to determine in which grade experts thought the complexity of manufacturing a specific automotive part varies due to material, mold or areal weight. And hence, validate our material complexity factor estimation.

In order to determine if there were significant complexity differences within one geometry when other material conditions are considered, the one-way analysis of variance (denote as ANOVA) is employed. The term one-way, also called one-factor, indicates that there is a single explanatory variable, complexity in this case, with two or more levels, here denoted as influencing factors, and only one level is applied at any time for a given subject. That is to say, the experts rate geometries considering one influencing parameter at each time.

There is a population of experts for which there is a quantitative complexity, for each of the  $k$  factors. Expert outcomes for each group have mean parameters that can be label  $\mu_1$  through  $\mu_k$  with no restrictions on the means distribution. To apply the ANOVA analysis, expert variances for the rating for each of the possible influencing parameters all have the same value. In other words, the rating variances between factors must be similar. Fact that it is verified in the present survey, as each expert is assumed to apply the same criteria when evaluating different parameters. The distribution of the outcome is presumed to follow a Normal distribution with mean  $\mu_i$  and variance  $\sigma^2$ .

The overall null hypothesis and starting point for one-way ANOVA is that the means between factors are equal. Evaluating the outcomes with the “F-statistic” factor will allow the retention or rejection of the null hypothesis. If the estimated



“F-statistic” value is lower than a critical value of the Fisher distribution, known as  $F_{crit}$  the null hypothesis is rejected and hence, the assumption that all influencing parameters have equal mean. Therefore, at least two of the influencing parameters means significantly differ.

In the thesis on hand, unlike means is indicative of an influence over the complexity rating. Two cases were studied:

**1<sup>st</sup> Case:** For each of the rated geometries, is it analyze if there is a notably variation on complexity rating between employing a female mold, woven fabrics or reinforcements with a higher areal weight.

**2<sup>nd</sup> Case:** The aim in this case is to evaluate if woven or areal weight influence on general complexity is the same for each part or it is dependent on the complexity of the part.

Additionally, as mentioned in Section 5.3, further questions were included in the survey and thereby they will be here examined. These questions pretended to determine if there is an additional effort on manufacturing when using sandwich structure o larger (increasing either width or length) parts.

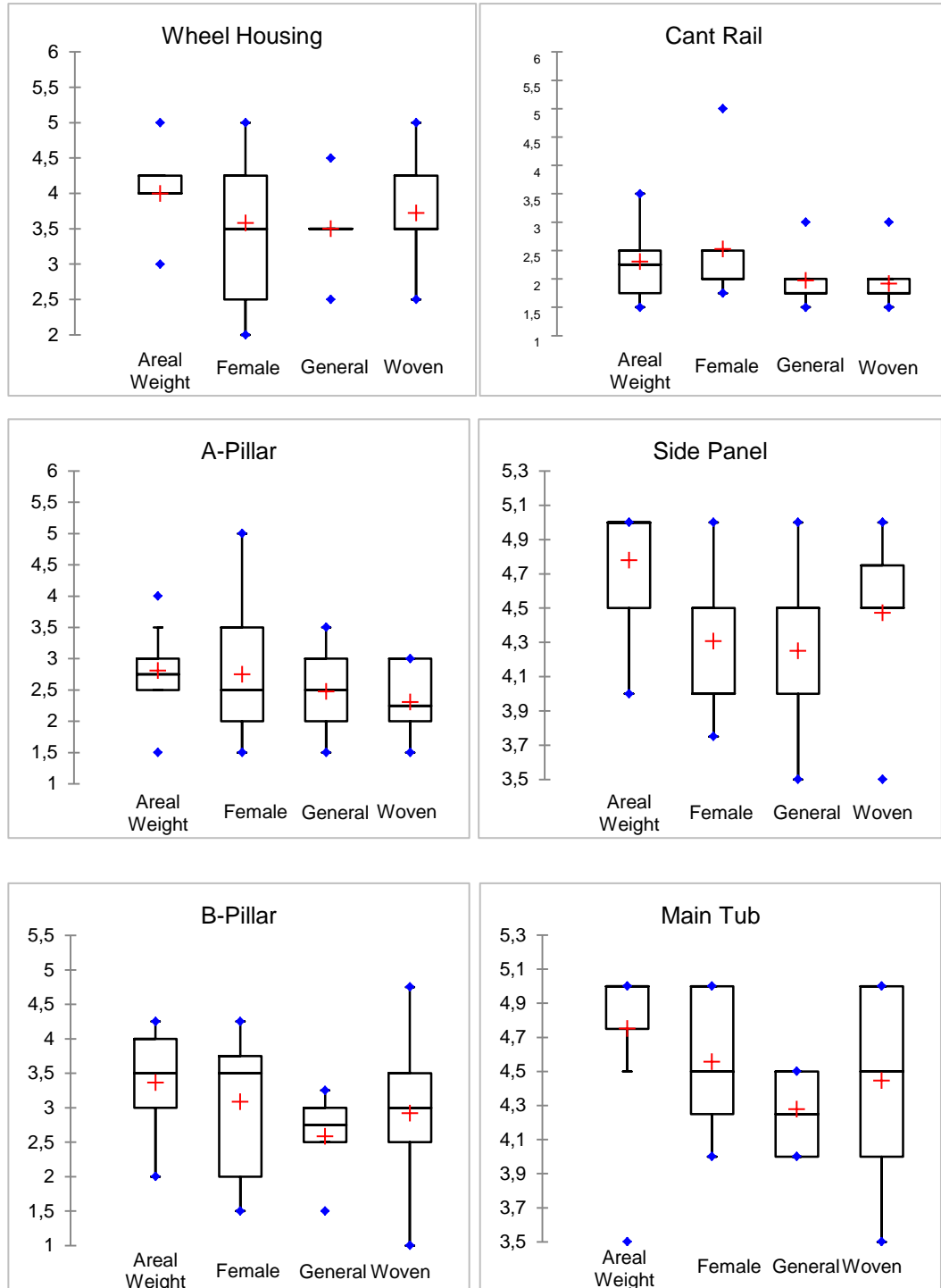
### ***6.2.1.1 Influential parameters analysis***

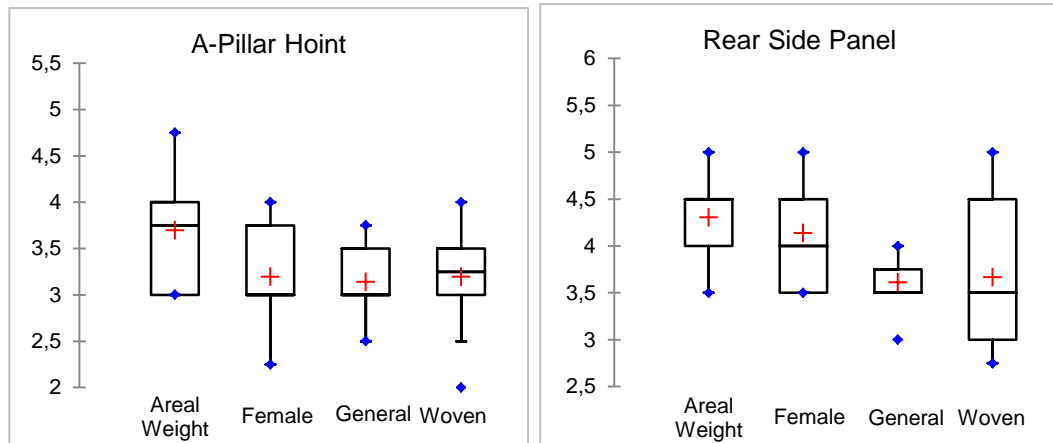
As just noted, each geometry outcome rating was evaluated independently with the goal of determining the role that plays the use of a different reinforcement or of a heavier fabric.

As a resume for the analysis below are illustrated the box plots for the different geometries. Each box-plot collects and evaluates experts rating data in compliance with the use of either female mold, woven fabrics, larger areal weights or none of them. Box-plots constitute a graphical interpretation of the survey results. Substantial variations among parameters means are synonym of a large influence on complexity.



Result and discussion





On the basis of analysis conducted and results, it can be concluded that none of the geometries showed to be significantly influenced by the use of either of the influential parameters, except for the rear side panel, whose complexity was remarkable altered by the utilization of higher areal weights, and less determinant for use, by the employment of a female mold. Probably, due to the sharp folds that hinders the demolding process, in case of the mold influence, and the fabric corners fitting, in case of areal weight.

As an overall view of the complexities mean variations when considering different factors while evaluating different geometries Figure 6.1 Is plotted:

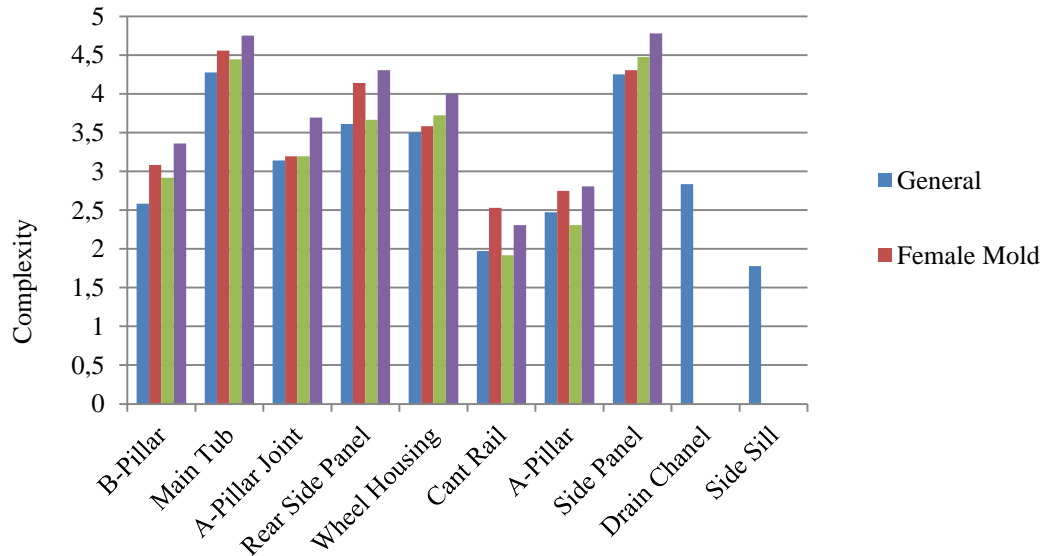


Figure 6.1 Complexity values overview

In the subsequent section, the 2<sup>nd</sup> case results and discussion is presented.

### 6.2.1.2 Geometry influence analysis

The object of study at this section is the determination of a possible relationship between the geometrical complexity factor and the degree of influence of either woven fabrics or areal weight over the named factor as stated in Section 5.3.1.

Making use of the mean squared error (MSE) to measure the average of the squares of the difference between the influenced complexity value and the general value, an examination on the errors amongst the geometries is here introduced in Figure 6.4:

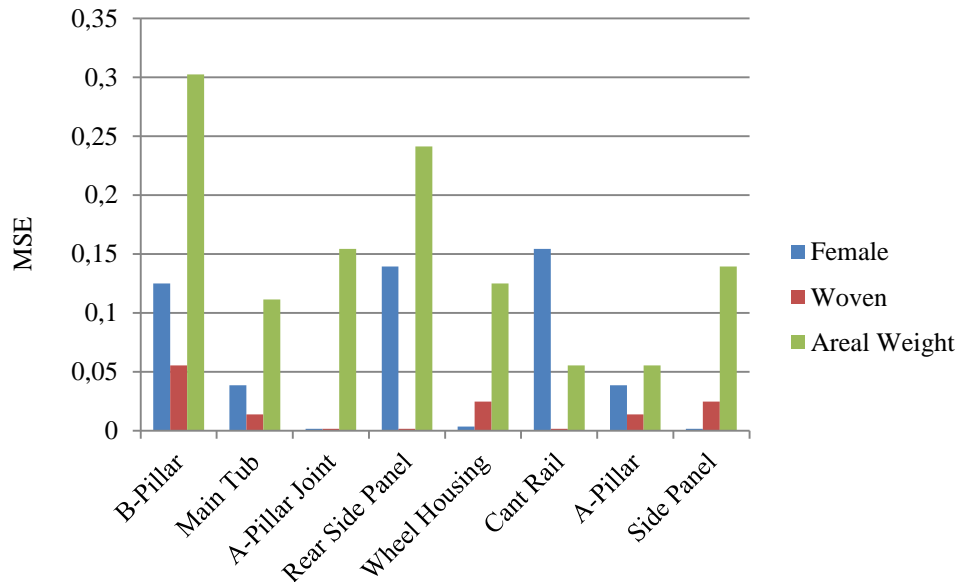


Figure 6.2 Factors Error vs. GCF

The histogram above verified that the degree of influence of a factor is related with the geometry involved. However, not all the factors are influenced by the form on the same proportion. This can be inferred from the graphic on Figure 6.2 where areal weight seem to be larger affected than when using woven fabrics.

In order to verified the beforehand mentioned difference. Each factor is examined independently based on a lineal regression model. Firstly, woven fabrics will be uniquely considered; and secondly, higher areal weight fabrics.

In first place, it was observed that woven fabrics influence is independent from the geometrical form of the part. This was deduce from the slope value of the following linear regression model, where is shown that the additional complexity associated with the use of this type of reinforcements is unconnected to the respective GCF of the geometry:

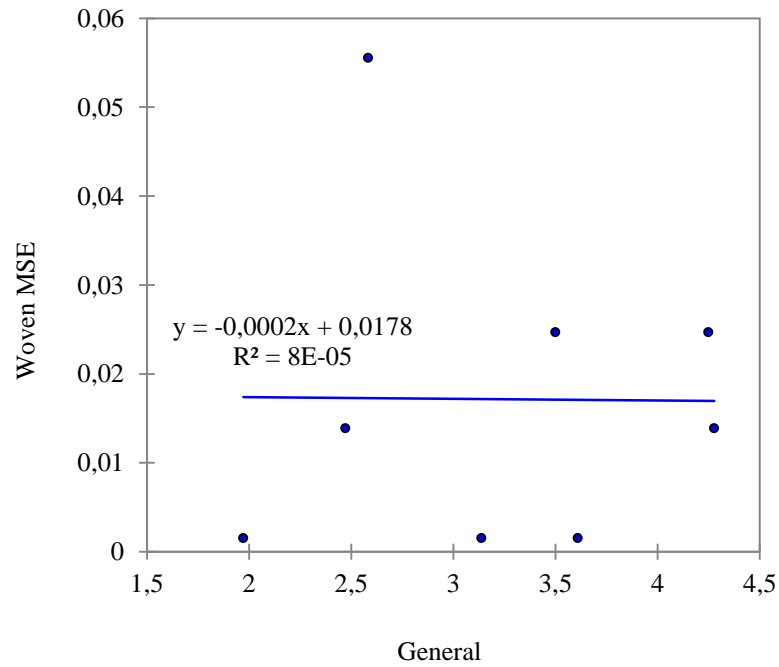


Figure 6.3 Woven fabric influence

Following the same procedure for higher areal weights:

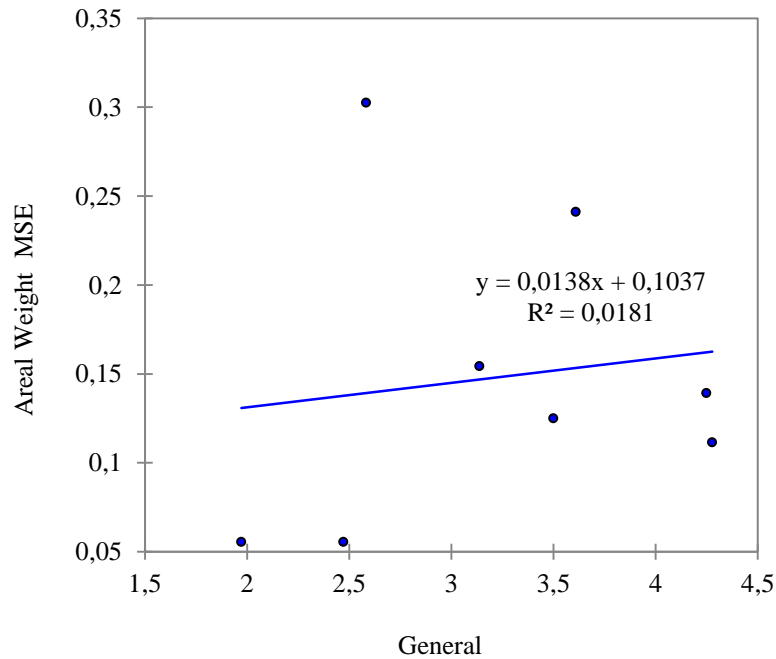


Figure 6.4 Areal Weight influence

In this case, a lineal relation is inferred from Figure 6.4. Thus, areal weight grade of influencing on complexity varies with the GCF.

In conclusion, it is more relevant areal weight influence rather than fabric reinforcement. Hence, the draping complexity factor can be redefined as a function exclusively of areal weight.

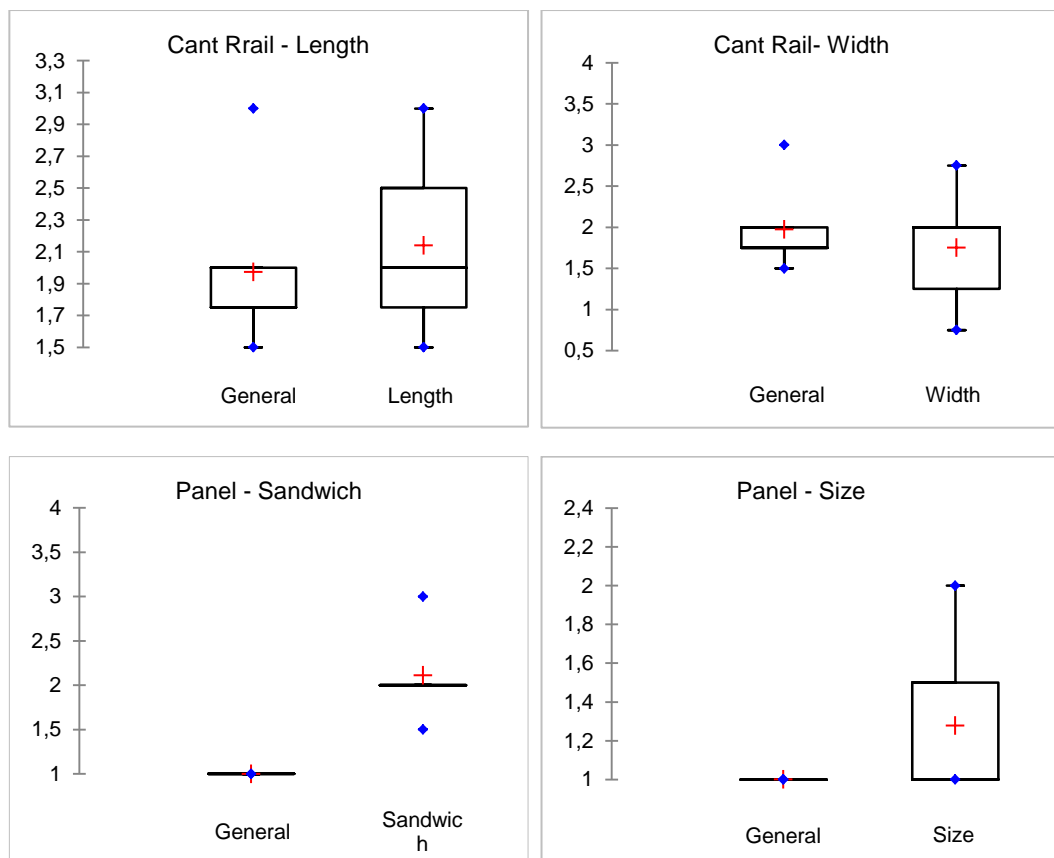
$$Y = a + c \cdot W \quad (6.1)$$
$$DC = 44.9 + 0.127 \cdot m_{m^2}$$
$$C_{draping} = \alpha \cdot (0,0138 \cdot GCF + 0,1037) \cdot DC$$

A second analysis on manufacturing times will be evaluated in the following section. It would help validating and consolidating this second approach.



### 6.2.1.3 Special factors analyze

An additional study was developed for two geometries: flat panel and side sill. The experts were asked to rate both geometries under new constraints. In case of the flat panel, these new factors where the use of a sandwich structure and the increase of size; while for the cant rail, experts were inquire for a new complexity value in cases of increasing cant length and width. For both cases a one-way analysis of variance (ANOVA) is used.



On the basis of the results obtained, it can be concluded that no significant variation in complexity was shown when increasing cant rail length and width, while it can be established that there is a weighty complexity increase if either a



sandwich structure is used or the size is increased (length & width). This is justified by the presence of an additional step in the manufacturing process, in case of the sandwich structure.

Lastly, several specific comments from experts highlight that:

- Fabrics with higher areal weights are more difficult to drape
- Fabrics with higher areal weights are more complex to fit into corners.
- Sandwich required more time due to the draping around the edges.
- Plain woven fabrics are harder to align in the correct direction.
- Woven fabrics are more complex to lay-up when decorative aim is pursued.
- Hand-lay-up requires more time.
- Laminate orientation while laying-up influence drapability since some corners are easier to achieve depending on the fiber direction.
- From a manufacturing point of view, female molds normally increased demolding complexity as well as fiber loading accessibility.

### 6.2.2 TIME MEASUREMENT

---

In a second evaluation, a set of four automotive parts (flat panel, cant rail, A-pillar and B-pillar) were produced under different process and material conditions (For further information referred to Section 5.3.2.) The total amount of time required for every stage of the composites manufacturing process was measured and



analyzed. The thesis at hand focuses on material influence, thereby and owing to the present section, an exclusively examination on lay-up process is here developed.

The results obtained are summarized on the next graphic:

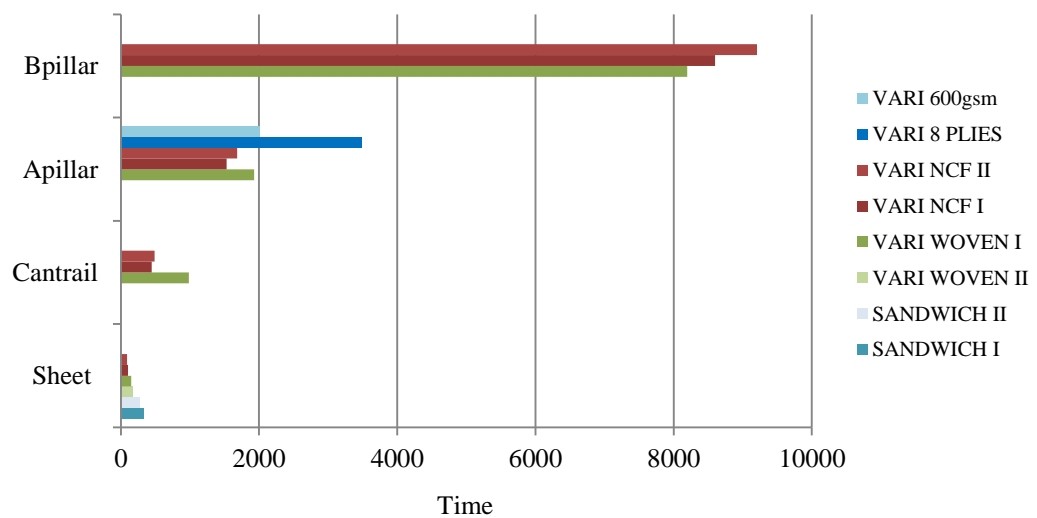


Figure 6.5 Draping time measurement

In a first observation, it can be seen that process required-time increases alongside complexity. To verify the statement previously inferred, a box plot of the complexity mean values is hereafter used:

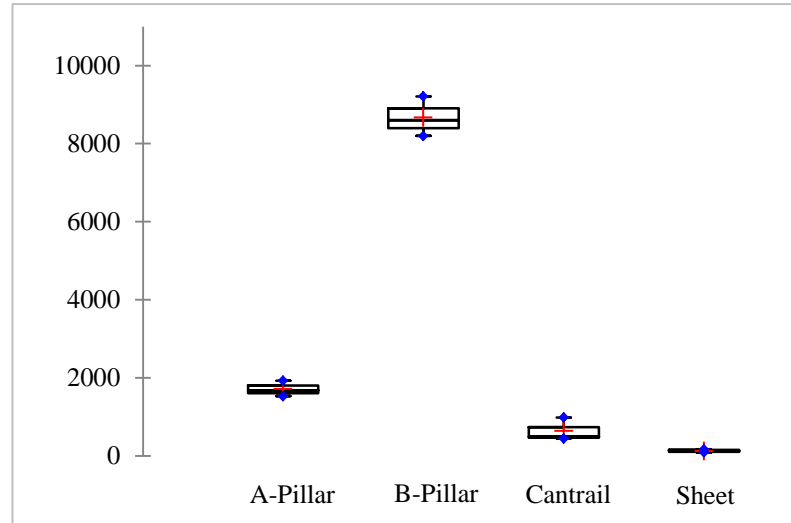


Figure 6.6 Complexity mean values

As expected, the values differ notably from each other. It is to remark that just woven and NCF tests were considered.

On the same way, the analysis of time increment due to the use of woven fabrics against NCF (Figure 6.10) showed that while in the B-Pillar the draping procedure was longer for NCF, the rest of parts inferred the opposite information.

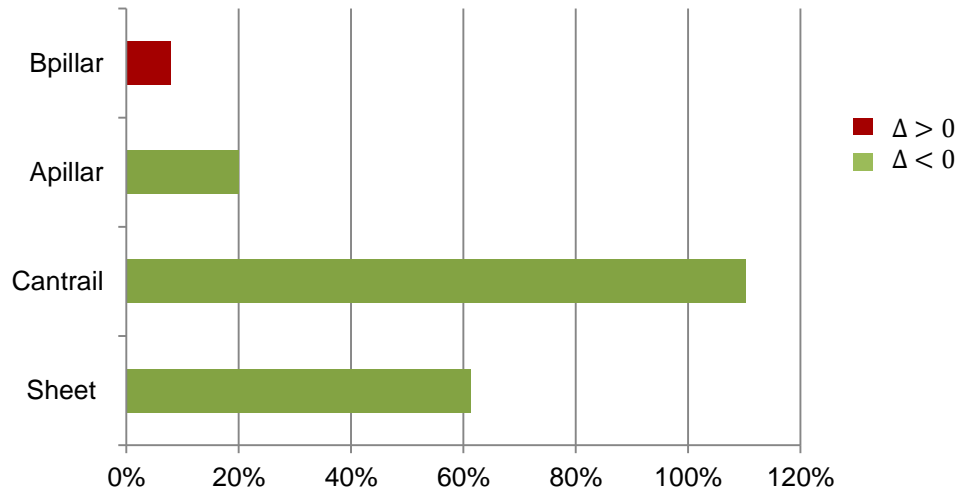


Figure 6.7 Time increment related to woven fabric use

Figure 6.7 must be carefully analyzed as it shows a couple of inconsistencies. As it can be seen in case of the sheet, there was a time increment of approximately  $\sim 60\%$ , what must be due to non-material factors rather than to a material complexity since during the process no difficulty compared to the other fabrics either on handling or draping and fitting was observed. However a deeper look into each of the steps that occur when draping is required to verify this hypothesis.

The manufacturing process of a flat sheet draping procedure consists of the following steps [46]:

Table 6.3 Draping steps

Cluster	WLU	RIFT	RTM	Process Steps
Lay-up (Manual)	✘	✘		Drape layer. Apply Binder/ glass type. Cut fabric edges
Consolidate (Draping press)			✘	Drape all layers



Thus, draping time measurement includes other sub-steps that may play a role on the overall time although they have nothing to do with material. A new scheme can be shown in Figure 6.11 where drape layer times were uniquely considered:

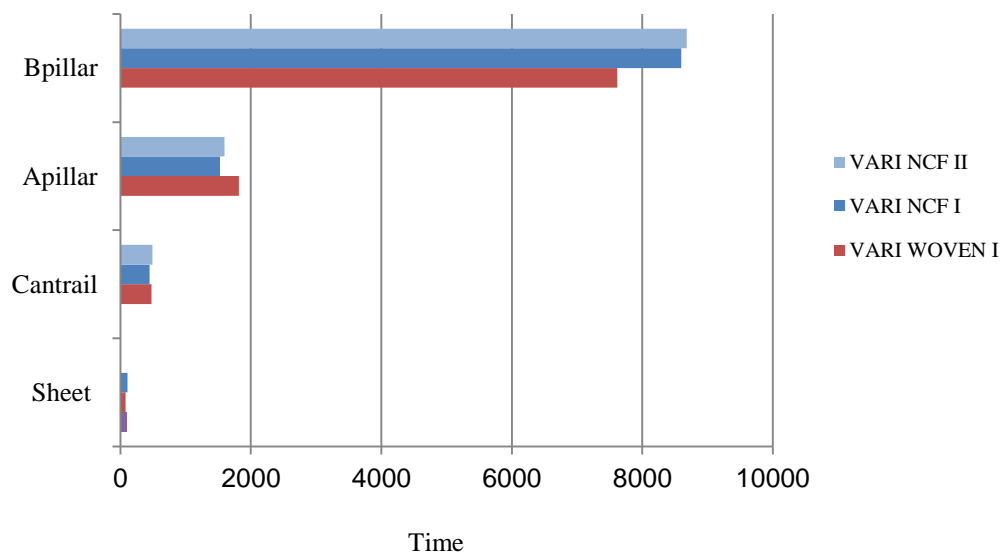


Figure 6.8 Drape layer measured times

It is therefore demonstrated that the time variances were due to additional steps of the draping process. Thus, no significant time difference was shown by reason of material. In fact, even B-Pillar test with woven fabrics were shorter than those realized with NCF under the same conditions.

Other setups, such as the use of sandwich structure, doubling the number of plies or the employment of higher areal weight (600gsm) plies were also tested with a sheet part and an A-Pillar, respectively. Each part is studied separately thereupon:

### 1<sup>st</sup> Case: Sheet Panel

Extra tests using sandwich structure (extra core ply) were realized for the sheet. The time dissimilarities, although they have been already seen in Figure 6.12, are hereunder shown in order to evaluate more accurately the possible differences.



Taking the mean values of the necessary time for each of the groups and evaluating inter-comparison, it was founded that:

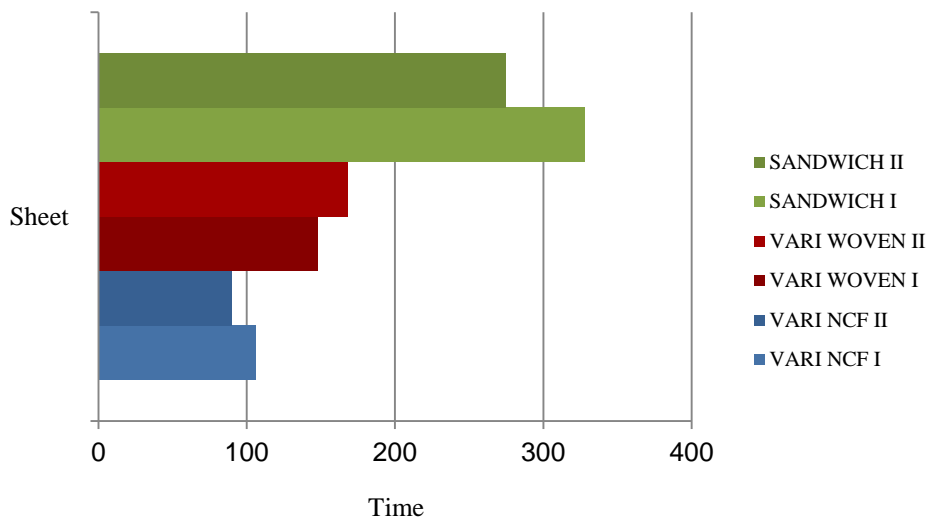


Figure 6.9 Sheet time measurements

Taking the mean values of the necessary time for each of the groups and evaluating inter-comparison, it was founded that:

$$\begin{aligned}t_{woven} &= (1 + 0,612) \cdot t_{NCF} \\t_{sandwich} &= (1 + 2,077) \cdot t_{NCF}\end{aligned}\quad (6.2)$$

On the basis of the above equations, the use of sandwich structures has a notable effect on the draping required time. This is mainly due to the presence of a core in between layers that demands extra time to bring it into the right position. It is difficult to affirm that the core presence has no influence on complexity, as although this extra-time should be included in time-estimation models as an extra layer time, it is true that the draping of later layers could be more complex, and hence more time consuming, than the first ones. To obtain a more accurate

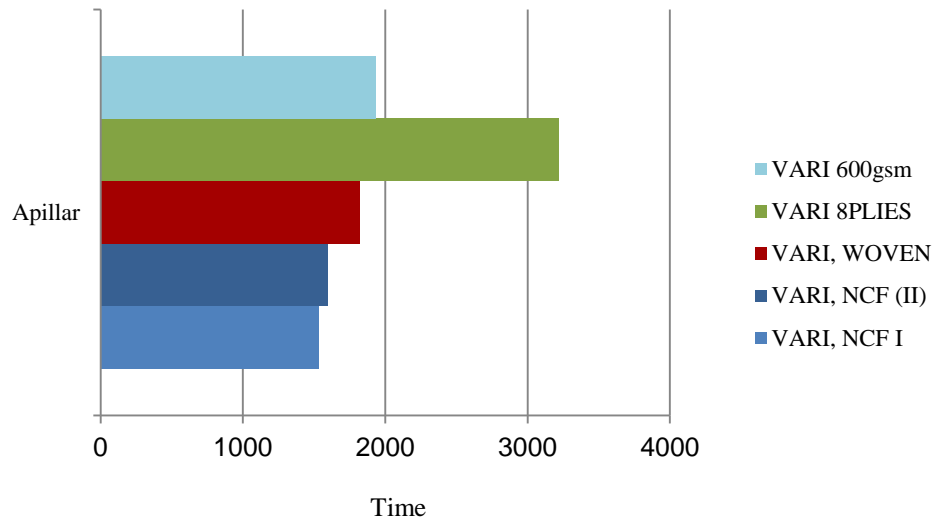


distinction amongst both situations an exhaustive experiment considering parts with a variety of complexities is recommended for future work.

The influence of woven fabrics for this case was already analyzed above.

## 2<sup>nd</sup> Case: A-Pillar

Applying the same procedure as in the 1<sup>st</sup> case, but considering solely drape layer measurements:



Where:

$$\begin{aligned}t_{woven} &= (1 + 0,163) \cdot t_{NCF} \\t_{8plies} &= (1 + 1,059) \cdot t_{NCF} \\t_{600gsm} &= (1 + 0,2352) \cdot t_{NCF}\end{aligned}\tag{6.3}$$

The aim of developing a test with double number of plies was to validate the assumption that there is not a material complexity when it comes to number of layers, and rather new parameters on time-estimation model equations. Equation 6.3 verified this initial hypothesis, as the time required for 8 plies was



approximately equal to two times the time employed for draping 4 plies of reinforcement.

On last term, it is important to emphasize that during the process additional cuts were done to the fabrics to increase de fitting accuracy. The number of cuts seemed to be larger in case of woven fabrics, especially when draped along double curvature forms, what, as mentioned before, detract mechanical properties. In order to guarantee component integrity, the thickness should be increased to compensate this possible cuts.

One of the major aims of the thesis at hand was to analyze the influence of using different reinforcement on manufacturing time. As a result of the survey and time measurement study it was found that time increment due to material is not significant, and hence, the development of a complexity factor is meaningless. However, it is equally recognized that such minor increment is mainly affected by the fabric areal weight and, in a lesser degree, by fabric shear rigidity; always under the premise, that their respective grade of influence is directly related with the part geometrical complexity.

### **6.3** *PERMEABILITY VALIDATION*

---

At the start of the complexity factor analysis, two processes were considered, the recent examined draping and in second instance permeability, o more generally speaking, infusion. This second process was declined (Section 5.3) as it was assumed to be more an optimization stage rather than an influence. Probably thanks to the grade of the process automation.

Nonetheless, this initial hypothesis is hereby verified by evaluating the infusion time measurements for the different parts and variations as done in the previous section.

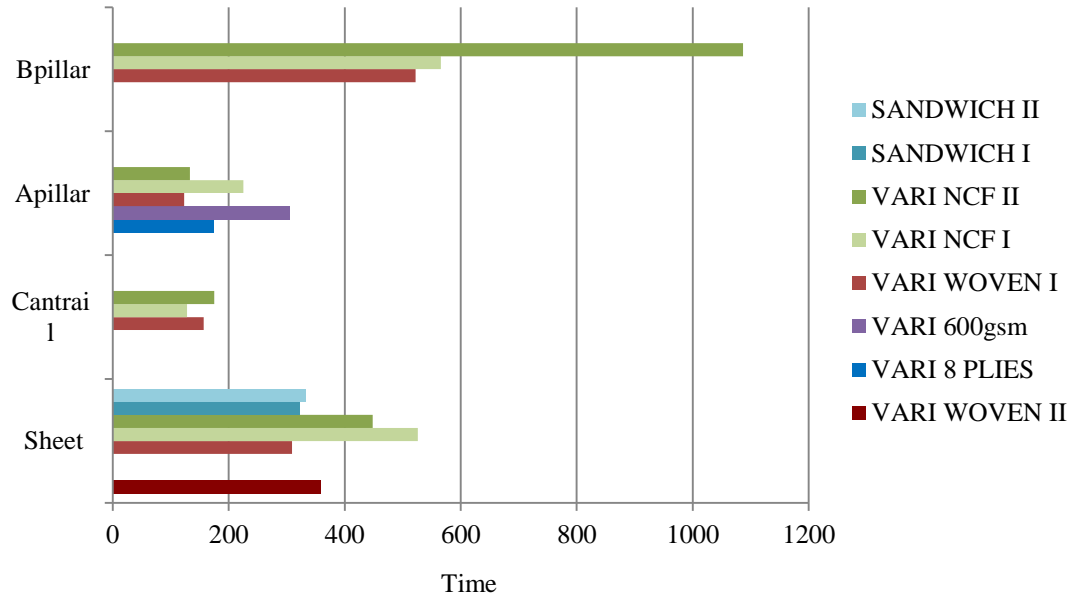


Figure 6.10 Infusion time measurement

As it can be inferred from Figure 6.10, for each of the geometries the infusion time remains approximately similar. Differences are seen on individual cases such as the second B-Pillar NCF test, but an earlier case ( VARI NCF I) developed on the same terms showed normal times.

Therefore, it can be concluded that there is no material complexity over infusion processes.

## 6.4 PLY STACKING COMPLEXITY

Observing the lay-up process, it was inferred that one parameter influencing the lay-up time was associated with the location, optimization and placement of successive plies on top of one other. This is due to the fact that all the plies that



should be laid are not equal and they rather have different sizes, shapes and orientations.

The lay-up process can be seen as a T-steps process where each step is the draping of one ply. If all plies are the same, only one configuration is possible, and hence the probability associated to this configuration is 1. This way of quantifying complexity as probability factor is known as Information Theory.

When number of type of plies, denoted by  $n$ , changes, reflecting different ply orientation, the number of possible configurations also varies, and consequently to a different probability of obtaining a certain configuration. The figure bellow illustrates different configurations for the same T and n:

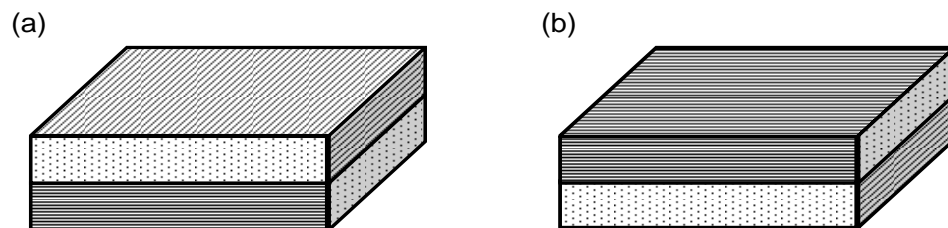


Figure 6.11 Different configurations for the same T and n

Equation 6.1 determines the probability of a particular configuration of T-ply and n types of plies:

$$p = \frac{1}{n^T} \quad (6.4)$$

For simplicity and due to the LOA optimization n is assumed to be 4, the four possible orientations a ply can be stacked.

From Equation 6.1, the information content of a ply drape can be determined as:



$$I = \log_2 \left( \frac{1}{p} \right) = \log_2(n^T)$$
$$I = T \cdot \log_2 n \quad (6.5)$$

In our case, where  $n = 4$  ( $0^\circ, 90^\circ, 45^\circ, -45^\circ$ ):

$$I = 2 \cdot T \quad (6.6)$$

This complexity seems to be a significant cost driver not just in hand lay-up, but also in cutting processes where ply orientation plays a role when optimizing scrap fabric.

As the present study refers to an early design phase, the lay-up is already optimized and thereby given to the manufacture. Hence, the ply stacking complexity is avoided. It is, however, true that cutting processes are highly influenced, but it can also be evaded by designing a cutting plane of the fabric roll.

## **6.5 DRAPING SIMULATION**

---

Draping simulation is the most accurate path to determine the fabric behavior. The main problem when considering draping software regards to the amount of input required or the lack of fabric mechanical properties consideration.

Nonetheless, as an example, the software Interactive Drape was used to simulate the draping of a woven fabric over the A-Pillar, under no mechanical properties influence.

Two simulations were performed varying the geometrical compaction of woven fabrics, hence, the pin-joint mesh. It is shown, that when no mechanical properties



are involved, compacting the fiber (Figure 6.13), this means, decreasing the fish net, decreases fabric deformation.

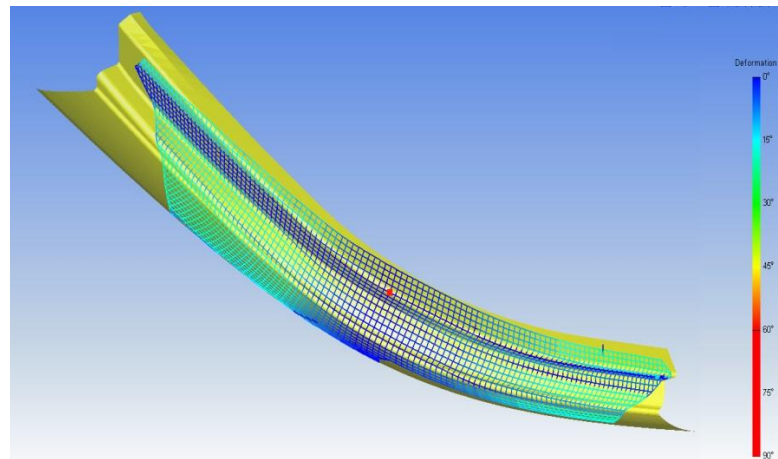


Figure 6.12 Draping I

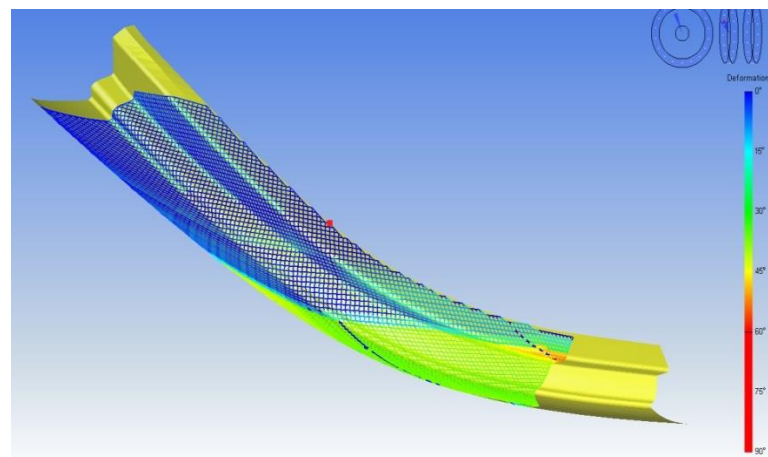


Figure 6.13 Draping II



## Chapter 7. SUMMARY AND OUTLOOK

CFRP design and optimization involves the study of four major fields, such as the analysis of the interactions between them. Interactions that might have more influence on the overall process than either of the major fields.

In order to evaluate how a factor exercise influence on another factor, it is vital to understand the behavior and mechanisms behind. It was shown that the main process influenced by material complexity was lay-up, or more specifically, layer draping. In order to estimate an influential factor or complexity several research was realized in order to reject possible material factor. Most of the research found on draping evaluation was from the textile industry, pioneer on the textile forming techniques that can be found today for composites manufacturing. Due to the lack of mechanical tests for measuring either this locking angle or fabric geometries parameters, common parameters given by the manufacturer where hence considered. It was finally stipulated that material complexity was a function of fabric areal weight and shear modulus, which is directly proportional to fabric locking angle.

Knowledge-based rating and time measurement analysis decline the initial hypothesis, and hence, the existence of a material complexity factor.

Looking for a reason to explain the lack of such factor, it was concluded that the difference amongst the use of unlike reinforcements or fabrics is negligible when compared to other complexities such as GCF.



## **7.1** *FUTURE WORK*

---

---

The realignment of fibers during preforming produces mechanical properties variations, along with variations in permeability. Hence, new values for sheared reinforcements must be estimated in order to stipulate if they are longer useful, or the mechanical properties detriment is significantly big to require a new material.

Other point proposed for future work follow:

- Braiding technology : Nowadays, braiding technologies are earning increasing attention, as parts can be manufactured at very low cost. However the main disadvantages still remain on the lack of variety parts. Further investigation is here proposed, as a method to estimate braid mechanical properties.
- Similarly can be done with PREPREGs, widely used in racing cars.
- Twill and Satin Woven Fabrics, optimize the methods here introduced for other pattern.
- Likewise realignment of the fibers when draping. Methods that model the mechanical degradation should be further introduced.
- On the thesis at hand material influence on CFRP composites manufacturing process was analyzed, but it has been shown that inversely, manufacturing process affects the properties of the fabrics and thus, their performance. One major example of this situation is the composites properties detriment by reason of voids presence; or due to the undercuts that are done to the fabric during draping process to avoid wrinkling.
- New tendencies are looking forward the analysis of natural fibers. An analysis on the worth application of natural fibers in the automotive industry is proposed.



**UNIVERSIDAD PONTIFICIA COMILLAS**  
ESCUELA TÉCNICA SUPERIOR DE INGENIERÍA (ICAI)  
INGENIERO INDUSTRIAL

## Summary and Outlook

---

CFRP Materials are the future and thereby a field on constant investigation and development, advanced driven mainly by the automotive and aerospace industry

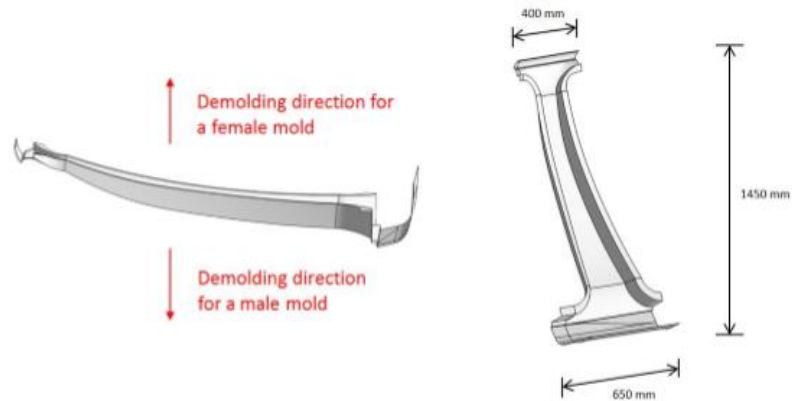


## APPENDIX : SURVEY

Geometry	#	Description
	1	Automotive chassis, structural: B-Pillar exterior part. Main dimensions: [1450/650/400]
	2	No specific function, non-structural: Plate. Main dimensions: [400/400]
	3	Automotive chassis, structural: Complete main tub. Main dimensions: [3517/1659]
	4	Automotive chassis, structural: A-Pillar joint. Main dimensions: [965/980]
	5	Automotive chassis, structural: Front drain channel. Main dimensions: [1625/470/280]
	6	Automotive chassis, structural: Rear side panel. Main dimensions: [1175/1470]
	7	Automotive chassis, structural: Side sill. Main dimensions: [230/500/265]
	8	Automotive chassis, structural: Rear wheel housing. Main dimensions: [1100/679]
	9	Automotive chassis, structural: Cant Rail. Main dimensions: [500/100/65]
	10	Automotive chassis, structural: A-Pillar. Main dimensions: [965/500]
	11	Automotive chassis, structural: Side Panel. Main dimensions: [500/100/65]



**Geometry 1/11: B-Pillar**



Rating:

1. General geometric complexity: [1 ... 5]

2. Specific attributes:

Specific complexity: [1 ... 5]

- ❖ Male mold
- ❖ Biaxial non-crimp fabrics
- ❖ 4 plies  
with an areal weight of 200 gsm

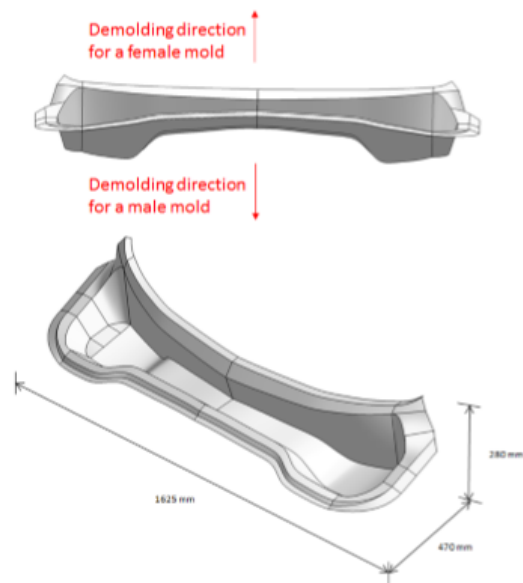
3. How does the specific complexity change if we use ...

	Tendency [+,-]	Value [0.5 ... 2.5]
...a female mold?	<input type="text"/>	<input type="text"/>
...plain woven fabrics?	<input type="text"/>	<input type="text"/>
...plies with an areal weight of 600 gsm?	<input type="text"/>	<input type="text"/>

Comments:



**Geometry 5/11: Drain channel**



Rating:

1. General geometric complexity: [1 ... 5]

2. Specific attributes:

Specific complexity: [1 ... 5]

- ❖ Male mold
- ❖ Biaxial non-crimp fabrics
- ❖ 4 plies  
with an areal weight of 200 gsm

Comments:



## USED SYMBOLS

Symbol	Description
$V_f$	Fiber Volume
$V_m$	Matrix Volume
$E_1$	Young's modulus parallel to the fiber direction
$E_2$	Young's modulus perpendicular to the fiber direction
$\rho$	Density
$G_{12}$	Shear Modulus
$\nu_{12}$	Poisson's ratio
$A_{ij}$	Extensional Stiffness Matrix
$B_{ij}$	Extensional Bending Matrix
$D_{ij}$	Bending Matrix
$\Omega_{weft}$	Weft
$Q$	Stiffness Matrix
$h$	Ply thickness
$a$	Crimp geometrical factor
$a_o$	Crimp geometrical factor
$a_u$	Crimp geometrical factor
$\eta_l$	Length correction factor
$\eta_o$	Reinforcement correction factor



$\varepsilon$	Strain
N	Force
$X_t, X_c$	Ultimate Tensile and Compressive strength in fiber direction
$Y_t, Y_c$	Ultimate Tensile and Compressive strength in matrix direction
$I$	Information Content
$T$	Ply- steps
$t$	Time
$\alpha$	Automation grade
$C_{draping}$	Overall Draping Complexity
$W$	Areal Weight
$\theta$	Shear angle
$\varphi_{min}$	Locking angle
$\varphi$	Inter yarn angle
$E_x, E_y$	Effective Extensional Young's Modulus of the laminate in longitudinal and transverse direction
U	Strain Energy
$\delta$	Interfiber spacing
$K_x, K_y$	In-Plane Permeabilities
$K_z$	Through-thickness Permeability
$.degraded$	Degraded values



## ABBREVIATIONS

CFRP	Carbon Fiber Reinforced Plastics
BIW	Body-In-White
SFP	Semi-Finished Products
NCF	Non-crimp-fabrics
ROM	Rule of Mixtures
CLT	Classical Laminate Theory
PW	Plain Woven
SW	Satin Woven
TW	Twill Woven
EAM	Element Array Model
SAM	Slice Array Model
MSE	Mean Squared Error
LOA	Layerwise Optimization Algorithm
UD	Uni-Directional Fabric
DC	Draping Complexity
GCF	Geometrical Complexity Factor
IFF	Inter Fiber Failure
FF	Fiber Failure



## LIST OF TABLES

Table 3.1	Properties Comparison [28] .....	32
Table 3.2	Mechanical properties comparison.....	33
Table 3.3	<i>no</i> typical values .....	36
Table 3.4	Tsai-Chou approaches comparison .....	46
Table 3.5	Yarn Strengths for Tsai-Wu failure mode.....	50
Table 3.6	Empirical degradation constants .....	52
Table 3.7	Woven vs. NCF .....	55
Table 4.1	Forming research overview .....	69
Table 5.1	Summary of published locking angles .....	91
Table 6.1	Material Data.....	103
Table 6.2	Results comparisson.....	104
Table 6.3	Draping steps.....	117



## LIST OF FIGURES

Figure 1.1	Emissions reduction strategies [39] .....	10
Figure 1.2	Expectations towards CFRP implementation .....	11
Figure 2.1	CLT Flowchart.....	21
Figure 2.2	IFF Failure modes .....	24
Figure 2.3	FF Failure modes .....	25
Figure 2.4	Manufacturing processes .....	26
Figure 2.5	Sequential vs. direct .....	27
Figure 3.2	Weave pattern styles .....	31
Figure 3.4	Spread vs. standard .....	33
Figure 3.5	RVE Examples.....	34
Figure 3.6	Idealization of the mosaic model .....	38
Figure 3.7	Series-model flowchart .....	41
Figure 3.8	Parallel-model flowchart.....	41
Figure 3.9	Cross-ply model .....	47
Figure 3.10	Braiding process.....	56
Figure 3.11	Braid styles.....	57
Figure 3.12	Braids mechanical properties .....	58
Figure 3.13	Prepreg production volume.....	59
Figure 4.1	Composites manufacturing process .....	64
Figure 4.2	Woven and UD lay-up equations .....	65
Figure 4.3	Draping influencing parameters.....	66
Figure 4.4	SFP Drapability.....	68



---

Figure 4.5	Macro-level deformations .....	70
Figure 4.6	Meso-level deformations .....	71
Figure 4.7	Micro-level deformations.....	71
Figure 4.8	Gaps simplification .....	75
Figure 5.1	Tool overview .....	79
Figure 5.2	SFP GUI flowchart .....	81
Figure 5.3	Mosaic model flowchart .....	82
Figure 5.4	Material Optimization flowchart.....	83
Figure 5.5	LOA for (a) laminate (b) woven fabrics .....	85
Figure 5.6	Tsai-Wu failure mode implementation .....	87
Figure 5.7	Shear angle [22] .....	89
Figure 5.8	Shear angle measurement methods (a) parallelogram (b) bias-extensional.....	90
Figure 5.9	Locking angles for different fabrics.....	92
Figure 5.10	Carbon fabrics locking angles.....	93
Figure 5.11	Locking angles .....	94
Figure 5.12	Molding directions .....	101
Figure 5.13	Time-measurement scheme .....	102
Figure 6.1	Complexity values overview.....	109
Figure 6.2	Factors Error vs. GCF.....	110
Figure 6.3	Woven fabric influence.....	111
Figure 6.4	Areal Weight influence .....	112
Figure 6.5	Draping time measurement .....	115
Figure 6.6	Complexity mean values.....	116
Figure 6.7	Time increment related to woven fabric use.....	117



Figure 6.8	Drape layer measured times.....	118
Figure 6.9	Sheet time measurements.....	119
Figure 6.10	Infusion time measurement.....	122
Figure 6.11	Different configurations for the same T and n.....	123
Figure 6.12	Draping I.....	125
Figure 6.13	Draping II.....	125



## BIBLIOGRAPHY

- [1] Amjad. 2014. *Analysis and Development of Parametric Model and Design Variants of Composite Vehicle Structure*, Nanyang Technological University.
- [2] Berthelot, J.-M. 1999. *Composite Materials. Mechanical Behavior and Structural Analysis*. Mechanical Engineering Series. Springer New York, New York, NY.
- [3] Byun, J.-H. and Chou, T.-W. Modelling and characterization of textile structural composites: A review. *The Journal of Strain Analysis for Engineering Design* 24, 4, 253–262. DOI=10.1243/03093247V244253.
- [4] Callahan, K. J. and Weeks, G. E. 1992. Optimum design of composite laminates using genetic algorithms. *Composites Engineering* 2, 3, 149–160.
- [5] Chen, Z., Ye, L., and Liu, H. 2004. Effective permeabilities of multilayer fabric preforms in liquid composite moulding. *Composite Structures* 66, 1-4, 351–357.
- [6] Chou, T.-W. and Ko, F. K. 1989. *Textile structural composites*.
- [7] Chou, T.-W. and Ko, F. K. 1989. *Textile structural composites*.
- [8] Chou, T.-W. and Nowinski, J. L. 1992. *Microstructural design of fiber composites*. Cambridge solid state science series.
- [9] Chretien, N. 2002. *Numerical constitutive models of woven and braided textile structural composites*. [University Libraries, Virginia Polytechnic Institute and State University], [Blacksburg, Va.].
- [10] Clayton, G. and Howe, C. 2004. Cost as a driver in advanced composites aerospace research. *Proceedings of the Institution of Mechanical Engineers, Part L: Journal of Materials Design and Applications* 218, 2, 79–85.



- [11] Curran, R., Kundu, A. K., Wright, J. M., Crosby, S., Price, M., Raghunathan, S., and Benard, E. 2006. Modelling of aircraft manufacturing cost at the concept stage. *Int J Adv Manuf Technol* 31, 3-4, 407–420.
- [12] Dow, N. 1987. *Analysis of Woven Fabrics for Reinforced Composite Materials* NASA CR-178275. NASA, Hamton, Virginia.
- [13] Drapier, S. 2002. Influence of the stitching density on the transverse permeability of non-crimped new concept (NC2) multiaxial reinforcements. Measurements and predictions. *Composites Science and Technology* 62, 15, 1979–1991.
- [14] Eric, C. 1991. *Composites Cost Modeling: Complexity*, University of Illinois.
- [15] Fiebig, C. 2014. The influence of fiber undulation on the mechanical properties of FRP-laminates. *58th IWK, Ilmenau Scientific Colloquium*.
- [16] Florian Mayer. 2014. *Analysis and Implementation of a parametric vehicle body component out of CFRP*, Technische Universität München.
- [17] Gebart, B. R. 1992. Permeability of Unidirectional Reinforcements for RTM. *Journal of Composite Materials* 26, 8, 1100–1133.
- [18] George, A. 2011. *Optimization of resin infusion processing for composite materials. Simulation and characterization strategies*. s.n.], [S.l.
- [19] Hashin, Z. 1980. Failure Criteria for Unidirectional Fiber Composites. *J. Appl. Mech.* 47, 2, 329.
- [20] Hashin, Z. and Rotem, A. 1973. A Fatigue Failure Criterion for Fiber Reinforced Materials. *Journal of Composite Materials* 7, 4, 448–464.
- [21] HEXCEL. *Technical Fabrics Handbook. Reinforcements for Composites*. [http://www.hexcel.com/Resources/DataSheets/Brochure-Data-Sheets/HexForce\\_Technical\\_Fabrics\\_Handbook.pdf](http://www.hexcel.com/Resources/DataSheets/Brochure-Data-Sheets/HexForce_Technical_Fabrics_Handbook.pdf). Accessed 25 July 2015.



- [22] Huebner, M. 2012. Simulation of the Drapability of Textile Semi-Finished Products with Gradient-Drapability Characteristics by Varying the Fabric Weave. *Fibres & Textiles in Eastern Europe* 20.
- [23] Jee, D.-H. and Kang, K.-J. 2000. A method for optimal material selection aided with decision making theory. *Materials & Design* 21, 3, 199–206.
- [24] Jones, R. M. 1998. *Mechanics Of Composite Materials*. Taylor & Francis.
- [25] Krenchel, H. 1964. *Fibre reinforcement : theoretical and practical investigations of the elasticity and strength of fibre-reinforced materials*.
- [26] Kulichenko, A. V. 2005. Theoretical Analysis, Calculation, and Prediction of the Air Permeability of Textiles. *Fibre Chemistry. Fibre Chem* 37, 5, 371–380.
- [27] Laszlo P. Kollar, George S. Springer. 2009. *Mechanics of composite structures*. Cambridge University Pres, [Place of publication not identified].
- [28] LCC. 2012. *Production Technologies for Composite Parts*, Technical University of Munich, Munich.
- [29] LeBlanc, D. J., Lorenzana, J., Kokawa, A., Bettner, T., and Timson, F. 1976. *Advanced Composite Cost Estimating Manual. Volume II. Appendix*. Defense Technical Information Center, Ft. Belvoir.
- [30] Lundstrom, T. 2000. *The permeability of non-crimp stitched fabrics*.
- [31] Ma, W. 2011. *Cost modelling for manufacturing of aerospace composites*, Cranfield University.
- [32] Miravete, A. 1999. *3-D textile reinforcements in composite materials*. CRC Press, Boca Raton.
- [33] Mogavero, J. and Advani, S. G. 1997. Experimental investigation of flow through multi-layered preforms. *Polym. Compos.* 18, 5, 649–655.
- [34] Naik, R. 1994. *Failure Analysis of Woven and Braided Fabric Reinforced Composites*. NASA, Hamton, Virginia.



- [35] Narita, Y. and Turvey, G. J. 2004. Maximizing the buckling loads of symmetrically laminated composite rectangular plates using a layerwise optimization approach. *Proceedings of the Institution of Mechanical Engineers, Part C: Journal of Mechanical Engineering Science* 218, 7, 681–691.
- [36] Puck, A. 1996. *Festigkeitsanalyse von Faser-Matrix-Laminaten. Modelle für die Praxis*. Hanser, München, Wien.
- [37] R.S. Sandhu. 1971. *Parametric Study of Optimum Fiber Orientation for Filamentary Sheet*.
- [38] Rechfeld, M. 2015. *Development and implementation of a CAx data interface system for the design, analysis and optimization of automotive body components consisting of CFRP.*, Technische Universität München.
- [39] Reid Paquin. 2014. *How Prepared is the Automotive Industry? Solutions for Meeting Fuel Efficiency and Emissions Standards*. Aberdeen Group.
- [40] Reifsnider, K. L. 1982. *Damage in Composite Materials: Basic Mechanisms, Accumulation, Tolerance, and Characterization*. ASTM International, 100 Barr Harbor Drive, PO Box C700, West Conshohocken, PA 19428-2959.
- [41] Roy R. 2003. *Cost Engineering: Why, What and How?* Cranfield University, United Kingdom.
- [42] Schönborn, C. 2015. *Methodology to Assess and Optimize the Automotive Assembly Process for Bodies Consisting of Carbon Fiber Reinforced Plastics*, Technische Universität München.
- [43] Siemens Product Lifecycle Management Software. 2015. *Fibersim 14: Siemens PLM Software*. [http://www.plm.automation.siemens.com/en\\_us/products/fibersim/fibersim-14.shtml](http://www.plm.automation.siemens.com/en_us/products/fibersim/fibersim-14.shtml). Accessed 24 August 2015.
- [44] Soykasap, O. 2006. Micromechanical Models for Bending Behavior of Woven Composites, 0022-4650.



- [45] Spallino, R., Giambanco, G., and Rizzo, S. 1999. A design algorithm for the optimization of laminated composite structures. *Engineering Computations* 16, 3, 302–315.
- [46] Surek, F. 2015. *Development of a Manufacturing Cost Assessment Method and an Optimization Heuristic for the Design of Composite Vehicle Bodies*, Technische Universität München.
- [47] *Technologies | Oxeon.se*. <http://oxeon.se/technologies>. Accessed 25 July 2015.
- [48] Tsai, S. W. 1992. *Theory of composites design*. Think Composites, Dayton, Ohio.
- [49] Tsai, S. W. and Massard, T. N. 1984. *Composites Design*. Defense Technical Information Center, Ft. Belvoir.
- [50] Verette RM. 1970. *Stiffness, strength and stability optimization of laminated composites*. NOR-70-138. Northrop Corporation, California.
- [51] Vigo, T. L. and Turbak, A. F. 1991. *High-tech fibrous materials. Composites, biomedical materials, protective clothing, and geotextiles / Tyrone L. Vigo, editor, Albin F. Turbak, editor*. ACS symposium series, 0097-6156 457. American Chemical Society, Washington, D.C.
- [52] Wemyss, A. M. and Boos, A. G. de. 1991. Effects of Structure and Finishing on the Mechanical and Dimensional Properties of Wool Fabrics. *Textile Research Journal* 61, 5, 247–252.